(36)

DNA Target Selection by Calicheamicin

by

Aaron A. Salzberg

B.S. Aerospace Engineering, University of Maryland, 1983
M.S. Aerospace Engineering, University of Maryland, 1986

SUBMITTED TO THE DIVISION OF TOXICOLOGY IN PARTIAL FULFILLMENT OF THE REQUIREMENTS FOR THE DEGREE OF

Ph.D. IN TOXICOLOGY
AT THE
MASSACHUSETTS INSTITUTE OF TECHNOLOGY

May, 1998

Signature of Author.....
Division of Toxicology
May 15, 1998

Certified by.....
Peter C. Dedon
Associate Professor of Toxicology
Thesis Supervisor

Accepted by.....
Peter C. Dedon
Chairman, Committee on Graduate Students
Division of Toxicology

This doctoral thesis has been examined by a Committee of the Division of Toxicology as follows:

Professor William Thilly.....
Chairman
Division of Toxicology
Massachusetts Institute of Technology

Professor Peter C. Dedon.....
Supervisor
Division of Toxicology
Massachusetts Institute of Technology

Professor John Essigmann.....
Division of Toxicology and Department of Chemistry
Massachusetts Institute of Technology

Professor Alexander Rich.....
Department of Biology
Massachusetts Institute of Technology

Professor James Williamson.....
Department of Molecular Biology and the Skaggs Institute of Chemical Biology
The Scripps Research Institute

DNA Target Selection by Calicheamicin

by

Aaron A. Salzberg

Submitted to the Division of Toxicology
on May 15, 1998 in Partial Fulfillment of the
Requirements for the Degree of Ph. D. in Toxicology

Abstract

The research presented here has evolved from the general hypothesis within our laboratory that DNA *in vivo* has characteristics which modulate its sensitivity to DNA damaging compounds. As one component of this overall paradigm, this work sets out to explore the material and structural properties of DNA that mediate the targeting of drugs to specific sites within the DNA.

To examine these issues, we have studied the clinically relevant antitumor antibiotic calicheamicin. Calicheamicin binds DNA non-covalently in the minor groove and abstracts hydrogen atoms from both sugar phosphate backbones causing site-specific double-stranded DNA damage. The reactivity of the drug is affected by both the topology and sequence context of the binding site, suggesting that calicheamicin recognizes some form of structural perturbation rather than sequence *per se*. However, the true mechanism for calicheamicin target selection is unknown.

To investigate the role of both calicheamicin structure and DNA structure and dynamics in target recognition, two approaches were taken: First, gel mobility studies were performed to evaluate whether calicheamicin binding sites possessed a common element of curvature. Second, DNA cyclization experiments were conducted to assess and measure the structural changes that occur in DNA when calicheamicin or its oligosaccharide binds. (Novel modifications were introduced to facilitate the rapid detection and analysis of DNA bending.) Our results show that calicheamicin binding sites are not curved, but that both the drug and oligosaccharide bend DNA upon binding. These data support a model for calicheamicin target selection where the drug prefers to bind those sequences that can be easily bent (*i.e.*, flexible) into a conformation that maximizes its electrostatic and hydrophobic interactions with DNA.

In addition to these experiments, we exploited calicheamicins' ability to bend DNA to study the affect of topology on the kinetics of DNA bimolecular association. We show, that when the ends of the DNA molecule are in close proximity,

intermolecular reactions are inhibited; a result that calls into question indirect methods for measuring bimolecular association reaction rates.

These results contribute to our understanding of small molecule-DNA interactions and lay the groundwork for understanding how molecules select genomic targets.

Thesis Supervisor: Associate Professor Peter C. Dedon

Title: Associate Professor of Toxicology

Dedication

Bruce Becker
David Monius
David Price
Samuel Rosenthal

Acknowledgments

I am extremely grateful to the Division of Toxicology at MIT, the National Institutes of Health and the Hugh Hampton Young Fellowship Committee for their support and commitment to my work.

Table of Contents

Abbreviations and Symbols

(in alphabetical order)

a, b	Mathematical constants as defined in the text
bp	Base-pairs
AL	Apparent length (base pairs)
[B]	Concentration of binding sites (molar)
[B-CAL]	Concentration of occupied binding sites (molar)
C_i	Integration constants
CAL	Calicheamicin γ_1^I
[CAL]	Concentration of calicheamicin γ_1^I (molar)
CAL-ε	Calicheamicin ε
[CAL-ε]	Concentration of calicheamicin ε (molar)
$C(t)_r$	Radioactivity measured in the circularized DNA band (cpm)
[C(t)]	Concentration of circles (molar)
d	Change in mean circle size $(m_{ul} - m_{ll})/100$
$D(t)_r$	Radioactivity measured in the dimerized DNA band (molar)
[D]	Concentration of uncyclized substrate (molar)
[D']	Concentration of undimerized substrate (molar)
$[D_i(t)]$	Concentration of dimers (molar)
$[D_m(t)]$	Concentration of measured undimerized dimerized substrate (molar)
$[D_{mo}]$	Total measured concentration of undimerized substrate (molar)
[E]	Free enzyme concentration (molar)
$[E_o]$	Total enzyme concentration (molar)
[ES]	Concentration of the enzyme-substrate complex (molar)
f_d	Fraction of unligatable substrate
f_s	Ratio of ligatable substrate to total DNA (circularization)
f_s'	Ratio of ligatable substrate to total DNA (bimolecular association)
[H]	Concentration of half molecules (molar)
J	Ring closure probability (molar)
k_1	Rate constant for cyclization (s^{-1})
k_2	Rate constant for dimerization ($M^{-1}s^{-1}$)

k_{xy}	Rate constant going from step "x" to step "y"
K_a	Bimolecular association equilibrium constant
K_c	Cyclization equilibrium constant
K_m	Rate constant for DNA ligase
[L]	Concentration of DNA substrate (molar)
$[M_o]$	Concentration of monomers (molar)
m	Mean circle size
m_{ll}	Lower limit of the mean circle size
m_{ul}	Upper limit of the mean circle size
M W	Molecular weight (grams/mole)
[P]	Concentration of covalently closed circles (molar)
[P']	Concentration of covalently linked monomers (molar)
pUC19-Sap	The pUC19 cloning vector with the *Sap* I restriction site removed
pAS1	Cloning vector created from pUC19 as described in Figure 1
pAS1/nmx	The pAS1 cloning vector incorporating the "n"th polymer of the "x" monomer
R_L	Ratio of apparent length to actual length
[S]	Concentration of ligatable substrate (cyclization)
$[S_a]$	Concentration of ligatable substrate (bimolecular association)
X	Migration distance (cm)
α	Bend angle of a regular polygon with respect to a local tangent (degrees)
α_{cal}	Bend angle caused by calicheamicin binding (degrees per site)
α_f	Average bending due to the intrinsic flexibility of DNA (degrees per base-pair)
β	Enclosed angle of a regular polygon (degrees)
δ^-	Partial charge (negative)
δ^+	Partial charge (positive)

List of Figures

List of Tables

Biographical Note

Publications and Conference Presentations

Biochemistry

Salzberg, A.A., and P.C. Dedon (1997) Calicheamicin target recognition: DNA structure and dynamics in small molecule-DNA interactions. *Proc. Natl. Acad. Sci. USA*, submitted.

Salzberg, A.A., and P.C. Dedon (1997) An improved method for the rapid assessment of DNA bending by small molecules. *J. Biomol. Struc. Dyn.* **15**: 277-284.

Salzberg, A.A., and P.C. Dedon (1997) DNA bending by small molecules: Studies with calicheamicin, in Structure, Motion, Interaction and Expression of Biological Macromolecules (ed. R.H. Sarma and M.H. Sarma) Adenine Press (in press).

Salzberg, A.A., P. Mathur, and P.C. Dedon (1996) The intrinsic flexibility and drug-induced bending of calicheamicin DNA targets, in DNA Cleavers and Chemotherapy of Cancer or Viral Diseases (ed. B. Meunier). Kluwer Academic Publishers: The Netherlands, pp. 23-36.

Yu, L., A.A. Salzberg, and P.C. Dedon (1995) New insights into calicheamicin-DNA interactions derived from a model nucleosome system. *Bioorg. Med. Chem.* **3**: 729-741.

Dedon, P.C., A.A. Salzberg, and J. Xu (1993) Exclusive production of bistranded DNA damage by calicheamicin. *Biochemistry* **32**: 3617-3622.

Salzberg, A.A. (1997) DNA bending by small molecules: Studies with calicheamicin, *10th Conversation in the discipline of Biomolecular Stereodynamics.*

Salzberg, A.A., and P.C. Dedon (1997) Calicheamicin bends DNA, *Proc. of the Amer. Assoc. Cancer Res.* **38**: 228.

Salzberg, A.A., and P.C. Dedon (1997) Determinants of calicheamicin binding, *New England Pharmacologists.*

Salzberg, A.A. (1995) Does DNA flexibility play a role in target selection by genotoxins? (Observations with calicheamicin), *Boston Mutagenisis Society.*

Salzberg, A.A., and P.C. Dedon (1995) The structure and dynamics of calicheamicin binding sites, *Proc. of the Amer. Assoc. Cancer Res.* **36**: 353.

Engineering

Haughton, J., and A.A. Salzberg (1990) Combined high level acoustic and mechanical vibration testing and analysis. *Proceedings of the 8th International Modal Analysis Conference.*

Salzberg, A.A. (1989) Validation of LACE spacecraft vibroacoustic prediction model, *J. Env. Sciences*, **32**: 53-59.

Salzberg, A.A. (1989) Deriving component pyroshock test specifications from system level test data, *Proceedings of the 60th Shock and Vibration Symposium 1989.*

Salzberg, A.A., and J. Haughton (1989) Combined high level acoustic testing and mechanical vibration testing for vibration prediction, *35th Institute of Environmental Sciences technical meeting.*

Salzberg, A.A. (1988) Spacecraft vibroacoustic response prediction, *NRL Review*, 93-94.

Salzberg, A.A. (1988) Validation of LACE spacecraft vibroacoustic prediction model, *Proceedings of the 59th Shock and Vibration Symposium 1988.*

Salzberg, A.A., and I. Chopra (1986) Tailoring the structural stiffness coupling in composite blade spars, *RPI Workshop on Composite Materials and Structures for Rotorcraft.*

Ethics and Sociology

Salzberg, A.A. (1997) Informed Discussion / Formal Authority, in Research Ethics: Fifteen Cases and Commentaries 1 (ed. B. Schrag). Association for Practical and Professional Ethics, Bloomington.

Salzberg, A.A. (1997) Commentary on "The Social Responsibilities of Biological Scientists." *J. Science Eng. Ethics*, **3**:149-152.

Awards

AAAS Science and Engineering Diplomacy Fellowship (1998)
Hugh Hampton Young Fellowship (1997)
AACR Young Investigator's Award (1995)
Alan Berman Research Publication Award (1990)

Prologue

Seminal to the research presented in this dissertation, is the view that DNA is a structure whose material and conformational properties play a role in regulating the intracellular environment. Within this paradigm, two hypotheses have emerged:

First, the degeneracy in the genetic code suggests that structurally different sequences can be used -- interchangeably -- to code for the same protein. In other words, while coding for the same gene product, the sequence -- by virtue of its intrinsic material and topological properties -- can use structure and dynamics to interact uniquely with its environment.

Second, as an anisotropic structure, DNA contains discontinuities in its material properties that lead to localized regions of high stress when the molecule undergoes dynamic motion. On an atomic level, this stress results in an increase in the reactivity of specific bonds within the structure. We call these hyper-reactive regions "hot spots".

The importance of these observations is the suggestion that there is more to DNA than first meets the eye and that to properly understand its behavior, we must discover and accept what it means to be a structure built from nucleotide bricks. Indeed, it is from this exploration of DNA structure that this thesis emerges.

CHAPTER I

Introduction

Deoxyribonucleic acid (DNA) is a molecule composed of two complementary polynucleotide chains twisted about each other in the form of a regular right-handed helix. The type and order of nucleotides within the chain directs the construction and function of cellular components necessary to sustain "life." If damage should occur to the DNA, the instructions may become modified or lost. In a healthy individuals, such alterations may result in physiological changes that can cause sickness or death. However, in unhealthy people, we may actually want to damage cellular DNA intentionally to selectively kill and destroy cells that are part of, or promote, a diseased state.

In addition to the "genetic code," the sequence of nucleotides in DNA creates series of uniquely charged chemical surfaces within the grooves of the double-helix that can act as recognition sites for proteins and other molecules. These regions play an important role in the proper functioning of the cell by regulating critical processes such as gene expression and DNA packaging. They also contribute to the targeting of DNA damaging compounds to specific regions within the molecule. However, DNA is more than a collection of chemical charges. As a polynucleotide chain, DNA possesses both material and structural properties that can also provide unique features that contribute to the recognition of specific sequences by DNA-reactive chemicals.

The research presented here has evolved from the general hypothesis within our laboratory that DNA *in vivo* has characteristics that modulate its sensitivity to DNA damaging compounds. These include phenomena that affect DNA generally -- such as chromatin packaging, DNA transcription and supercoiling -- and locally -- as in sequence-defined bending or flexibility. As one component of this overall paradigm, this work sets out to explore the material and structural properties of DNA that mediate the targeting of drugs to specific sites within the molecule.

To examine these issues, I have chosen to study the antitumor antibiotic calicheamicin and its interactions with DNA. Calicheamicin is a clinically relevant [1, 2], extremely toxic [3, 4] chemical that binds non-covalently to the minor groove of DNA causing site-specific strand cleavage. My goals were to 1) determine whether the structural or dynamic properties intrinsic to specific DNA sequences were responsible for the sequence selectivity of calicheamicin-induced DNA damage, and 2) discover what, if any, components of calicheamicin were responsible for these interactions.

This work is significant for several reasons. First, by defining -- at the local level -- the structural properties that govern DNA binding by calicheamicin, we can begin to interpret differences in drug-induced DNA damage that are observed under physiologically relevant conditions in whole cells. In addition, since calicheamicin targets a wide variety of sequences, we may uncover a common structural motif unique to specific DNA sequences that increases their susceptibility to damage by certain compounds. Next, by developing an assay for quickly measuring and quantifying the effects of calicheamicin binding on DNA structure, we further the techniques available for the study of similar DNA distorting phenomena. This is particularly significant given the extreme hydrophobicity and weak binding affinity of calicheamicin for DNA. And last, by rigorously examining the empirically observed results from carefully designed cyclization experiments, it may ultimately be possible to refine theoretical models of DNA structure and to extract -- biochemically -- the topological changes that occur in DNA as a result of drug binding. In all cases, the research adds to the growing body of data that may one day allow us to design drugs that target sequence-defined structural or dynamic properties rather than sequence *per se*. It will, perhaps, allow us to better understand why specific drugs target certain areas within the genome and, at the same time, begin to decipher this secondary "language" of DNA structure and dynamics.

Calicheamicin

Calicheamicin, a member of the enediyne family of antitumor antibiotics, has received significant attention both for its potency as a cytotoxic agent [5, 6] and for the chemistry of its DNA damage [7, 8]. Isolated from *Micromonospora echinospora* ssp *calichensis*, the antibiotic has demonstrated as much as a 1000-fold

greater activity against some tumors than other similar compounds such as adriamycin [6]. Shown below, the drug consists of a reactive enediyne core (common to enediyne antitumor antibiotics) attached to a five membered oligosaccharide chain (aryltetrasaccharide).

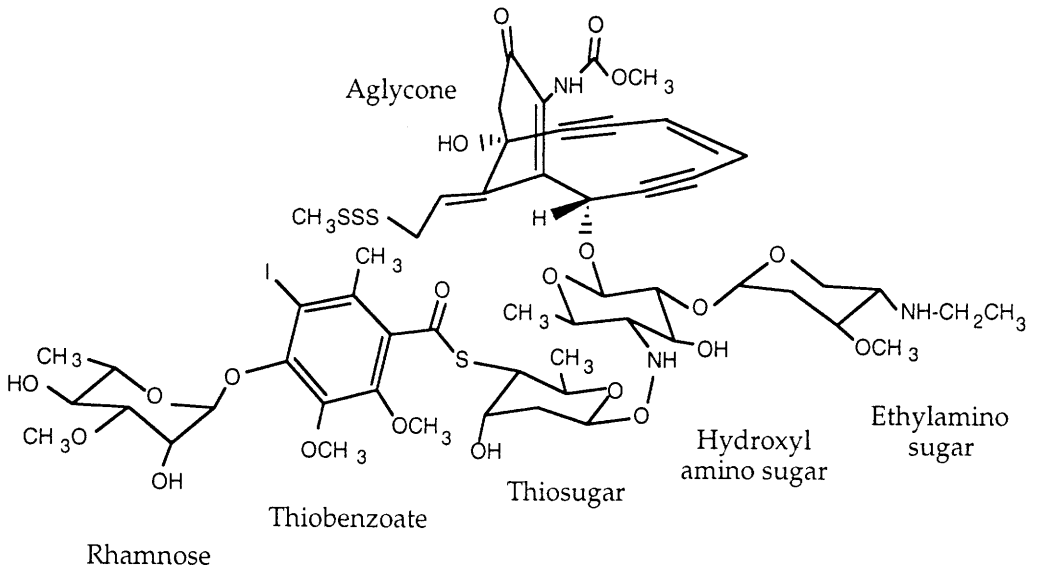

Calicheamicin γ_1^I

Aside from its practical relevance as a tumor fighting agent, the benefit in using calicheamicin as a model compound for investigating the interactions of DNA and drug structure, is that it represents one member of a group of functionally similar, yet structurally diverse, enediyne compounds. This allows us to investigate DNA-drug interactions by comparing and contrasting the effects of drug structure on the affinity and reactivity of these compounds with DNA under a variety of functional and topological settings [9-12].

Calicheamicin and DNA

Like other members of the enediyne family, calicheamicin produces DNA damage *via* a diradical intermediate that, when positioned in the minor groove, abstracts deoxyribose hydrogen atoms from the DNA backbone (see figure below). The drug is activated by reduction of the trisulfide moiety which initiates formation of a relatively stable dihydrothiophene intermediate [13]. The activated drug,

positioned in the minor groove of DNA, then begins a Bergman-type cycloaromatization to the highly reactive diradical species which then abstracts hydrogen atoms from the deoxyribose sugars [7, 8]. As a result, the diradical intermediate is reduced to its inactive form, calicheamicin ε, and the oxidized sugar radicals undergo oxygen-dependent reactions to form abasic sites or strand breaks [14].

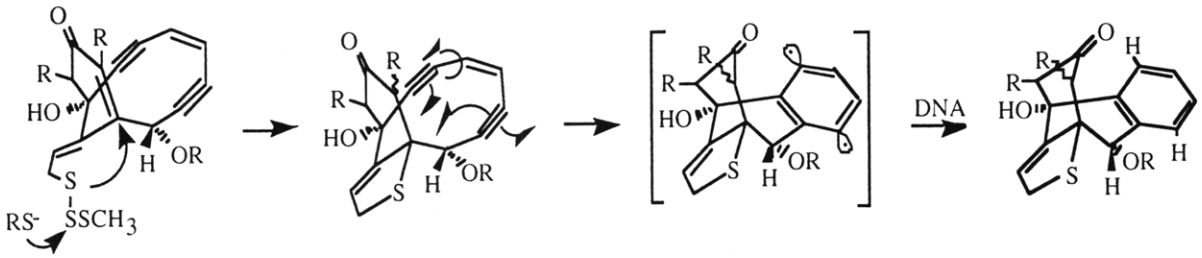

Single molecules of calicheamicin produce predominantly double-stranded DNA lesions with damage in each strand staggered by two base pairs (bp) [6, 7, 15, 16]. The oxidative damage to the deoxyribose results in products that are specific to the position of the abstracted hydrogen atoms and are detectable in gel-shift mobility assays [17-21]. These experiments, combined with deuterium transfer studies, have shown that hydrogen abstraction occurs in the deoxyribose sugars at the 4' and 5' positions [13, 22]; the latter, as shown below, positioned three base pairs in a 3'-direction on the complementary strand.

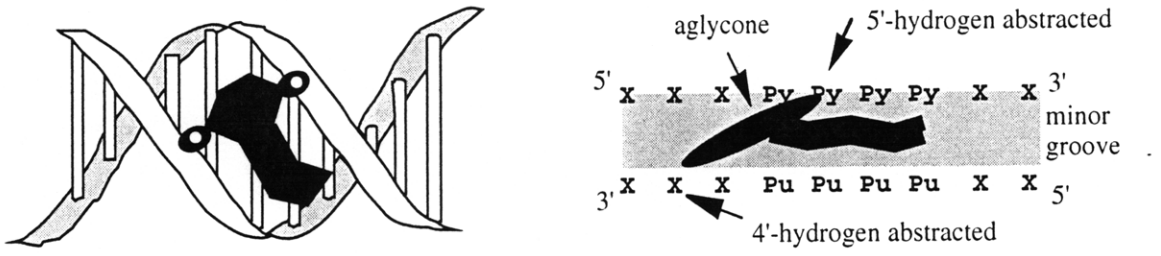

These results are consistent with hydroxyl radical footprinting and NMR solution structures of the calicheamicin-DNA complex which suggest that the drug binds DNA such that the aglycone warhead spans the minor groove with the ethylamino sugar reaching over the phosphate backbone and the carbohydrate tail adopting a right-handed screw conformation that extends down the minor groove in a 3'-direction [22-27].

Calicheamicin damages DNA site-specifically; showing a general preference for a wide variety of tetrapurine sequences such as AGGA, AGAG, AGGT, TGGA, AGGC, GAGA and AAAA [6, 7, 28, 29]. This targeting may reflect differences in binding affinity, if every drug molecule bound leads to a measured damage event; or in reactivity, if the binding site sequence plays a role in the activation of the drug to the diradical intermediate or in the rate of the formation of the final damage products. Most likely, DNA targeting involves some combination of both. In the case of calicheamicin, it is now generally accepted that the apparent tetrapurine sequence selectivity reflects a recognition of sequence-dependent local DNA conformation and dynamics rather than a direct reading of specific base sequences or issues of reactivity [6, 24-27, 30-37].

The oligosaccharide tail of calicheamicin appears to be the structure responsible for the sequence selectivity. Damage studies with derivatives of calicheamicin have shown that the molecule retains site specificity without the ethylamino or rhamnose sugars, but requires the remaining elements of the oligosaccharide tail for sequence recognition [38]. The aglycone alone, or with the hydroxyl amino and ethylamino sugars, is not sequence specific; it binds and damages DNA indiscriminately with significantly lower affinity [35]. Interestingly, hydroxyl radical footprinting experiments demonstrate that the oligosaccharide does not bind in the exact same location as the parent calicheamicin but is instead shifted slightly [34, 38]. Taken together, these results suggest that the affinity of calicheamicin for specific DNA sequences is primarily a function of the oligosaccharide tail with some "small," as yet unknown, contribution from the aglycone.

How the aryltetrasaccharide recognizes DNA sequence is unclear. In target sequences with a 5' penultimate cytidine, it has been shown that the presence of the exocyclic amine from the complementary guanosine (located in the minor groove) is important to, but not necessary for, recognition [34, 39]. Indeed, molecular dynamics studies suggest that the thiobenzoate ring changes its orientation completely when binding to DNA without such an amine present [40]. However, despite these observations, no pattern of bonding interactions appears to account for the ability of calicheamicin to uniquely recognize the wide variety of purine sequences it does.

Several observations suggest that calicheamicin targeting may reflect the ability of specific sequences to undergo structural changes in response to drug binding. NMR studies indicate that the relatively rigid carbohydrate side chain

contacts the pyrimidine strand and that the minor groove widens to accommodate the aglycone [26, 27, 39]. Additionally, observations have been made that calicheamicin binding causes DNA overwinding and increases the negative superhelical content of DNA [41, 42]. These data, combined with experiments that show base changes outside the target recognition sequence affects calicheamicin-induced damage [38], suggest that DNA topology and dynamics is influenced by calicheamicin binding. As a result, it may be energetically favorable for calicheamicin to bind those sequences that can undergo these changes most easily. As yet, however, there is no unified model for the calicheamicin target recognition process.

Recent work within the Dedon laboratory has contributed significantly to resolving many of these issues. In a comparison of calicheamicin-induced damage in naked DNA to DNA reconstituted into nucleosomes we found that: 1) bending of nucleosome DNA increased drug-induced cleavage at one site; 2) there is little correlation between minor groove width *per se* and calicheamicin target selection; and 3) calicheamicin appears to recognize the structural discontinuity at the 3'-ends of purine tracts [43].

The observation that bending could influence DNA damage suggested that calicheamicin may have a preference for curved DNA; DNA that could accommodate drug structure with a smaller expenditure of energy. This is consistent with previous observations that calicheamicin binding caused some, albeit small, modifications to DNA structure and that some form of an "induced fit" was responsible for drug binding.

Together, the last two observations suggest the existence of a structural feature, common to the 3' ends of purine tracts, that increases the susceptibility of DNA to damage by calicheamicin. This finding is further supported by a review of the literature which shows that many of the most reactive sites occur at the 3' ends of purine tracts, as shown below.

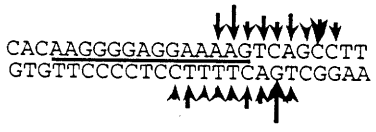

Yu *et al.*, *Bioorg. Med. Chem.* **3**: 729, 1995

Nicolaou *et al.*, *J. Am. Chem. Soc.* **114**: 7555, 1992

Mah *et al.*, *Tetrahedron* **50**: 1361, 1994

Myers *et al.*, *J. Am. Chem. Soc.* **116**: 125, 1994

Mah *et al.* came to a similar conclusion in their work [24]. They propose that the 3' end of the A-tract is curved, creating a structure which deviates from canonical B-DNA making it a better target for calicheamicin.

These observations suggest a new model for calicheamicin's interaction with its DNA targets [43]. Within this paradigm, the drug does not recognize sequence *per se*. Instead, a sequence-dependent structural perturbation (*i.e.*, a bend or hinge), lying 3' to the purine tract at or beyond the purine-pyrimidine junction, facilitates the reaction of the drug with DNA. It is further suggested that the aglycone plays some role in the recognition of these DNA features. This is somewhat analogous to observations of anthramycin and tomaymycin binding to, and bending, target DNA sequences [44].

To investigate the appropriateness of this model, experiments were performed to:

1) Identify, if any, the intrinsic characteristics of calicheamicin binding sites (Chapter II).
2) Qualitatively determine the effects of calicheamicin and oligosaccharide binding on DNA structure (Chapter III).
3) Quantitatively measure the effect of calicheamicin and oligosaccharide binding on the kinetics of DNA cyclization (Chapter IV).

To accomplish these objectives, it was necessary to develop techniques to measure the changes in DNA structure under conditions which allowed the drug to bind the DNA.

Measuring the Cyclization Properties of DNA

Three methods are most often used to detect DNA curvature or bending:[1] electron microscopy, gel electrophoresis and circularization of DNA molecules [45]. The first, electron microscopy, is useful for observing macroscopic structural phenomena that can be captured and visualized within the operating conditions of the microscope. Typical results have been estimates of large bend angles or population profiles, reflecting the proportion of molecules captured in a curved or

[1] Curvature is a change in the direction of the helical axis that is sequence defined. In other words, a property intrinsic to the DNA. Bending is a change in the direction of the helical axis due to external forces, such as protein or drug binding.

bent conformation [46]. Small changes, however, are often undetectable. Gel electrophoresis methods take advantage of the abnormally slow migration rate that macroscopically curved or bent DNA molecules exhibit when compared with "straight" DNA [47]. The technique is versatile and reliable, in some cases allowing -- with the proper experimental design -- the estimate of bend angles, the direction of curvature/bending and even, under some circumstances, changes in twist and flexibility [48-50]. Unfortunately, the electrophoretic properties of a DNA molecule are relatively insensitive to small changes in curvature and non-planar superhelical conformations [51]. Furthermore, it is unclear how flexibility and twist affect gel migration. As a result, it is often difficult to ascribe specific changes in electrophoretic mobility to a unique structural or dynamic change in the DNA molecule.

The T4 DNA ligase-catalyzed cyclization assay, originally described by Shore *et al.* [52], has become the most sensitive method for measuring the static and dynamic properties of a DNA molecule [53]. Under the proper conditions, both bend and twist changes can be identified and quantitatively defined. The extreme sensitivity of this technique derives from the conditions required for a DNA molecule to circularize. To successfully ligate into a circle, a DNA molecule must:

- have ends that are in close proximity to one another,
- have helical axes that are nearly aligned at the ends, and
- be torsionally aligned such that the helical backbone is continuous at the site of the newly formed bond.

Changes in the first two, due to planar curvature, bending or anisotropic flexibility;[2] or the third, as a result of over- or under-winding and torsional stiffness, dramatically affect the overall rate of cyclization.

Cyclization experiments are often conducted in one of two ways. The first allows a DNA molecule, with self-complementary ends, to self-ligate and form either circles or polymers [54, 55]. The process is allowed to continue for long a period of time after which the circular and linear products are separated by two-dimensional gel electrophoresis. For each polymer size, the ratio of circles to linear

[2] Isotropic flexibility implies that the stiffness of the molecule is the same in all directions. An example would be a round broom handle. Anisotropic flexibility means that the stiffness properties are dependent upon the direction that the molecule is being bent. A flat plastic ruler, easily bent across the thickness but almost impossible to bend across the width, is an example of an anisotropically flexible structure.

products gives a qualitative measure of the probability of cyclization. The change in this ratio over the entire range of polymer sizes gives a relative measure of the cyclization properties of the DNA molecule with respect to other similarly constructed and tested DNA molecules. The method has several disadvantages. Since the measured linear products do not faithfully represent the amount of a specific size polymer that was, or was not, a substrate for further polymerization; no kinetic information, concerning the rates of cyclization or dimerization, can be obtained. In addition, it is not clear how, or if, these observations can be analyzed in a quantitative fashion to reveal the underlying characteristics of the DNA or the response of DNA to external forces. In Chapter III, an approach is developed to overcome these difficulties and this assay is used to qualitatively examine the effects of calicheamicin binding on DNA structure.

The second form of the circularization assay consists of a time course experiment in which a single DNA molecule is ligated under conditions which allow either circularization, dimerization or both to occur but limits further polymerization [56, 57]. The reaction is performed over a short period of time so that all the reaction products, and their relative proportions, can be identified and measured. As described in detail in Chapter IV, this allows the individual reaction kinetics to be determined and the probability of cyclization to be calculated for a specific DNA molecule under defined conditions.

The relationship between the probability of cyclization and changes in DNA trajectory or twist for a given molecule have been worked out using statistical mechanics and polymer chain theory [58]. Monte Carlo simulations have been used to extract twist and bend data from empirical determinations of the probability of cyclization over a range of conditions [56, 59, 60]. Therefore, with the proper experimental approach, it may be possible to precisely determine the structural changes occurring within a DNA molecule biochemically.

Fundamental to many of these calculations, is the assumption that the rate of bimolecular association is independent of the rate of cyclization [52]. In other words, if a DNA molecule is highly curved and cyclizes easily, the rate of bimolecular association is assumed to be the same as if it were a "straight" DNA that had little, or no, propensity to circularize. In performing these experiments, we observed that this may not be the case. In Chapter V, additional experiments are performed to determine whether DNA length and topology can affect intramolecular reactions. Regardless, by conducting experiments in which we incrementally change -- by the addition of drug -- the structural or dynamic characteristic of the same DNA

molecule, we will establish a benchmark for the validation of theoretical models predicting the dynamic behavior of DNA.

CHAPTER II

The Intrinsic Properties of Calicheamicin Binding Sites

As discussed Chapter I, there is evidence to suggest that calicheamicin targets DNA sequences that possess some form of a structural perturbation. In other words, is it possible that the drug has an affinity for a topological characteristic unique to specific DNA sequences. Since the nucleosome studies described in Chapter I indicate that calicheamicin-induced DNA damage is sensitive to DNA bending, it may be that the drug targets regions of DNA that are intrinsically curved. To test this hypothesis, an experiment was designed to qualitatively assess whether different calicheamicin binding sites possessed similar curvatures. While it may be important in some cases, the results shown here demonstrate that DNA curvature is not a necessary perquisite for calicheamicin binding.

Experimental Design

To determine whether calicheamicin binding sites are -- as a group -- intrinsically curved, we examined the migration of DNA polymers containing two different, but phased, calicheamicin binding sites on non-denaturing polyacrylamide gels. The studies are premised upon the anomalously slow migration of curved DNA sequences when compared to "straight" DNA of the same size [45, 47-50, 61, 62]. This behavior is thought to arise from the fact that a rigid, curved molecule has a larger enclosed volume or surface area which excludes gel fibers. This interferes with the ability of the curved DNA to reptate smoothly. In general, the greater the enclosed area the slower the DNA migrates. Therefore, long DNA molecules will migrate much more slowly than short molecules with an identical radius of curvature. As a result, small DNA bends can often be detected by repeating the bent sequences in-phase with the helical repeat of canonical DNA (10.5 bp) such that all

the bends occur in the same direction to form a longer DNA molecule with an observable degree of planar curvature.

To establish that any electrophoretic anomaly was the result of curvature at the calicheamicin binding sites, three duplex oligonucleotides were tested. The "in-phase" DNA construct, shown below, contained two calicheamicin binding sites, AGGA•TCCT [7] and ACAA•TTGT [35], spaced 10 base-pairs (bp) apart in a 21 bp DNA duplex.

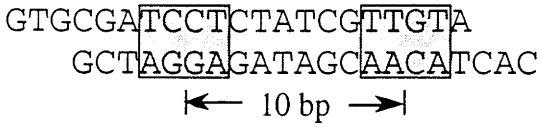

in-phase construct

These sequences have been shown to be high affinity binding sites for both calicheamicins γ_1^I and ε [33, 35]. At each site, the purine-rich sequence was positioned on the same strand to ensure that the aglycone portion of the drug molecule was at the 3' end with the oligosaccharide tail extending in the 5' direction across the recognition site [22, 23, 33]. When self-ligated, the 21 bp DNA monomer would form polymers with binding sites aligned -- on average -- with the 10·5 bp helical repeat of B-DNA. Since all the binding sites in the polymer were in-phase with each other, any small localized sequence-dependent curvature would add constructively, effectively magnifying a small localized bend into a planar macroscopic curve observable by polyacrylamide gel electrophoresis.

The three base pair CAC•GAG complementary ends of the DNA oligomers were designed to allow the cloning and preparation of large quantities of purified polymers. No other combination of two or three base pairs would allow integration of the polymer into a standard cloning vector without introducing an additional calicheamicin binding site at the junction between two monomers formed during self-ligation.

To verify the dependence of any observed DNA curvature on the calicheamicin binding sites, two additional constructs were tested. The "out-of-

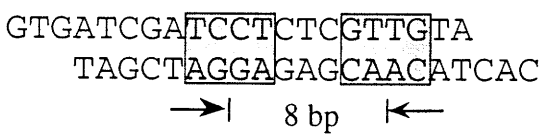

out-of-phase construct

phase " 21 bp duplex oligonucleotide has the same binding site sequences as the in-phase monomer except that they are now spaced 8 bp apart. If the calicheamicin binding sites were curved, then polymers formed from the self-ligation of this construct would form a 3-dimensional zig-zag or superhelical structure which would migrate more like "straight" DNA than the planar curved generated from the in-phase polymers.

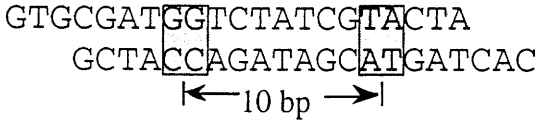

no-site construct

The "no-site" construct contains the same sequence as the in-phase DNA duplex except that the calicheamicin binding sites have been abolished by exchanging the central two base pairs on opposite strands. If polymers created by the self-ligation of this construct migrate normally, then any observed anomaly with the in-phase monomer must be the result of the intact calicheamicin binding sites and not curvature arising from adjacent sequences. (This is necessary since all the sequences are repeated every 21 bp and are therefore in-phase with each other.)

Two additional duplex oligomers served as positive and negative controls. When self-ligated, the A-tract monomer forms curved polymers that exhibit anomalous migratory behavior on polyacrylamide gels [54]. Conversely, polymers of the 10 bp *Bam*H I linker DNA have been used historically as a benchmark for "straight" DNA in gel mobility assays [49].

A-tract *Bam*H I linker

To verify that each of the above constructs contained the desired calicheamicin binding sites, damage studies were performed using calicheamicin γ_1^I on restriction fragments from cloned vectors containing polymers of the DNA monomer constructs.

Materials and Methods

Synthesis and purification of DNA oligonucleotides. DNA oligomers were either synthesized (391 DNA synthesizer from Applied Biosystems, all reagents from Biogenex) or purchased from Oligo's Etc. (Portland, OR). Synthesized oligomers (2 μmoles) were deprotected by an overnight incubation at 55°C in 1 ml of ammonium hydroxide, lyophilized and resuspended in 500 ml of water. All oligomers were purified by gel elution from 20% polyacrylamide sequencing gels [63] and desalted using C18 Sep Pack cartridges (Waters).

Construction of the pAS1 cloning vector. Plasmids containing DNA polymers of multiple monomer units were created by inserting polymers into a modified pUC19 cloning vector and transfecting the vector into a non-methylating *E. coli* host for culture. To modify the pUC19 vector for this purpose, the native *Sap* I site at 683 was removed by digesting pUC19 with *Tfi* I, gel purifying the larger DNA fragment and religating the vector (pUC19-Sap). The pUC19-Sap was prepared to accept the polymer constructs by inserting a new *Sap* I restriction site at the *Bam*H I site of the polylinker region as shown in Figure 2.1. The 24 bp insert contained a *Sap* I recognition element that would leave, after digestion, a GTG overhang at the 3' end and a CAC overhang on the 5' end. Since the insert was small and reading frame maintained, the ability of the new vector, pAS1, to α-complement was preserved.

Construction of pAS1/nmx plasmids. A family of clones containing the same monomer element "x" repeated "n" times was created by digesting pAS1 with *Sap* I, dephosphorylating the vector, and ligating in either gel purified polymers of a specific size or a mixture of polymers resulting from the self-ligation of monomers. The ligation was performed at micromolar duplex monomer concentrations for 4 minutes at 0°C to prevent further polymerization or cyclization of the polymers. The mixture of polymers was then ligated into *Sap* I-digested pAS1 at a molar ratio of 50:1, vector to polymer. GM2163 *E. coli* cells were transformed with the resulting vectors and the individual clones characterized by plasmid minipreps, DNA sequencing and gel electrophoresis [63, 64]. Particularly useful in this process was the modified mini-prep protocol developed by Lee and Suraiya [65]. The GM2163 strain was chosen since it is *dam* methylase deficient and can undergo α-complementation (NEB). Each clone was characterized by the type and size of the polymer insert. For example, a pAS1 vector containing a polymer of 12 repeated monomer elements of

the in-phase DNA duplex was named pAS1/12m9 (9 for in-phase, 10 for out-of-phase and 11 for no-site constructs). For larger quantities, plasmids containing the desired insert were grown under appropriate conditions for the host GM2163 cells (NEB fact sheet #316) with chloramphenicol to increase copy number and reduce contamination by genomic DNA [63]. Plasmid DNA was then extracted and purified using Qiagen Giga Preps.

Identification of calicheamicin binding sites. To verify the location of calicheamicin binding sites, specific cloned DNA constructs (*i.e.*, pAS1/5m9, pAS1/6m10 and pAS1/3m11) were digested with *Eco*R I, 5'-[^{32}P] end-labeled with T4 polynucleotide kinase and γ-[^{32}P]-ATP, purified on G25 Quick-spin Columns (Boehringer), and digested with *Hind* III [63]. The labeled fragment containing the insert was purified by elution from a 10% polyacrylamide gel [63]. Damage reactions consisted of labeled DNA (~50,000 cpm), 30 μg/ml of calf thymus DNA, calicheamicin γ_1^I (0-30 nM), 1% methanol, 10 mM glutathione, 50 mM HEPES, 1 mM EDTA, pH 7. The reaction was initiated by adding calicheamicin. After 1 hr at 0°C, the DNA was purified and resolved on an 8% sequencing gel.

Gel mobility assay. The electrophoretic migration studies on the DNA constructs were conducted as follows. Monomers were 5'-[^{32}P] end-labeled and ligated with T4 DNA ligase in a reaction containing 7·5 mM labeled monomer, 50 mM Tris-HCl (pH 7·8), 10 mM $MgCl_2$, 10 mM dithiothreitol, 1 mM ATP and 50 μg/ml bovine serum albumin. Ligase was added to a final concentration of 8 units/ml and the mixture was incubated overnight at 16°C. The DNA was extracted once with phenol/chloroform, precipitated in ethanol, and resolved by electrophoresis on an 8% non-denaturing polyacrylamide gel. Gels were then dried and subject to autoradiography or phosphorimager analysis (Molecular Dynamics).

Results and Discussion

Synthesis, cloning and purification of DNA constructs. In general, the cloning strategy worked well and a variety of plasmids containing different sized polymers of the three monomer inserts were created. Transformed cells showed a propensity for removing whole monomers from the polymer chain, converting from a pAS1/nmx to a pAS1/(n-1,2...)mx when cultured in large quantities. In some cases,

the vector would loose the entire insert. *E. coli* strains deficient in a variety of recombinant proteins fared worse that the GM2163 strain. In any case, the presence of multiple polymer sizes within a recovered plasmid sample had no effect on the damage assays.

Calicheamicin damage in DNA constructs. To ensure that the DNA constructs possessed the predicted binding sites, multimers of each monomer were damaged by calicheamicin γ_1^I and the cleavage products analyzed on sequencing gels. As shown in Figure 2.2, the mixed-site polymers were damaged only at the expected sites. Consistent with previous studies, damage at the AGGA site occurred more frequently than the ACAA site [24, 35]. The absence of a similar damage pattern in the no-site construct, under the same conditions, indicates that the primary binding sites have been abolished by the change in sequence. However, a closer look at Figure 2.2 does show the presence of one, perhaps two, low affinity binding sites at different locations.

If we assume that the frequency of drug-induced damage reflects the binding affinity of calicheamicin for these sequences then the drug binds the DNA oligomers as designed.

Calicheamicin binding sites are not intrinsically curved. To determine whether calicheamicin binding sites possessed any intrinsic curvature, each monomer was 5'-end labeled, self-ligated and resolved on an 8% non-denaturing polyacrylamide gel. From Figure 2.3, it appears that the binding site constructs migrated normally with respect to the *Bam*H I linker. As expected, the curved A-tract migrated much slower than similarly sized DNA in the adjacent lanes.

The mobility of these polymers relative to the *Bam*H I linker DNA can be quantitatively expressed as the ratio of the polymers apparent length to its true length (R_L). The apparent length is determined by measuring the migration distance of a specific DNA polymer and determining the length of "straight" DNA that would migrate the same distance. The following equation, describing the migration behavior of "straight" DNA, was derived empirically by finding the best fit to the *Bam*H I Linker data ($R^2 > 0{\cdot}995$, see Figure 2.4; least squares analysis performed in Cricket Graph by Cricket Software).

$$\ln(X) = 6{\cdot}41 + 0{\cdot}29 \ln(MW) \qquad (2.1)$$

where X is the migration distance in centimeters and MW is the molecular weight of the polymer. Rearranging and assuming the molecular weight of each base pair is 650g/mole, gives the following equation for the apparent length (in base pairs) of a DNA polymer migrating X (cm) on the gel:

$$AL_{bp} = (6.13 \times 10^{6})\, X^{-3.45} \qquad (2.2)$$

Dividing equation 2.2 by the true length of the polymer, gives the R_L value for that specific DNA molecule. The R_L values for the polymers shown in Figure 2.3 are plotted in Figure 2.5.

None of the binding site constructs exhibited significant migration anomalies relative to a "straight" DNA standard [66]. These results stand in striking contrast to the abnormally slow migration of the A-tract. These data suggest that neither in-phase, out-of-phase or no-site constructs possess a significant degree of intrinsic curvature. This does not, however, rule out the possibility that calicheamicin targets curved or bent DNA. Therefore, it can only be concluded that two of the DNA sequences recognized by calicheamicin are not curved and that DNA curvature is not necessary for calicheamicin binding. It is important to note that these results do not preclude the possibility that other sequence dependent properties such as flexibility or twist are responsible for calicheamicin target recognition.

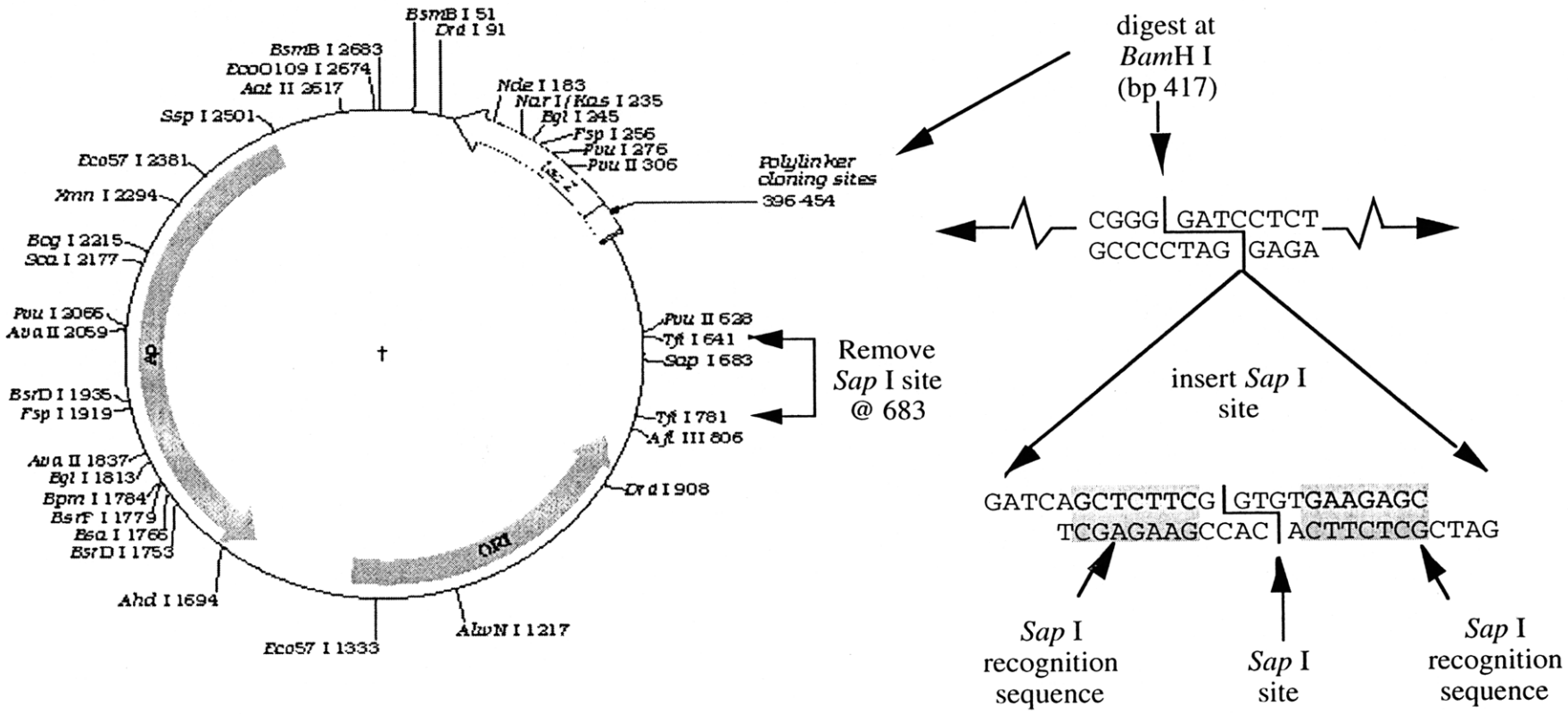

Figure 2.1. Synthesis of the pAS1 cloning vector. pUC19 was digested with *Tfi* I and religated to remove the existing *Sap* I site at 683. The 24 bp sequence, shown on the right, was then inserted into the polylinker cloning region at the *Bam*H I site; creating two new *Sap* I sites with recognition sequences on both sides of the shared restriction site.

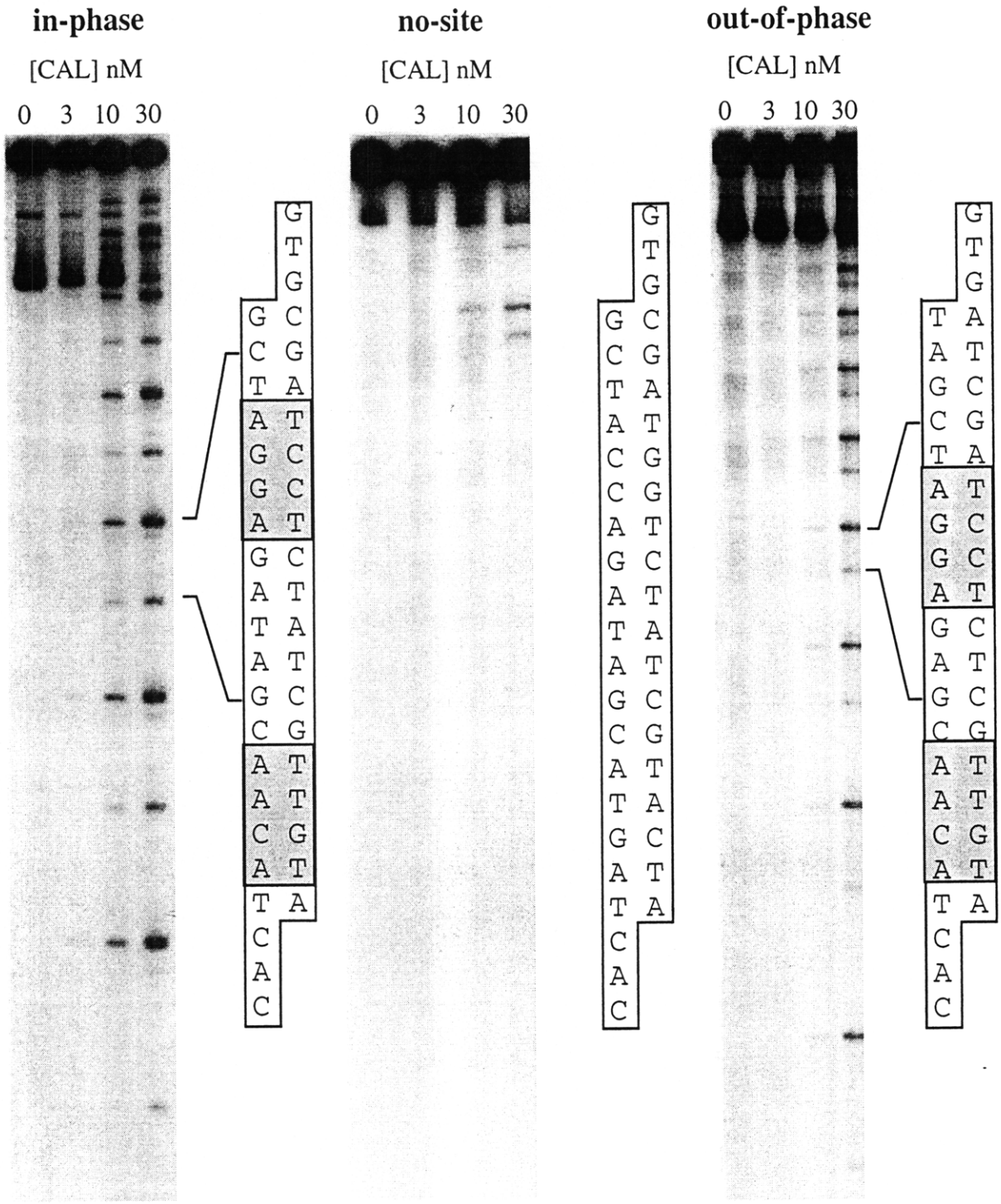

Figure 2.2. Damage produced by calicheamicin γ_1^I in the binding site constructs. Cloned polymers of each monomer were end-labeled, treated with calicheamicin γ_1^I (0-30 nM) and resolved on sequencing gels. Sequence diagrams, indicating the location of the damage sites in each of the constructs are shown to the right.

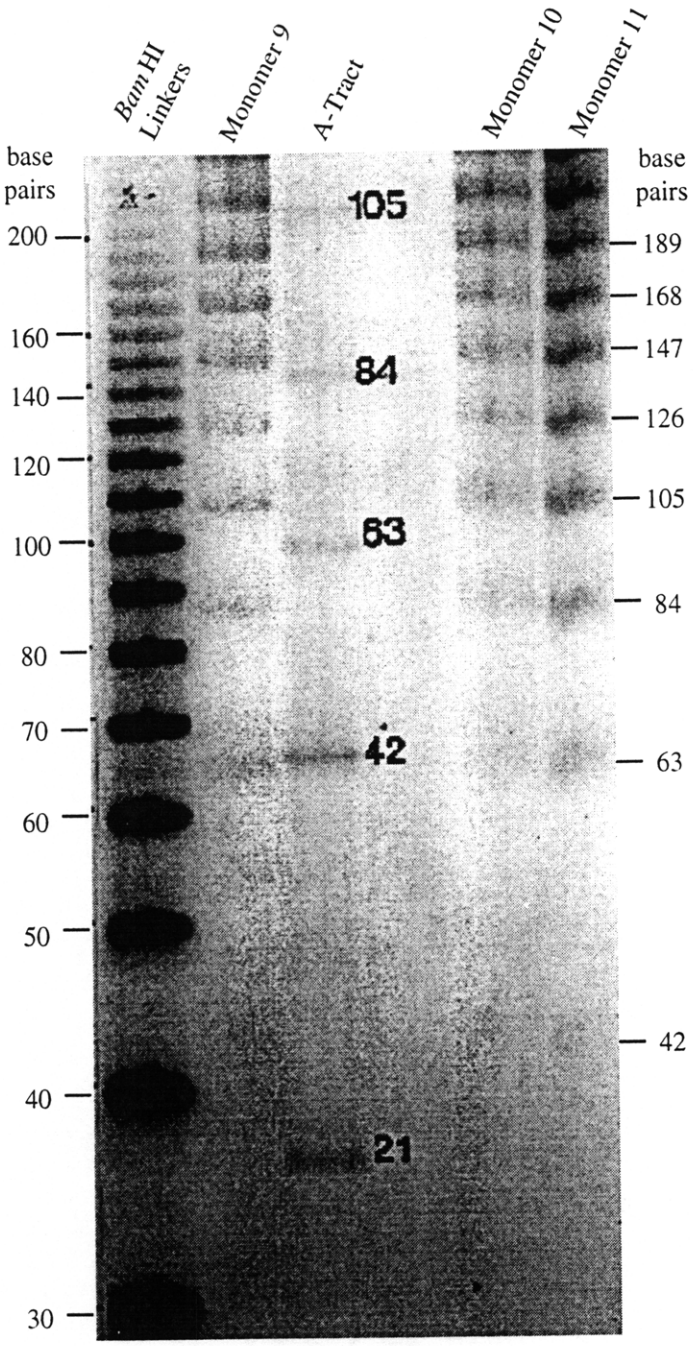

Figure 2.3. Gel migration of polymerized DNA constructs. Monomers were end-labeled, self-ligated and resolved on an 8% non-denaturing gel. *Bam*H I linker represents a "straight" control whereas the A-tract is known to polymerize into a molecule exhibiting planar curvature. The actual lengths for the polymers are shown, in base pairs, in the margins.

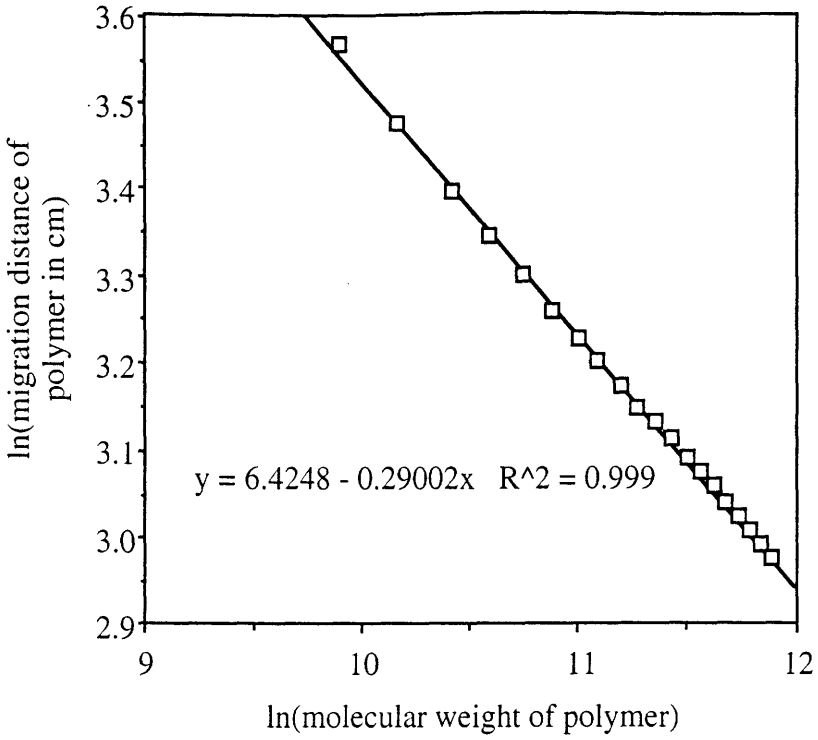

Figure 2.4. Curve fit of *Bam*H I linker data.

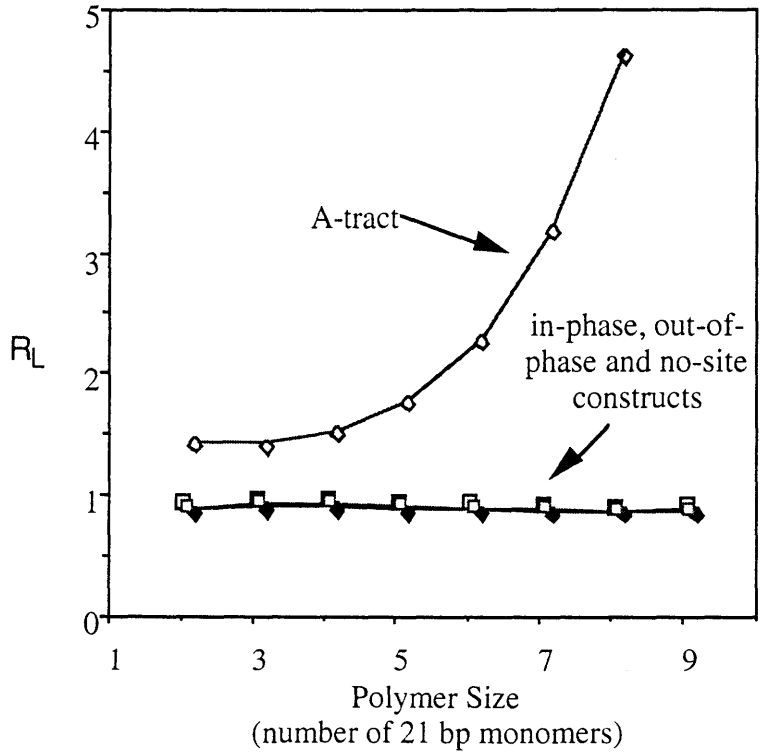

Figure 2.5. R_L values for the in-phase, out-of-phase, no-site and A-tract. The R_L value reflects the relative migration of the DNA compared to a "straight" standard.

CHAPTER III

The Effects of Calicheamicin Binding on DNA Topology

DNA is a chain-like structure whose mechanical properties are governed by the hydrophobic and electrostatic forces acting between its individual elements. The balance of these forces determines the overall trajectory, or shape, of the molecule while their interaction defines how the structure will respond to its external environment. In other words, like a solid bar, DNA has properties of form (*i.e.*, curvature and twist) and function (*i.e.*, lateral and torsional stiffness).

As discussed in Chapter I, there is evidence to suggest that calicheamicin selects its targets based -- at least in part -- on the topological characteristics of the binding site. In Chapter II, however, data were presented to show that DNA sequences bound by calicheamicin are not necessarily curved. To 1) explore this apparent inconsistency and 2) further understand the role of DNA flexibility in the target selection process, experiments were performed to investigate the changes that occur in DNA structure when calicheamicin binds. By finding what, if any, topological changes occur when the drug binds, we may be able to infer the sequence dependent properties that facilitate drug binding.

Experimental Design

As described in Chapter I, the biochemical methods for looking at DNA structure are rather limited. Measuring the changes in electrophoretic mobility of drug bound DNA can reveal drug-induced changes in DNA structure. However, the extreme hydrophobicity and weak binding affinity of calicheamicin for DNA make this approach difficult. The T4 ligase DNA cyclization assay, described in Chapter I, overcomes these problems and provides greater detection of drug-induced structural changes. The assay can be run under a wide variety of conditions and, because it relies on circle closure, is much more sensitive to bend and twist changes.

To determine whether a particular sequence is curved, bent or anisotropically flexible by DNA circularization, the sequence of interest is repeated in-phase with the helical repeat of B-DNA and the probability of the molecule forming a circle measured with respect to a random sequence DNA molecule of the same length. The propensity of these DNA molecules to form circles is then measured by "trapping" transiently cyclized products with T4 DNA ligase to form covalently closed circles which can then be separated from uncircularized reaction products [49, 52, 54, 57]. (The ends are "transiently" joined by non-covalently hydrogen bonding between complementary bases.) The proper phasing of the binding sites ensures that the structural changes at each site add constructively to magnify their individual effects. If the in-phase binding sites are bent, then the DNA molecule will curve in a plane and the ends will move closer together, thus increasing the probability of non-covalent binding of the ends and therefore, the number of covalently closed circles.

As discussed in Chapter I, factors other than bending can affect the rate of circle formation. They are:

1) *Molecule length* - Longer molecules possess greater intrinsic flexibility making it easier to bring the ends close together.
2) *End sequence* - Both the length and sequence of the complementary ends affect the association and disassociation rates of non-covalently closed DNA circles. Longer, or G•C rich, sequences promote non-covalent binding over shorter, or A•T rich, sequences.
3) *End Alignment* - When the phosphate backbones are aligned, hydrogen bonding occurs easily and facilitates covalent closure. Ends out-of-phase by ninety degrees hydrogen bond with much lower frequency and therefore, form fewer circles. This is not the case for long pieces of DNA (approximately 250 bp and larger) where an accumulation of torsional flexibility throughout the chain effectively decouples the rotational position of one end from the other. As a result, the sensitivity of DNA circularization to twist changes within the molecule decreases with increasing molecule length.

Each of these factors must be considered in both the design and interpretation of DNA cyclization experiments.

To assess the bend and twist changes that occur in DNA when calicheamicin binds, circularization studies were performed on the in-phase and out-of-phase DNA duplexes described in Chapter II. The oligomers were annealed with their

complementary strands, radiolabeled and polymerized with T4 DNA ligase under conditions that allowed circles to form once the DNA molecules had reached a reasonable length. Since components of the ligation reaction buffer activated calicheamicin into the DNA-damaging diradical species, the experiments were performed with calicheamicin ε, an inactive form of the drug. While the two compounds bind DNA at the same sequences [33], calicheamicin ε appears to bind with 10- to 15-fold lower affinity [67].

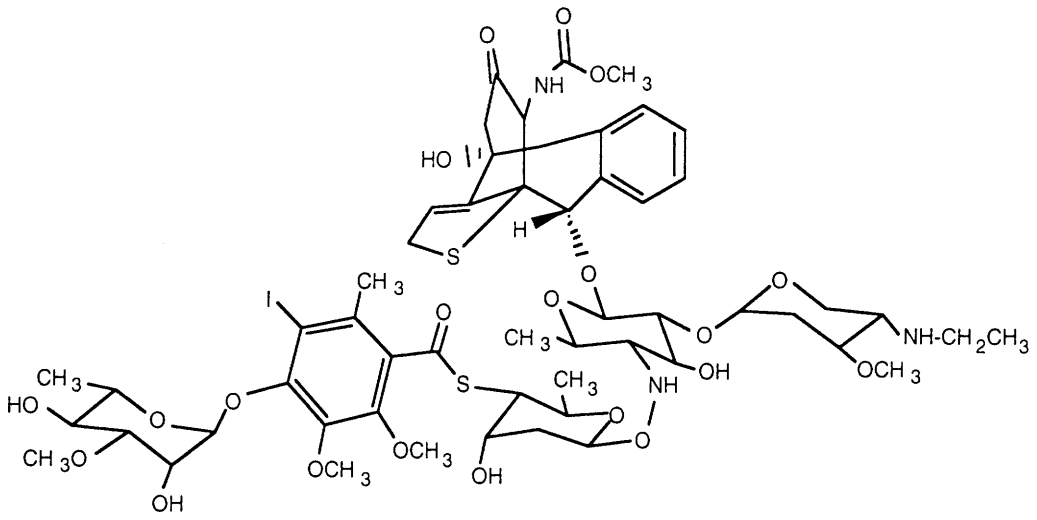

calicheamicin ε

To assess qualitatively the effects of calicheamicin binding on DNA structure, circularization experiments were performed with both the in-phase and out-of-phase DNA constructs over a broad range of drug concentrations. The reactions were repeated with the oligosaccharide portion of calicheamicin to determine which component of the parent compound was responsible for any observed effects.

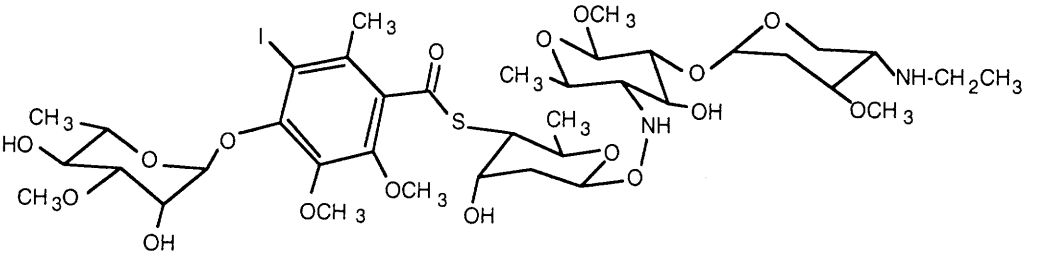

oligosaccharide (aryltetrasaccharide)

The circular reaction products were resolved by gel electrophoresis using a novel approach that obviated the need for two-dimensional electrophoresis. Identification

of individual circle sizes was accomplish by recovering and denaturing putative circular DNA prior to gel electrophoresis.

Seminal to the interpretation of any result, was the assumption that the relative proportion of calicheamicin binding between the two sites was the same for both the in-phase and out-of-phase DNA constructs. In other words, did moving the binding sites closer together, from 10 to 8 bp apart, cause binding at the higher affinity site to inhibit drug binding at the second site (negative cooperativity). The damage studies performed in Chapter II with calicheamicin γ_1^I did not rule out this possibility since the reactions were carried out under single-hit conditions. To address this issue, a second series of damage studies were performed with calicheamicin θ, a calicheamicin analog with a thioacetate trigger instead of a methyltrisulfide [68].

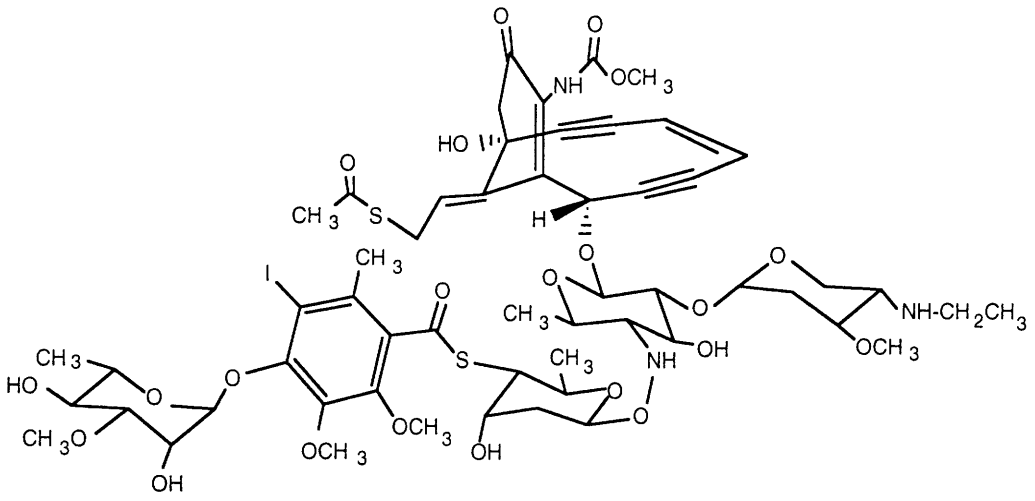

calicheamicin θ

With calicheamicin θ, it was possible to measure drug-induced DNA damage over a broad range of drug concentrations by titering the amount of glutathione activator so that similar levels of DNA damage were produced, even under saturating amounts of drug. If the no-cooperativity assumption was false, then at high calicheamicin concentrations the relative proportion of damage between the two binding sites would change.

Materials and Methods

Reagents and DNA substrates. Calicheamicins γ_1^I and ε were provided by Dr. George Ellestad (Wyeth Ayerst Research) or synthesized as described below; calicheamicin θ and the aryltetrasaccharide were provided by Prof. K.C. Nicolaou (Scripps Research Institute). All enzymes were obtained from New England Biolabs. Deoxyoligonucleotides were prepared as described in Chapter II.

Synthesis and purification of calicheamicin ε. Calicheamicin ε was synthesized using a protocal provided by Dr. George Ellestad (Wyeth Ayerst Research): 1 mg of calicheamicin γ_1^I in 330 µl EtOH was diluted with 330 µl of 0·5 M Tris-HCl (pH 7·5). The reaction was initiated by adding 330 µl of 0·5 M methyl thioglycolate (in EtOH) and stirred at room temperature for 2 hours. The reaction products were separated by HPLC using a linear gradient of 42·5 mM triethylamine (pH 6·0) in 15% acetonitrile to 20 mM triethylamine (pH 6·0) in 60% acetonitrile over 25 minutes. The peaks, shown in Figure 3.1, were collected, lyophilized and resuspended in 100% MeOH at 400 µM. Calicheamicin ε was verified by TLC and the concentration of the stock solution was determined by UV absorbance at 280 nm; ε_{280} = 11,536 $M^{-1}cm^{-1}$ [69].

DNA damage studies with calicheamicin θ. Cloned plasmids for the pAS1/13m11 were prepared as described in Chapter II, digested with *Xba* I and 5'-[^{32}P] end-labeled. Following digestion with *Eco*R I, the labeled fragment was purified by elution from an 8% polyacrylamide gel. Damage reactions consisted of labeled DNA (~30,000 cpm), 30 µg/ml of calf thymus DNA, 10 mM glutathione, 10 mM HEPES, 1 mM EDTA (pH 7). The reaction was initiated by adding calicheamicin θ and then glutathione as follows:

[Calicheamicin θ]final	[GSH]final	Incubation Time
0·1 µM	10 mM	1 hour
1 µM	10 mM	1 hour
10 µM	1 mM	1·5 hours
100 µM	0 mM	overnight

After incubation for the appropriate time at 37°C, the DNA was ethanol precipitated and resolved on a 6% sequencing gel. Bands were quantified by phosphorimager analysis.

DNA ligation experiments. The labeling and ligation reactions to produce circular DNA molecules from monomer substrates were performed as follows. Equal quantities of complementary oligomers were mixed and heated to 75°C and brought slowly to room temperature. Annealed DNA (1·4 μg) was 5'-end labeled in a 40 μl reaction with 450 μCi of γ-[^{32}P]-ATP (≈6,000 Ci/mmole) and 20 units of T4 polynucleotide kinase (NEB) in standard reaction buffer for 2 hrs at 37°C. The DNA was extracted with phenol/chloroform and purified on G25 Quick-spin Columns (Boehringer). The DNA was then quantified by UV absorption.

The ligation reaction was carried out in 50 μl of NEB T4 DNA ligase reaction buffer with 120 ng of radiolabeled DNA, 4% methanol, the appropriate concentration of calicheamicin ε or oligosaccharide (added in the methanol) and 400 units of T4 DNA ligase at 16°C overnight. The DNA was then extracted with phenol/chloroform and precipitated in ethanol. The reaction products were resolved by two- or one-dimensional electrophoresis as described below.

Resolving circular reaction products by two-dimensional gel electrophoresis. Two dimensional gel electrophoresis was performed to resolve circular DNA products. The DNA was resolved on an 8% non-denaturing polyacrylamide gel for approximately 2,700 V·Hrs. The gel was marked and placed for autoradiography so that the lane with the bands of interest could be located. A 3 cm x 25 cm gel slice, containing the DNA, was excised and placed at the top of a fresh set of plates. A second 8% non-denaturing polyacrylamide gel containing 50 μg/ml chloroquine was cast around the gel slice. The DNA was then run in the second dimension for approximately 2,700 V·hrs in TBE containing 50 μg/ml chloroquine. The gel was then dried and subject to autoradiography and/or phosphorimager analysis.

Resolving circular reaction products by one-dimensional gel electrophoresis. Visualization of circularized DNA products by one-dimensional electrophoresis was accomplished by first digesting the linear DNA with BAL-31. The DNA ligation reaction was carried out as described above and the DNA extracted with phenol/chloroform, precipitated in ethanol and then digested with BAL-31 using 1 unit per 120 ng of duplex DNA substrate for 1 hour at 30°C. The reaction was

stopped by adding EGTA to a final concentration of 20 mM and the DNA extracted with phenol/chloroform and ethanol precipitated prior to electrophoresis on either an 6 or 8% non-denaturing polyacrylamide gel.

Verification of DNA circle sizes. The nature and size of the putative circular DNA was established by denaturing gel electrophoresis. The bands remaining after BAL-31 digestion were excised, the DNA eluted from the gel slice, denatured by heating at 90°C for 5 minutes and then resolved on an 8% denaturing polyacrylamide gel containing 6M urea.

Quantitative analysis of reaction products. The ligation products were analyzed by phosphorimager analysis on a Molecular Dynamics Phosphorimager with ImageQuant software. The mathematical operations, described below, were performed in Microsoft Excel (MicroSoft), KaleidaGraph (Abelbeck Software) or Cricket Graph (Cricket Software).

Results and Discussion

Calicheamicin binding does not inhibit drug binding at adjacent sites. To verify that calicheamicin binding at one site did not interfere with binding at an adjacent site, we performed a second series of damage studies with calicheamicin θ, a calicheamicin analog with a thioacetate trigger instead of a methyltrisulfide [68]. In addition to activation by glutathione, the thioacetate moiety can undergo hydrolysis that also leads to a rearrangement of the aglycone to the reactive diradical species [68]. However, unlike direct activation, spontaneous hydrolysis of calicheamicin θ is a slow process when compared to formation of the drug-DNA complex. Therefore, using calicheamicin θ, it was possible to measure drug-induced DNA damage over a broad range of drug concentrations by titering the amount of glutathione activator so that similar levels of DNA damage were produced across a broad range of drug concentrations. If drug binding at the two closely spaced sites were inhibited, then we would expect to see a change in the relative proportion of damage occurring at the two sites at high drug concentrations.

Figure 3.2 shows the damage produced by calicheamicin θ in the out-of-phase construct over a broad range of drug concentrations. In the range of drug concentrations tested (1-100 μM), the ratio of calicheamicin θ-induced DNA damage

at neighboring binding sites was the same (approximately 3·5:1). Similar data were obtained for the in-phase DNA (data not shown). These results indicate that, even at high concentrations, calicheamicin binds without any difference in cooperativity between the binding sites in the in-phase and out-of-phase constructs. This is consistent with hydroxyl radical footprinting studies [33], and the calicheamicin γ_1^I damage studies described in Chapter II, which show that the ratio of damage between the two sites is the same for the in-phase and out-of-phase substrates.

From these results, we can conclude that calicheamicin binds equally well to the in-phase and out-of-phase DNA constructs and that negative cooperativity does not occur at high drug concentrations.

An improved method for the rapid assessment of circular DNA reaction products. Historically, two-dimensional gel electrophoresis has been the standard technique for resolving small circular DNA from linear DNA of the same size [54]. The method requires two gels. The first, is a standard polyacrylamide gel that separates all the reaction products by molecular weight. After the products are resolved in a single column, the strip of gel containing the DNA is removed and placed atop a second gel impregnated with a DNA intercalator such as chloroquine. The chloroquine supercoils the circular DNA, changing its electrophoretic mobility with respect to linear DNA of the same size. As a result, the second gel separates the two reaction products. An example of a two-dimensional polyacrylamide gel is shown in Figure 3.3.

To resolve circular DNA products formed under a broad range of reaction conditions would require two gels for each individual drug concentration and substrate tested; literally, fifty or more gels. Shore *et al.* [52] have addressed this issue by using mung bean nuclease to remove the [^{32}P]-labeled overhangs from linear DNA polymers. Unfortunately, the polymers used here have multiple radioactive phosphates throughout the linear DNA that are inaccessible to the enzyme.

Crothers suggested using the BAL-31 nuclease to distinguish between circular and non-circular DNA [53, 70, 71]. BAL-31 is an is an extremely stable enzyme which degrades both single- and nicked double-stranded DNA. On double-stranded molecules, the enzyme acts exonucleolytically from both the 3' and 5' ends [72, 73]. Therefore, uncyclized DNA (since it has ends that are accessible to the enzyme) are digested processively into smaller and smaller pieces. We have developed this technique by optimizing the reaction conditions so that BAL-31 removes nearly all

the linear polymers. After removing unincorporated nucleotides, the remaining DNA circles can be resolved by one-dimensional gel electrophoresis.

An example of the T4 ligase/BAL-31 technique applied to the in-phase calicheamicin binding site oligonucleotide is shown in Figure 3.4. In the absence of BAL-31 digestion, an intense ladder of linear polymers extends into the region of the gel containing circular DNA bands. However, BAL-31 digestion resulted in a reduction of linear DNA fragments by more than 10-fold relative to circles. The identity of the DNA bands was verified as described in the *Materials and Methods* section.

To establish that the population of DNA circles remaining after BAL-31 digestion faithfully reflected the original population, we examined the distribution of circle sizes as a function of both BAL-31 concentration and digestion time. Figures 3.5 and 3.6 show the change in products over a range of digestion conditions. In all cases, the distribution of circle sizes did not change as a function of digestion time or BAL-31 concentration, even though -- as expected -- the intensity of the circular DNA bands was reduced in the longer digestions (Figure 3.4).

Our findings suggest that BAL-31 digestion is an effective method for distinguishing circular from linear DNA. The procedure obviates the need for two dimensional electrophoresis, allowing multiple samples to be analyzed on one gel.

Calicheamicin ε bends DNA. To investigate the effect of calicheamicin binding on DNA structure, the in-phase DNA construct was polymerized under conditions that facilitated circle formation. The general conditions for these reactions are summarized in Table 3.1. After ligation, the DNA was digested with BAL-31 and the reaction products resolved by one dimensional electrophoresis on eight percent polyacrylamide (Figure 3.7). Bands corresponding to putative DNA circles were excised and eluted, denatured, and separating the products by denaturing gel electrophoresis. When denatured, double stranded circles convert to three products; catenanes, single stranded circles and linear DNA. Circle identification using this method is shown in Figure 3.8.

To assess the effect of drug binding, the amount of radioactivity in each band was quantified by phosphorimager analysis and normalized according to its corresponding circle size. The percentage of a specific circle size was then calculated by dividing the normalized radioactivity by the sum of the normalized radioactivity for all the circles measured. (See Table 3.2 for an example.)

As shown in the gel in Figure 3.7 and graphically in Figure 3.9, the distribution of circles formed shifts towards smaller circle sizes as drug concentration is increased. This can be seen more clearly in Figure 3.10, which is a plot of the mean of the individual circle distributions for two separate cyclization experiments with the in-phase monomer.

Three factors could account for the observed reduction in mean circle size for the in-phase construct:

- Binding of calicheamicin to sites in-phase with the helical repeat of B-DNA may introduce a planar bend, bringing the ends of the polymer closer together increasing the probability of cyclization.
- Calicheamicin binding may twist the DNA and alter the helical repeat such that the ends are moved into progressively better alignment as more and more the drug binds.
- Calicheamicin may act in a sequence independent manner to affect the rate of cyclization.

To address the last two possibilities, we repeated the cyclization experiment with the out-of-phase DNA construct. If the second scenario were true, then the out-of-phase construct would respond identically to the in-phase monomer since the effects of DNA twisting on the relative position of the ends does not depend on where in the molecule the twisting occurs. We would also expect the out-of-phase construct to respond like the in-phase monomer if the drug affected cyclization regardless of sequence.

The response of the out-of-phase construct to calicheamicin binding is shown in Figures 3.11 through 3.14. Unlike the in-phase monomer, the out-of-phase construct shows relatively little reduction in mean circle size as calicheamicin ε concentration increases. In other words, the change in the cyclization properties of the in-phase construct cannot be attributed -- solely -- to a twisting of the helix or some other sequence independent phenomena.

The small shift in the mean circle size for the out-of-phase construct may be the result of different binding affinities between the two sites, incomplete cancellation of the bend components or some degree of twist. Unfortunately, the sensitivity of our assay to twist is reduced due to the 3 bp overlap of the complementary ends in the DNA polymers [53]. However, since a significant calicheamicin-induced reduction in circle size was apparent only with the in-phase constructs, we can conclude that the majority of the change observed in the

cyclization properties must be a response to bending and not twisting. Given these observations, we conclude that DNA is bent in response to calicheamicin ε binding.

The oligosaccharide of calicheamicin ε bends DNA. The mean circle size assay was repeated using the in and out-of-phase DNA constructs over a wide range of oligosaccharide concentrations. The results are shown in Figure 3.15. The mean of the circle size distributions for both DNA constructs decreases with increasing oligosaccharide concentrations. The change is greatest for the in-phase construct which shows a decrease in mean circle size from 10 to 8·5. From these results, we can conclude that the oligosaccharide binding -- alone -- is sufficient to modify DNA structure. Whether this change in structure is a bend or twist remains unclear.

Several factors could account for the observed shift in the out-of-phase construct. First, since the oligosaccharide does not bind at "exactly" the same site as the parent drug, the shift could result from the oligosaccharide binding the in-phase construct slightly out-of-phase and the out-of-phase construct partially in-phase. This would reduce the shift seen in the in-phase construct and increase the shift in the out-of-phase construct. Second, the oligosaccharide may have a greater affinity for one binding site over the other. This would reduce oligosaccharide binding at sites out-of-phase with the high affinity site; thereby increasing the in-phase bending in the out-of-phase construct. Last, the oligosaccharide may be twisting rather than bending the DNA. This would mean that the aglycone suppresses this action in the parent drug and that our assay is sensitive enough to detect these changes. In any case, the oligosaccharide clearly introduces large structural perturbations into the DNA structure.

Estimating the degree of calicheamicin-induced DNA bending. Assuming that the bending stiffness of DNA is independent of the degree of flexure, we can roughly estimate the amount of calicheamicin-induced DNA bending by comparing the mean circle size of the bound and unbound DNA monomers.

The bending required to bring the ends of a DNA molecule together to form a circle can be determined by approximating the shape of the bent DNA polymer as an "n" sided regular-polygon. This assumes that all the bends are of the same magnitude and are equally spaced along the chain. From the figure below, the angle

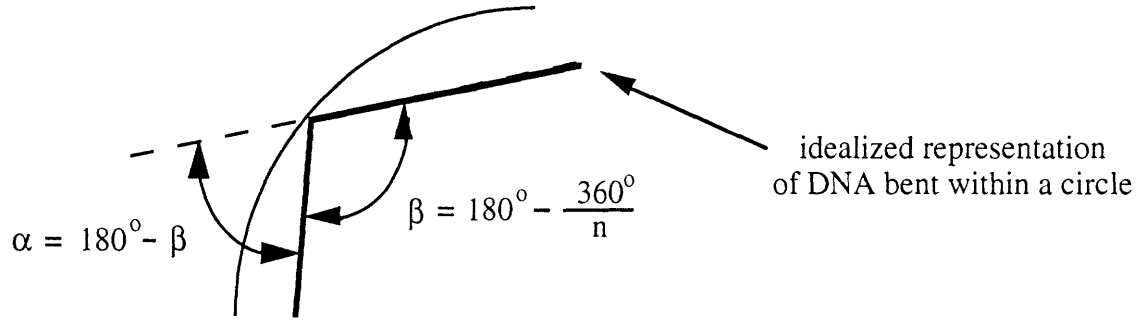

enclosed by two sides of a regular-polygon, β, is equal to

$$180^{\circ} - \frac{360^{\circ}}{n}$$

where n represents the number of bends in the perimeter of the polygon. The bend angle with respect to a local tangent, α, is $180^{\circ} - \beta$. Therefore,

$$\alpha = 180^{\circ} - \left[180^{\circ} - \frac{360^{\circ}}{(\text{number of bends})}\right].$$

As seen in Figures 3.11 and 3.12, even linear, as opposed to bent, DNA will form circles. The reason is that each base-pair has some freedom to move (*i.e.*, flexibility), which allows the molecule to bend in response to external forces. As the DNA chain lengthens, this intrinsic flexibility accumulates to the point where the random dynamic motions of the molecule brings the ends of the DNA close enough together to ligate. This "intrinsic flexibility" of the DNA polymer must be accounted for to reasonably estimate calicheamicin-induced DNA bending.

Based on the circle sizes observed for the in-phase monomer without calicheamicin (Figure 3.12), it appears that circles formed are arranged in a Gaussian distribution whose average behavior is well represented by the mean. If we model this "mean circle" as a regular-polygon where the circumference equals the perimeter, and each base-pair represents a bend, then we can calculate the per base-pair flexibility for the in-phase monomer under our experimental conditions. In this case,

$$\alpha_f = 180^{\circ} - \left[180^{\circ} - \frac{360^{\circ}}{\text{number of base-pairs in the mean circle}}\right], \text{ or}$$

$$\alpha_f = 180^\circ - \left[180^\circ - \frac{360^\circ}{\text{MCS x 21 (base pairs per monomer)}}\right] = \frac{360^\circ}{\text{MCS x 21}}$$

where α_f is the average bend angle due to intrinsic flexibility and MCS is the mean circle size in monomer units. Substituting the mean circle size for the in-phase monomer without calicheamicin,

$$\alpha_f = \frac{360^\circ}{9{\cdot}92 \times 21} = 1{\cdot}73^\circ$$

That is, each base-pair can -- on average -- bend 1·73 degrees without calicheamicin.

When the ligated monomers were bound by calicheamicin ε the mean circle size dropped from 9·92 to 7·98. The overall bending experienced by the DNA polymer is the sum of drug-induced bending and intrinsic flexibility. In other words,

$$\text{total bending} = 360^\circ = \alpha_f \times (\text{total number of base pairs}) + \alpha_{cal} \times (\text{number of calicheamicin binding sites})$$

where α_{cal} is the bending that occurs at each drug binding site. Therefore,

$$\alpha_{cal} = \frac{360^\circ - (\alpha_f \times \text{total number of base pairs})}{(\text{number of calicheamicin binding sites})}, \text{ or}$$

$$\alpha_{cal} = \frac{360^\circ - (1{\cdot}73^\circ \times \text{MCS} \times 21)}{2 \times \text{MCS}} = \frac{360^\circ - (1{\cdot}73^\circ \times 9{\cdot}92 \times 21)}{2 \times 9{\cdot}92} = 4{\cdot}4^\circ$$

That is, the bending introduced at each calicheamicin ε binding site can be estimated at 4·4 degrees.

This result is probably an overestimate of the actual bend angle since the original assumption is likely untrue. In fact, the change in the shape of the circle distributions as the mean circle size decreases, Figure 3.9, suggests that the flexibility of the DNA becomes more and more anisotropic at small circle sizes. This result implies a stiffening of the molecule as the DNA becomes more bent. However, since the DNA molecule has many degrees-of-freedom that may accommodate

conformational changes at relatively no energetic cost, the approximation may be reasonable over a small range of mean circle sizes and our estimate, not too far off.

A second assumption was that each calicheamicin-induced bend was identical in location, direction and magnitude. Given the wide variety of sequences recognized and the unique structural characteristics that each must have, this may not be the case. It is likely that different sequences respond uniquely to calicheamicin binding; some may bend a lot, some a little. Regardless, the bend of 4·4 degrees may prove useful in evaluating specific models of calicheamicin binding.

Mathematically modeling the change in mean circle size. The change in the mean circle size in response to calicheamicin ε binding to the in-phase DNA construct bears a strong resemblance to a standard titration curve. As a result, it may be possible to extract quantitative data about the drug-DNA binding relationship.

Assuming that calicheamicin-DNA binding can be described by

$$[B] + [CAL] \xrightarrow{k_a} [B\text{-}CAL]$$

where [B] is the concentration of binding sites, [CAL] the concentration of calicheamicin ε, [B-CAL] the concentration of bound calicheamicin ε, or occupied binding sites, and

$$k_a = \frac{[B\text{-}CAL]}{[B]\,[CAL]},$$

it can be shown that the amount of bound calicheamicin is described by

$$[B\text{-}CAL] = [CAL]_T - \left(\frac{-b + \sqrt{b^2 - 4c}}{2}\right) \qquad (3.3)$$

where $b = [CAL]_T - [B]_T + \frac{1}{k_a}$, $c = -\frac{[CAL]_T}{k_a}$ and the subscript T refers to total -- known -- concentrations. If we make the extremely simplistic assumption that drug binding and the change in mean circle size are directly proportional, then

$$m = m_{ul} + \left(\frac{m_{ll} - m_{ul}}{100}\right) x \left(\text{percentage of occupied binding sites}\right) \qquad (3.4)$$

where m is the mean circle size at a specific drug concentration and m_{ll} and m_{ul} are the lower and upper limits on the mean circle size respectively. Since the percentage of occupied binding sites is $[B\text{-}CAL]/[B]_T$, then

$$m = m_{ul} + d\left\{\frac{[CAL]_T}{[B]_T} - \frac{1}{[B]_T}\left(\frac{-b + \sqrt{b^2 - 4a}}{2}\right)\right\} \qquad (3.5)$$

where d is $(m_{ll} - m_{ul})/100$.

The above equation was fit to the data for the in-phase monomer optimizing the values of K_a and d to minimize the least square error using a Levenberg-Marquardt algorithm (KaleidaGraph). The results are shown in Figure 3.16. Interestingly, the estimate of the binding constant K_a is reasonable. The value of $4 \times 10^5\ M^{-1}$ is approximately half of that estimated for calicheamicin and approximately 7 times the binding constant for calicheamicin ε estimated by Chatterjee *et al.* [67] and Krishnamurthy *et al.* [42].

In the above derivation, many assumptions were used to simplify an extremely complicated behavior. It is unlikely that calicheamicin binding can be described by the model proposed and even less probable that the change in mean circle size is directly proportional to drug binding. A more rigorous approach would include nearest neighbor effects in the binding equation and develop a non-linear model for the variation of mean circle size with calicheamicin binding. Regardless, the results are reasonable enough to suggest that it may be possible to accurately determine binding constants from a DNA cyclization experiment.

Using the mean of the circle size distribution as a measure of the ring closure probability. While useful as a qualitative indicator of DNA behavior, is it possible that the distribution of circles in a ligation experiment provides a meaningful measure of the cyclization properties of the DNA substrate. In other words, how does the mean circle size relate to the actual kinetics of cyclization?

In the T4 ligase catalyzed cyclization experiments performed here, individual monomers polymerize until they reach a size where cyclization is favored over further polymerization. It is a complicated series of reactions involving molecules of many sizes cyclizing at different rates. An examination of the reaction products at a single point in time does not allow a determination of how fast an individual DNA polymer is converted to a circular or higher-order polymer product.

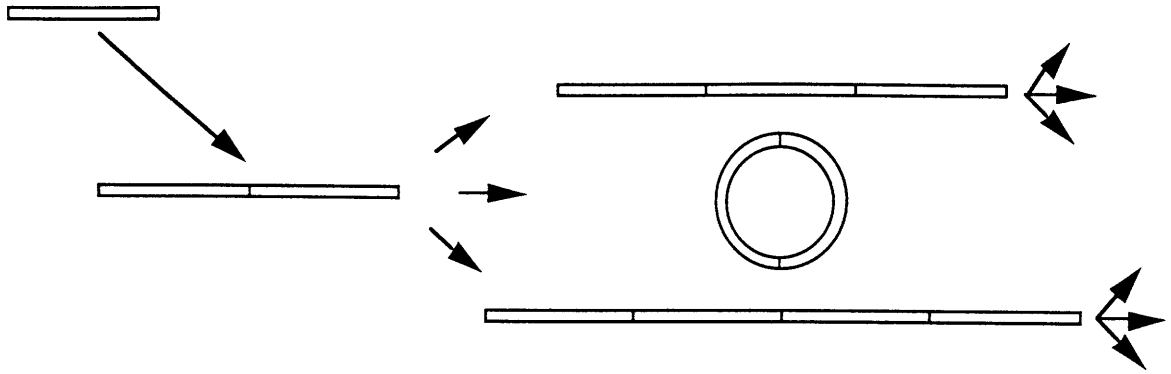

As a result, a true measure of the ring closure probability -- the ratio of the two equilibrium constants for the cyclization and dimerization reactions -- cannot be determined for a specific DNA molecule in the reaction. These experiments do, however, suggest that the mean of the circle distribution may be a relative measure of the average ring closure probabilities for the population of DNA molecules in the cyclization reaction.

To understand how the circle distribution from the polymerization assay reflects the kinetics of the competing cyclization and bimolecular association reactions, the experiments were repeated at multiple ligase and DNA concentrations. This is premised upon the fact that the reactions of unimolecular cyclization and bimolecular association are linearly dependent upon ligase concentration and are first and second order with respect to DNA concentration, respectively [52, 74]. (See Chapter IV for a detailed derivation of these expressions.) Over a range of ligase concentrations, from 40 to 40,000 U/ml in a 50 µl reaction with 120 ng DNA, there was little shift in the distribution of circles (data not shown). The DNA concentration (0.18 µM monomer oligonucleotide) was well below the estimated K_m for T4 ligase of ~0.6 µM [75, 76]. The observation that the distribution of circle sizes is insensitive to changes in ligase concentration suggests that the mean circle size may be a measure of the ratio of the two individual rates at which the two reaction products form.

This conclusion is further supported by the dependence of the mean on DNA concentration. Since cyclization and bimolecular association are first and second order reactions, respectively, the ratio of the rate constants, and thus the distribution of circle sizes, should not be constant as the DNA concentration varies. To test this hypothesis, the effect of DNA concentration on the mean circle size was determined. The results are shown in Figure 3.17. The mean circle size increases with increasing DNA concentration until a plateau is reached at ~500 nM bp (~24 nM monomer

oligonucleotide). This observation is consistent with the hypothesis that the mean reflects relative rates of product formation and not just cyclization alone. At low DNA concentrations, the probability that the ends of different DNA molecules will find each other is small when compared to the probability of intramolecular circle formation. As a result, smaller circles form more easily and the mean circle size is small. As the DNA concentration increases, the rate of linear polymer formation competes with the intramolecular cyclization thereby increasing the proportion of larger circles and thus increasing the mean circle size. Ultimately, the process is limited when, at high DNA concentrations, the longer polymers cyclize much faster than they polymerize. This has the effect of placing an upper bound on the observed mean circle size. As seen in Figure 3.17, our data reflect these characteristics and suggest that the mean circle size is a measure of the relative rates of product formation of both the cyclization and bimolecular association reactions. Further analysis may allow us to derive a direct relationship between changes in the mean circle size and the probability of ring closure, possibly allowing an explicit quantification of DNA bending.

Summary

We have found that calicheamicin ε bends DNA when it binds and that it is the oligosaccharide tail that appears to be a major contributor to these structural changes. These results suggest that calicheamicin likely prefers to bind sequences that can be easily bent or "trapped" (*i.e.*, flexible) into a conformation that maximizes its other interactions with DNA. This further implies that DNA sequences already bent into a conformation preferred by the drug would also be desirable substrates for calicheamicin binding. This situation is analogous to that of several antibiotics that modify DNA covalently (*e.g.*, [44, 77, 78]).

A structure and dynamics based paradigm for calicheamicin target recognition enables us to explain why, as discussed earlier, calicheamicin-induced DNA damage is influenced by the sequence context and overall topology of the binding site. Since calicheamicin binding depends on DNA flexibility, adjacent bases can affect drug binding by changing the dynamic behavior of the target sequence; an effect that may extend for several base pairs [79, 80]. In contrast, changes in DNA topology must precisely match the desired drug-bound conformation to facilitate drug binding. For example, in the nucleosome studies

described in Chapter I [24, 43, 81], DNA bending reduced or had no effect on calicheamicin-induced DNA damage except at one site. This is consistent with the suggestion that calicheamicin does not target curved or bent DNA indiscriminately but instead, binds only those sequences bent into a specific conformation.

Although important to the recognition process, DNA structure and dynamics are not the solitary determinants of calicheamicin binding. In fact, it is clear that calicheamicin target selection is a complex process involving several interactions that are optimized by the conformational flexibility of specific DNA sequences. In cases where the DNA is bent or "trapped," much of the energetic cost is taken from external forces that either bend or move the DNA. However, for those DNA targets considered "straight," a balance must be achieved between the DNA's intrinsic resistance to movement and those forces -- electrostatic and hydrophobic -- that bind calicheamicin to DNA. In addition, since the binding characteristics of individual sequences are heterogeneous, we should expect not one, but several, optimal binding scenarios; each unique to a particular sequence. As a result, the degree of flexibility required or the amount of bending induced, need not be uniform across all calicheamicin binding sites. A comprehensive model for calicheamicin binding and the other factors that contribute to the target identification process is presented in Chapter VI.

The results with calicheamicin also demonstrate the utility of the T4 ligase/BAL-31 approach. The circle distributions clearly reflect the kinetics of the competing reactions, though more studies are needed to rigorously define the quantitative relationships. With the appropriate DNA constructs, this technique should be useful for rapidly screening many small molecules and proteins for their ability to bend DNA.

Table 3.1 Reaction conditions for the DNA polymerization experiment.

[CAL-ε] μM	[DNA] mM bp	[binding sites] μM	% binding site occupied[a]	moles drug per bp[a]
400	2·4	352	99·8	108·3
40	2·4	352	97·5	10·8
20	2·4	352	95·2	5·42
10	2·4	352	90·6	2·71
5	2·4	352	82·5	1·354
2·5	2·4	352	69·3	0·677
1·88	2·4	352	62·3	0·508
1·25	2·4	352	51·7	0·339
0·63	2·4	352	33·6	0·169
0·31	2·4	352	19·6	0·085
0·08	2·4	352	5·5	0·022
0·02	2·4	352	1·4	0·005
0	2·4	352	0	0

[a] Calculations were based on two binding sites per monomer and an assumed binding constant $K_a = 1 \times 10^6\ M^{-1}$.

Table 3.2 Calculating the circle distribution.

Circle Size (monomers)	Radioactivity in band (cpm)	Normalized radioactivity[a]	Percentage of each circle[b]
14	338	24	1·2
13	783	60	2·9
12	1492	124	5·9
11	2369	215	10·2
10	3074	307	14·6
9	3504	389	18·5
8	3224	403	19·1
7	2563	366	17·4
6	1128	188	8·9
5	153	30	1·5
Total normalized radioactivity =		2109	
		Mean circle size =	8.83

a Radioactivity in each band divided by the circle size (in monomers) present in the band.

b Normalized radioactivity in each band expressed as a percentage of total normalized radioactivity.

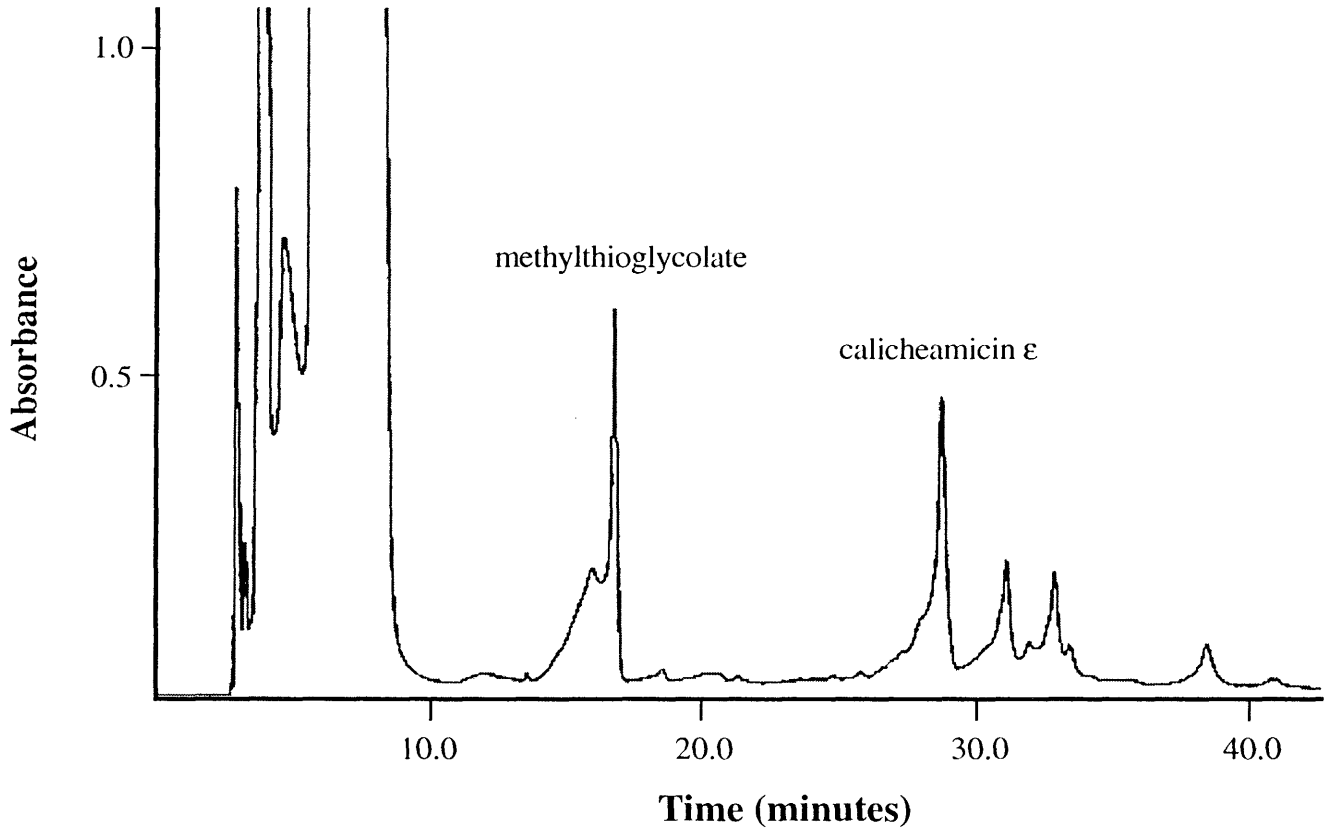

Figure 3.1. Calicheamicin γ_1^I was reduced to calicheamicin ε using methyl thioglycolate as discussed in the text. The reaction products were seperated by HPLC using a linear gradient from 42.5 mM triethylamine (pH 6·0) in 15% acetonitrile to 20 mM triethylamine (pH 6·0) in 60% acetonitrile in 25 minutes.

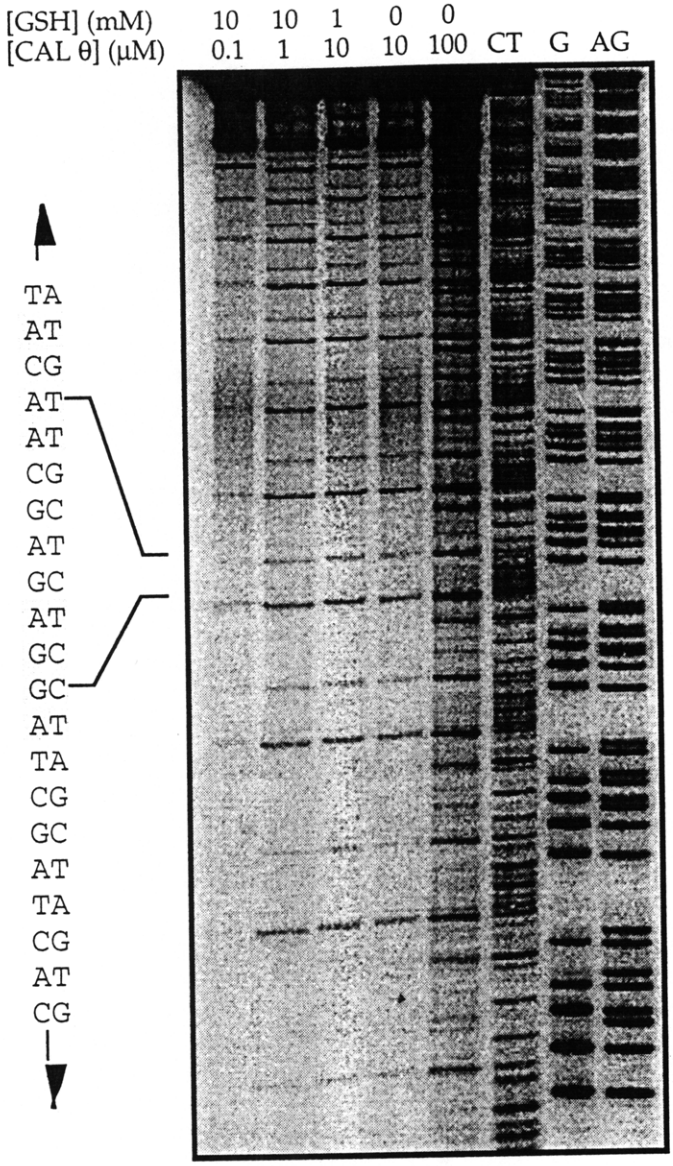

Figure 3.2. Calicheamicin θ induced DNA damage in the out-of-phase construct. Cloned plasmids containing 15 repeats of the out-of-phase DNA construct were digested with *Xba* I and 5'-[^{32}P] end-labeled. Following digestion with *Eco*R I, the labeled fragment was purified by elution from an 8% polyacrylamide gel. Damage reactions consisted of labeled DNA (~30,000 cpm), 30 μg/ml of calf thymus DNA, 10 mM glutathione, 10 mM HEPES, 1 mM EDTA (pH 7). The reaction was initiated by adding calicheamicin θ and then glutathione at the appropriate concentrations. After incubation at 37°C, the DNA was ethanol precipitated and resolved on a 6% sequencing gel. Bands were quantitated by phosphorimager analysis.

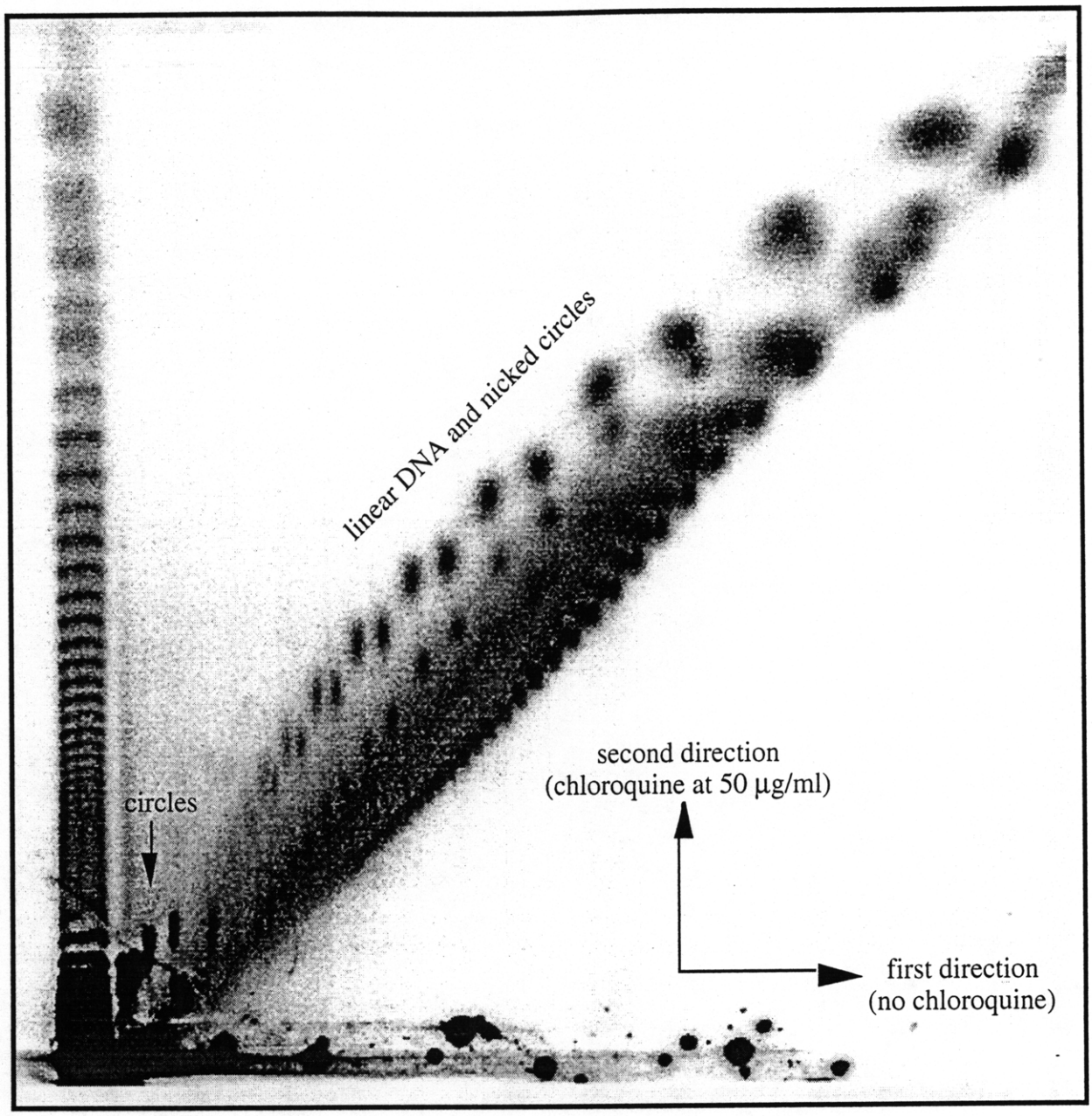

Figure 3.3. Resolving circular from linear DNA by two-dimensional gel electrophoresis. Products from a cyclization reaction are resolved first on an 8% non-denaturing gel and second on an 8% nondenaturing gel containing 50 µg/ml chloroquine. Bands along the diagonal are relaxed circles, supercoiled circles and linear DNA. Bands in the vertical lane on left are linear DNA markers run in the second dimension only.

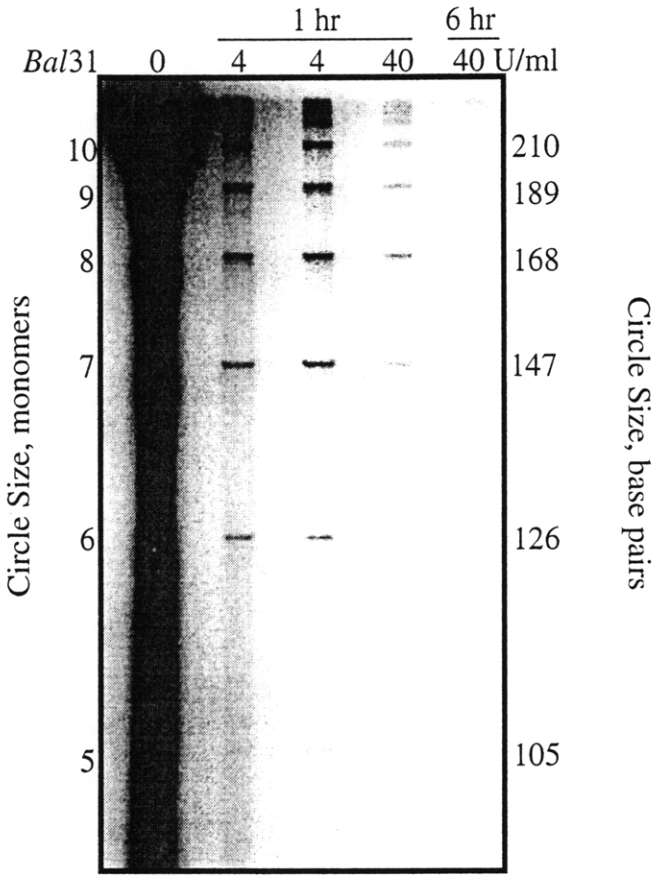

Figure 3.4. Effect of BAL-31 on the products of a T4 ligase reaction with the in-phase calicheamicin binding site construct. Following a ligation reaction of the oligonucleotide construct with T4 DNA ligase, linear DNA polymers were removed by digestion with BAL-31 as described in the text. The DNA was then resolved on a 6% non-denaturing polyacrylamide gel and subjected to phosphorimager analysis. The intensity of the radioactivity in the first lane is due to the high DNA concentration used in this experiment (3 μg/ml) to illustrate the effect of BAL-31 digestion.

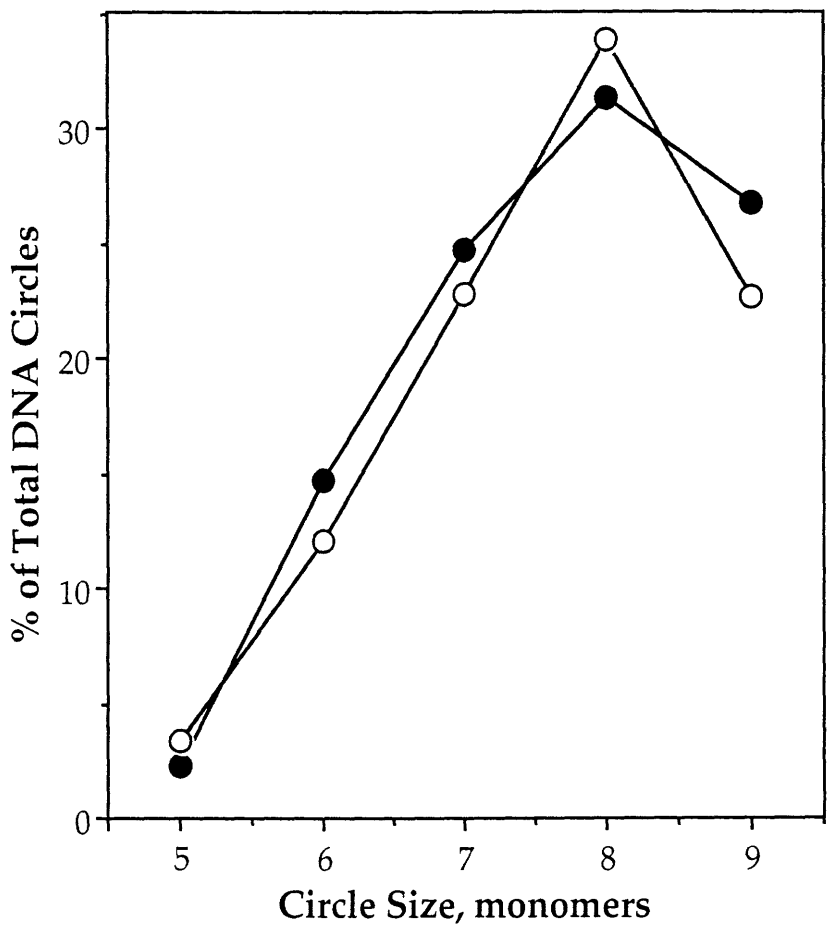

Figure 3.5. Effect of BAL-31 concentration on the distribution of DNA circles resulting from ligation of the in-phase calicheamicin binding site construct. DNA circle bands in the gel in Figure 3.4 were quantified by phosphorimager analysis and their intensities normalized to total radioactivity of all the circles measured. BAL-31 concentrations: 4 U/ml (open circles) and 40 U/ml (closed circles); 1 hr incubation for both concentrations.

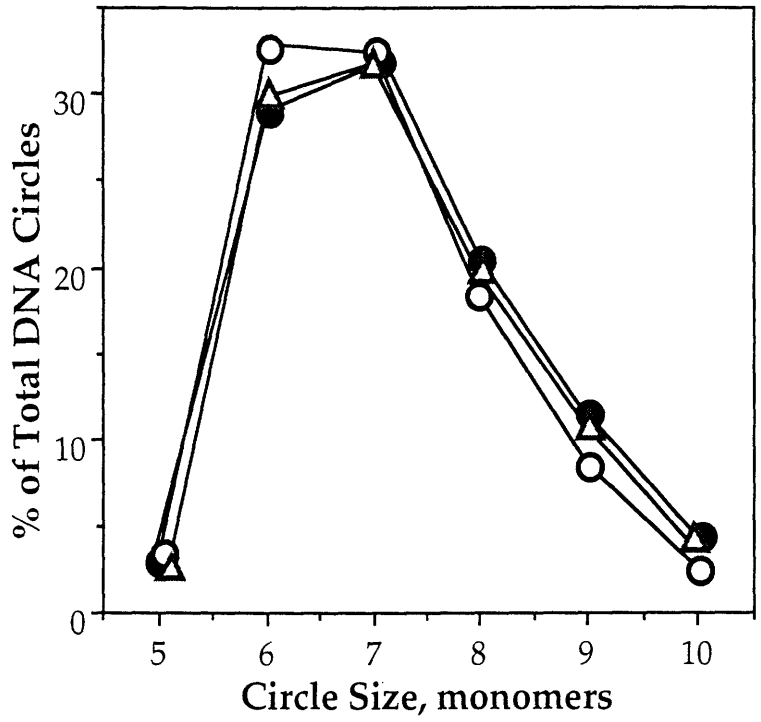

Figure 3.6. Effect of BAL-31 concentration on the distribution of DNA circles resulting from ligation of the A-tract construct. Following ligation of the A-tract construct with T4 DNA ligase, the products were subjected to digestion with BAL-31 as follows: 5 U/ml for 30 min (closed circles), 10 U/ml for 30 min (open circles), and 10 U/ml for 60 min (triangles). Digestion products were then resolved on an 8% non-denaturing polyacrylamide gel and the DNA circles quantified as described in *Materials and Methods*.

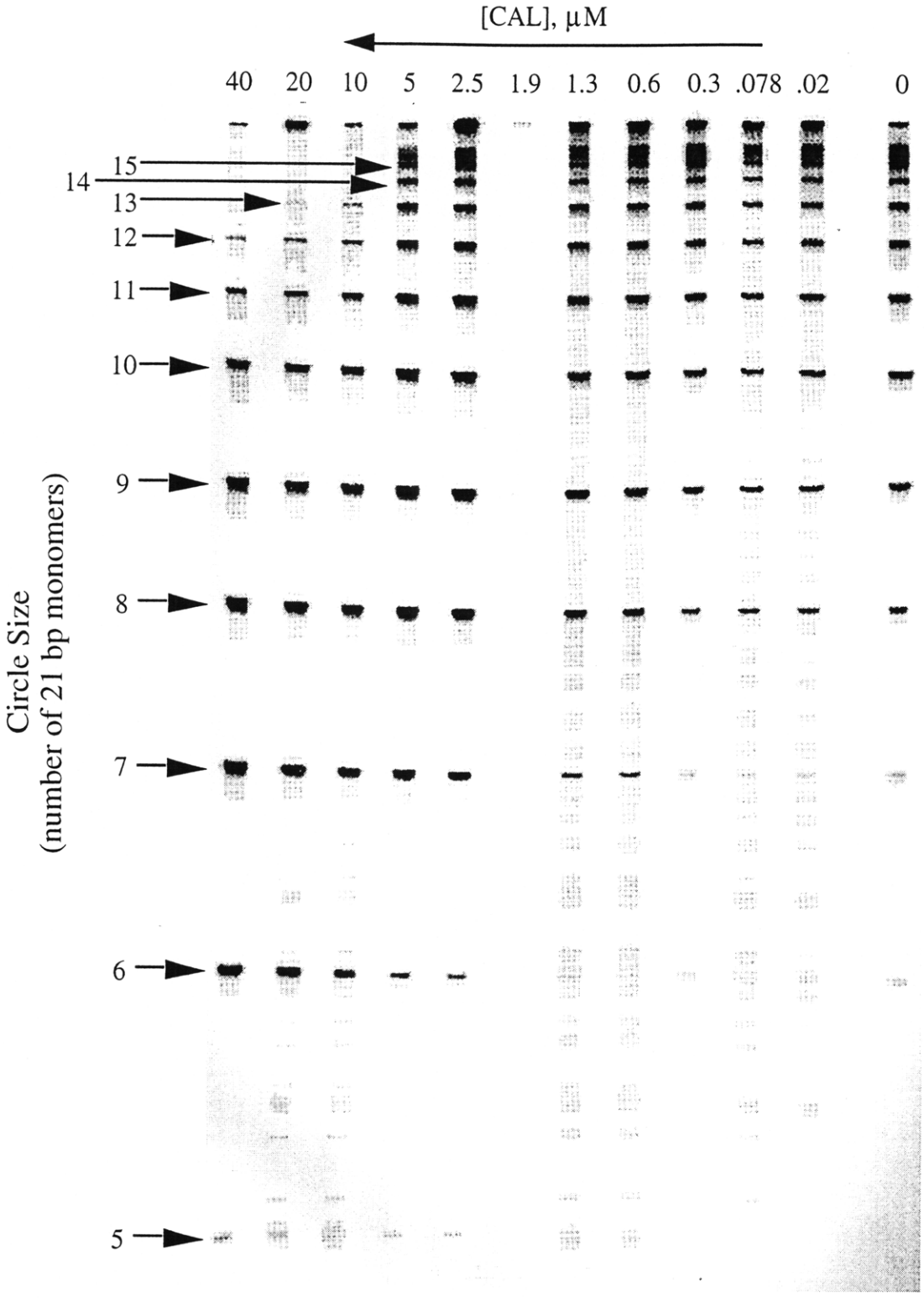

Figure 3.7. The effect of calicheamicin ε on the formation of DNA circles from the in-phase construct. Monomer DNA, ± calicheamicin ε, was treated with DNA ligase and digested with BAL-31 to remove linear polymers. Reaction products were resolved on a 10% polyacrylamide gel.

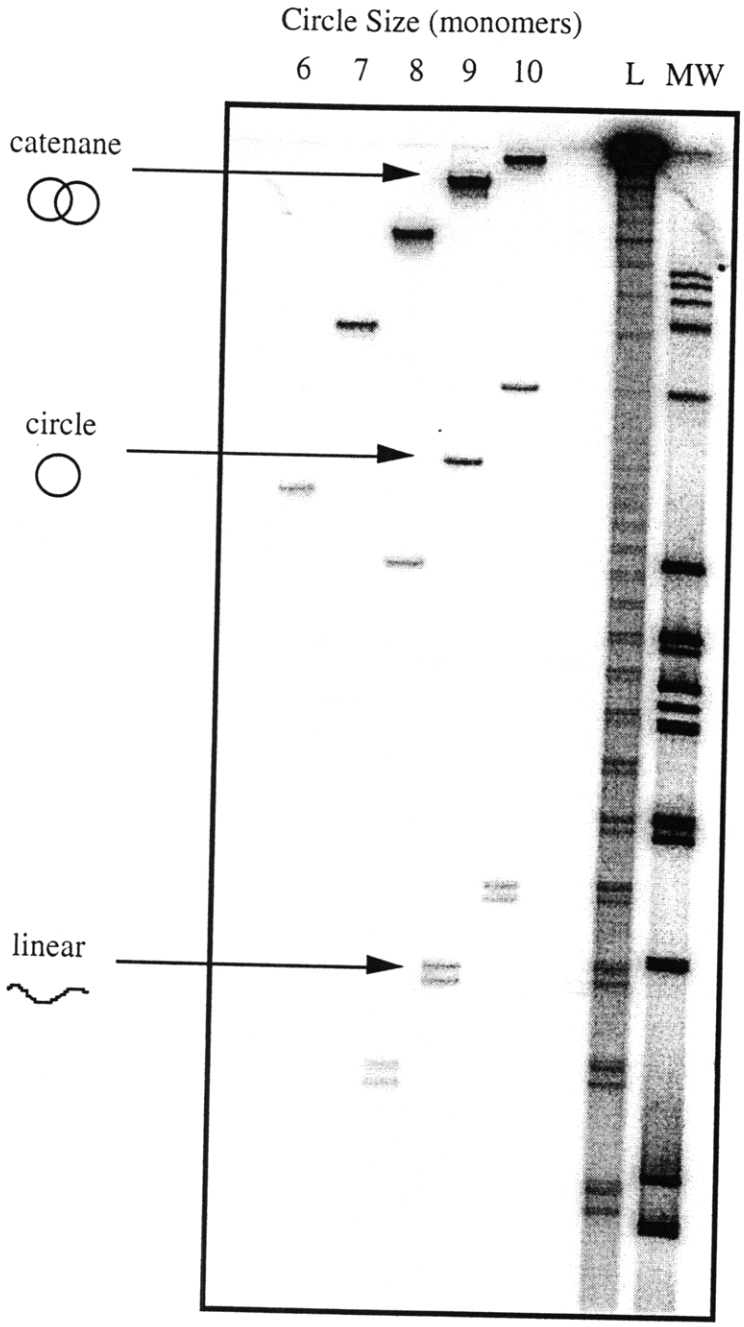

Figure 3.8. Identification of circle size by denaturing gel electrophoresis. Putative radiolabeled DNA circles were excised and eluted from an 8% nondenaturing polyacrylamide gel. DNA was heat denatured and resolved on an 8% denaturing gel with 6 M urea. Duplex DNA circles denature into three products: catenanes (from intact circles), single stranded circles and linear single stranded DNA (from nicked circles). Lane L contains denatured linear polymers adjacent to a molecular weight marker (lane MW) for size identification. The complementary strands of linear molecules migrate separately due to sequence differences.

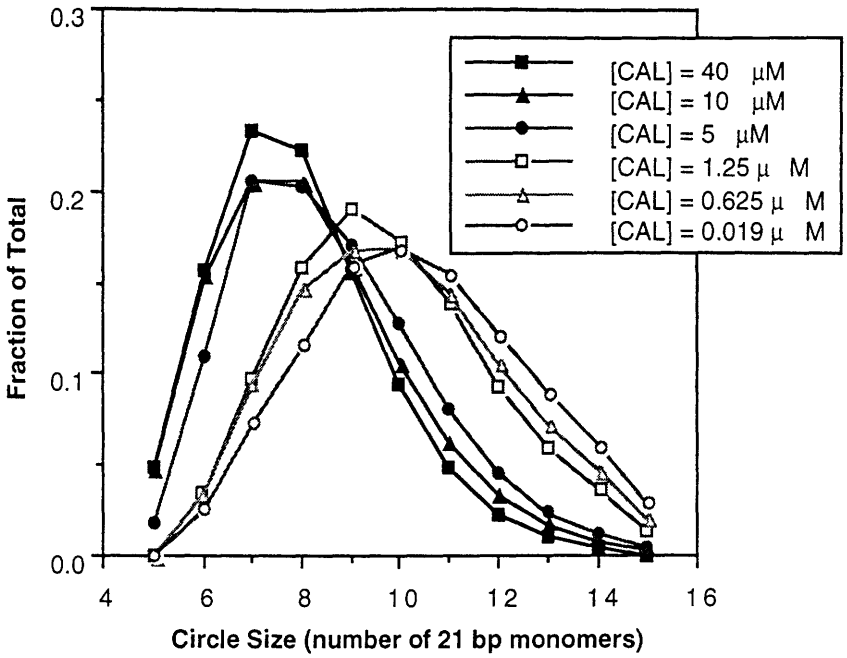

Figure 3.9. Distribution of DNA circles as a function of calicheamicin ε concentration for the in-phase construct. Individual circle populations were quantitated by phosphorimager analysis and normalized by size. The amount represents the fraction of total counts measured over the 10 circle sizes.

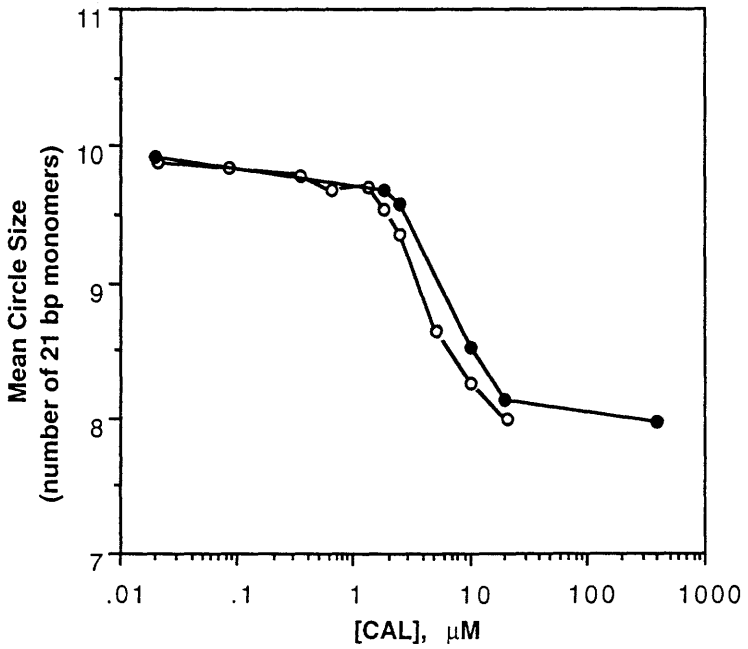

Figure 3.10. Plot of the mean circle size as a function of calicheamicin ε concentration for the in-phase DNA construct. Two separate trials are shown.

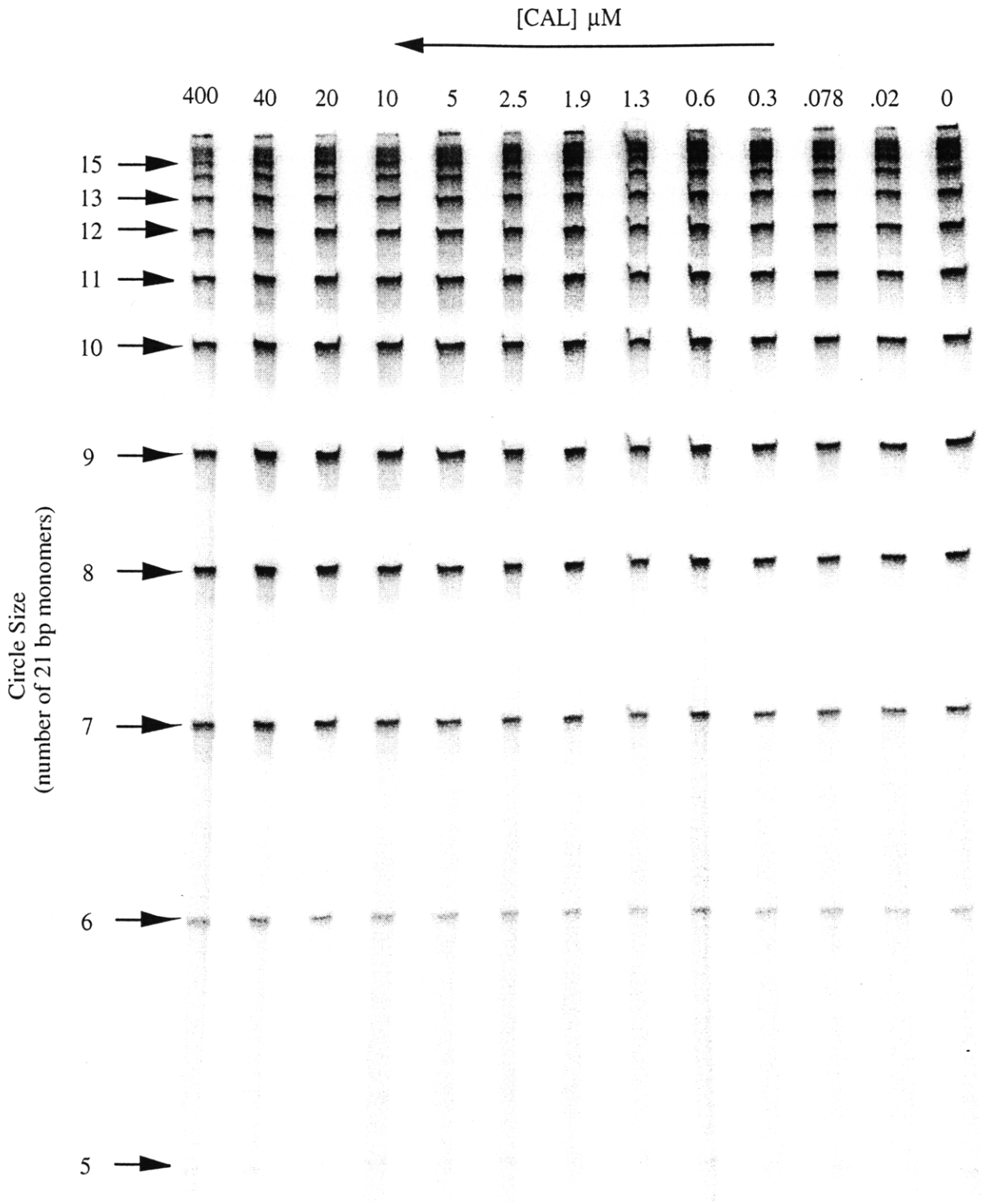

Figure 3.11. The effect of calicheamicin ε on the formation of DNA circles from the out-of-phase construct. Monomer DNA, ± calicheamicin ε, was treated with DNA ligase and digested with BAL-31 to remove linear polymers. Reaction products were resolved on a 10% polyacrylamide gel.

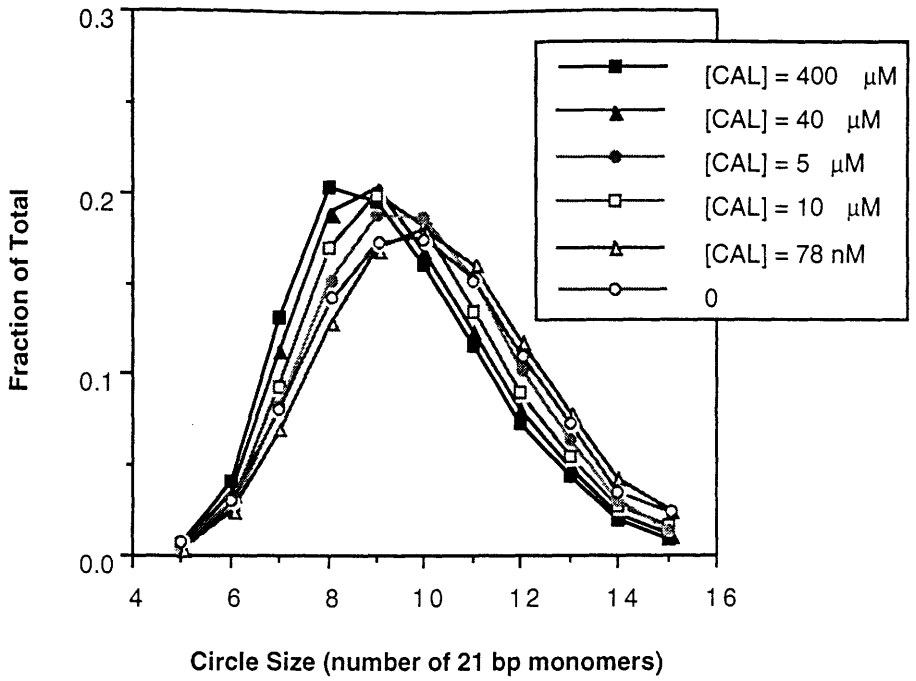

Figure 3.12. Distribution of DNA circles as a function of calicheamicin ε concentration for the out-of-phase construct. Individual circle populations were quantified by phosphorimager analysis and normalized by size. (Not all experiments are shown, the results at some drug concentrations have been left out for clarity.)

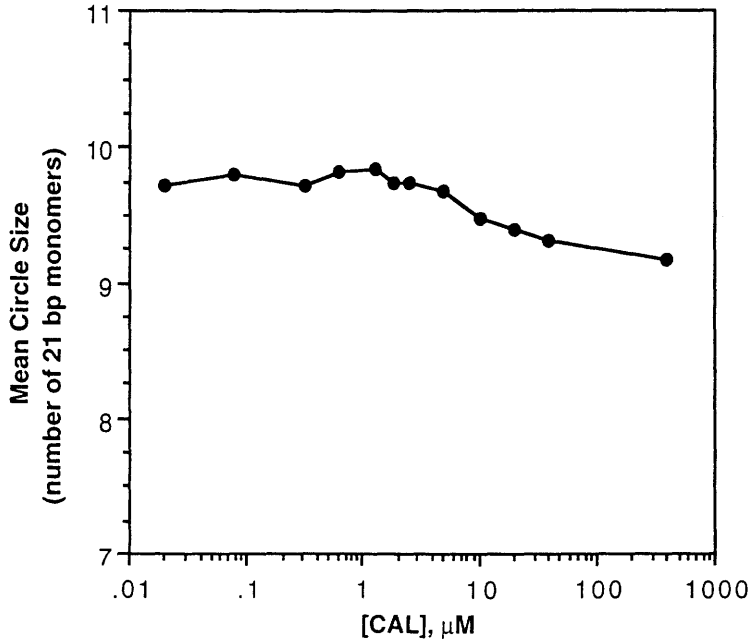

Figure 3.13. Plot of the mean circle size as a function of calicheamicin ε concentration for the in-phase construct.

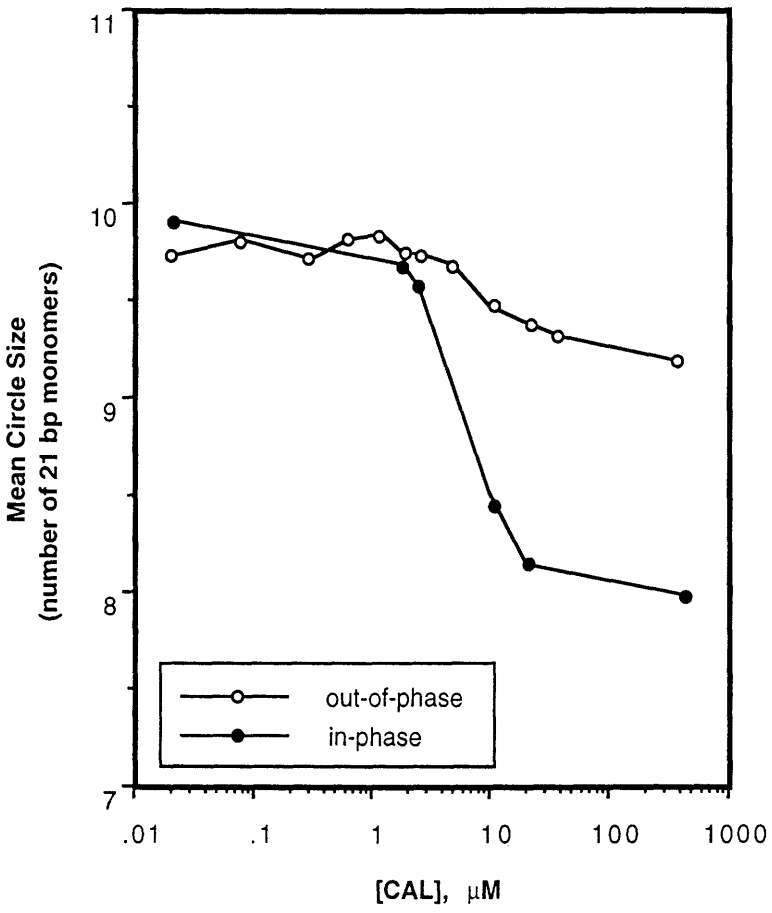

Figure 3.14. Mean circle size as a function of calicheamicin ε concentration for in- and out-of-phase DNA constructs.

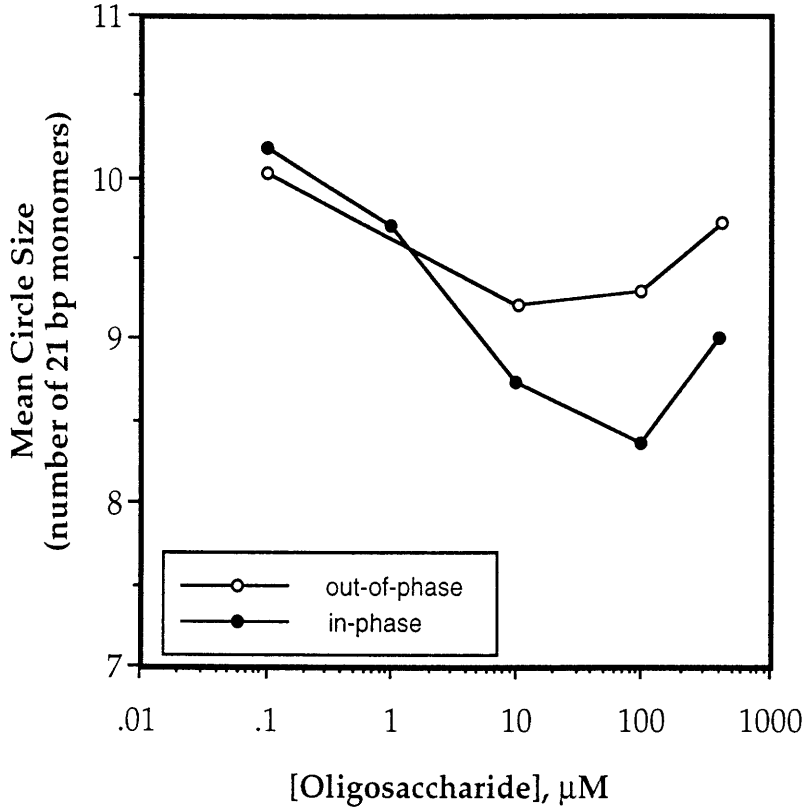

Figure 3.15. Mean circle size versus oligosacchride concentration. 120 ng of 5'-[^{32}P]-ATP end-labeled monomer (either the in-phase or out-of-phase construct) was polymerized in a 50 μl reaction containing standard T4 DNA ligase reaction buffer, the appropriate amount of oligosaccharide and 400 units of T4 DNA ligase. The reaction was carried out overnight at 16°C. The reaction products were then digested with BAL-31 and the circular products resolved by gel electrophoresis and quantitated by phosphoimager analysis.

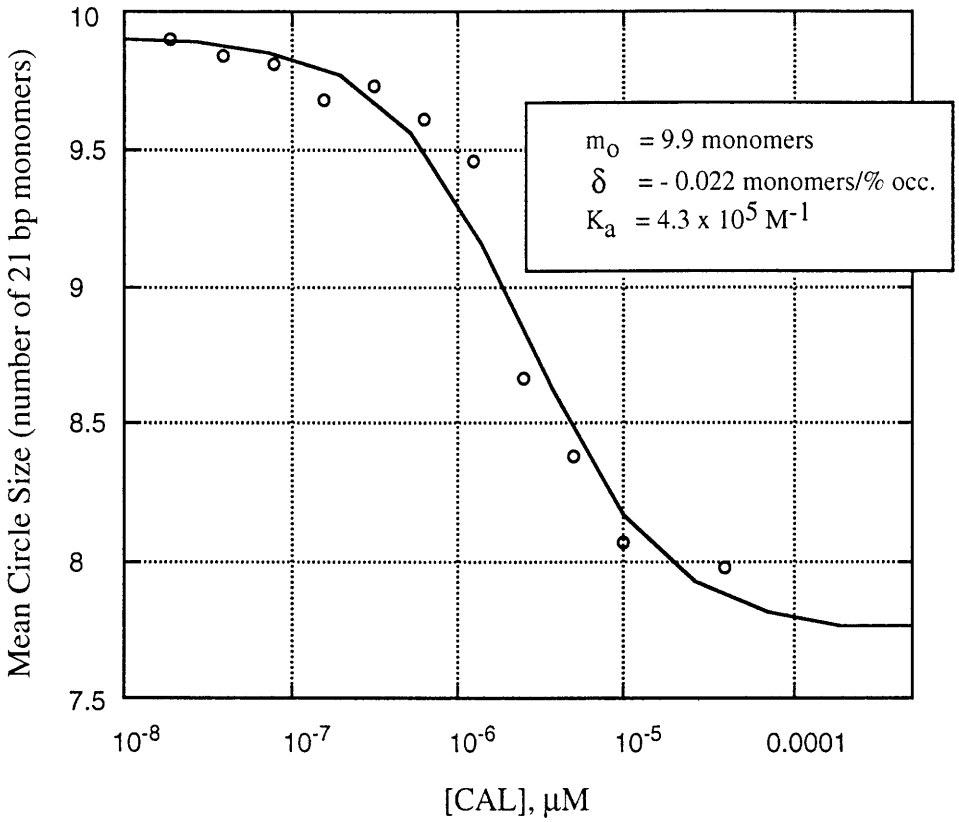

Figure 3.16. Estimating the binding constant of caleachimicin ε. Binding constant was determined by optimizing the fit of

$$m = m_{ul} + \delta \left\{ \frac{[CAL]_T}{[B]_T} - \frac{1}{[B]_T} \left(\frac{-b + \sqrt{b^2 - 4a}}{2} \right) \right\}$$

to the distribution of mean circle sizes for the in-phase DNA construct. (See text, equation 3.5, for definition of terms.)

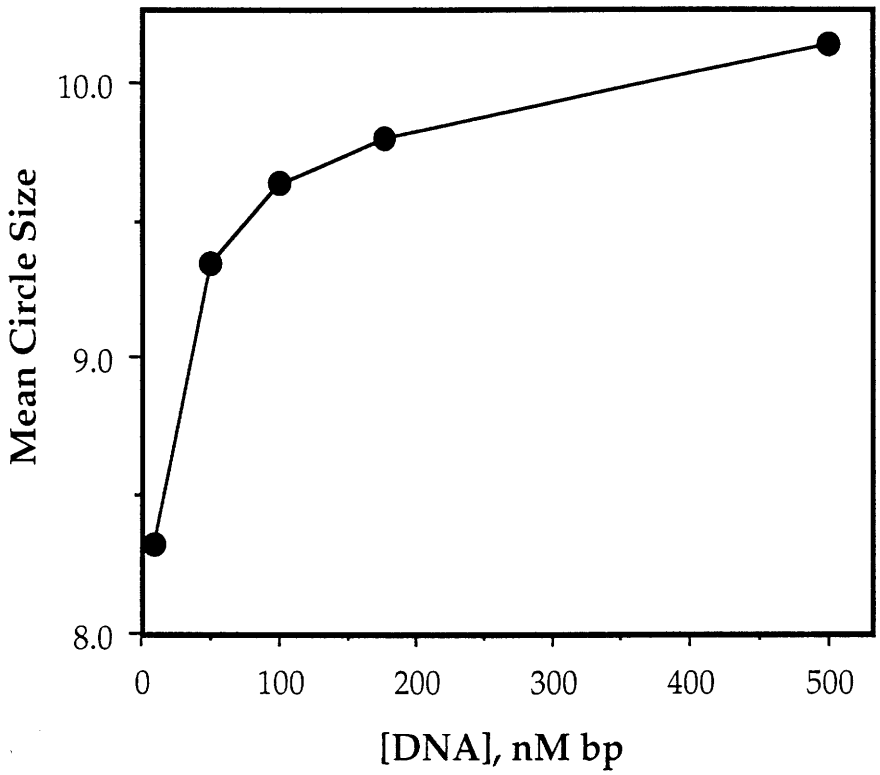

Figure 3.17. Effect of DNA concentration on the distribution of circle sizes resulting from the ligation of the calicheamicin binding site construct. Various concentrations of the calicheamicin binding site construct were subjected to reaction with T4 DNA ligase (8000 U/ml). The ligation products were then digested with Bal-31 (40 U/ml for 1 hr at 30°C) and the remaining circles were resolved on a 6% non-denaturing polyacrylamide gel. The mean circle size at each DNA concentration was determined as described in the text.

CHAPTER IV

Calicheamicin binding and DNA Cyclization Kinetics

The experiments described in Chapter III show that calicheamicin bends DNA upon binding. However, the mean of the circle size distributions is a relatively insensitive and -- at best -- a qualitative measure of cyclization probability. As reviewed in Chapter I, a more rigorous approach towards determining the structural changes that affect the probability of DNA circle formation is to examine the cyclization and dimerization behavior of a single polymer under conditions that allow all of the reaction products to be identified. An analysis of how these products vary over time allows an explicit evaluation of the reaction kinetics and a direct determination of the probability of polymer cyclization. Understanding how this probability changes as calicheamicin binds may then allow us to better understand -- and possibly quantify -- the structural changes in DNA resulting from calicheamicin binding.

The design of an experiment to measure the kinetic properties of a cyclizing molecule requires a careful consideration of the theoretical framework used to analyze the data. In other words, we must ensure that the test substrates and reaction conditions yield results that are consistent with the assumptions made in deriving the theoretical models used to calculate the reaction kinetics. To understand what these assumptions are and how they affect the experimental design we must first derive theoretical expressions for the rate constants we intend to measure.

Theoretical Background

Derived from polymer chain statistics, the ring closure probability (J factor or Jacobson-Stockmayer factor) is defined as the ratio:

$$J = \frac{K_c}{K_a}$$

where K_c and K_a are the equilibrium constants for cyclization and bimolecular association, respectively [67]. Depending on the concentration of one end about the other, J can be thought of as the molar concentration of DNA required to cause bimolecular joining to occur at the same rate as the corresponding cyclization reaction [53, 56, 82]. Since the formation of small DNA circles requires large fluctuations in the shape of the molecule, the cyclization equilibria are quite sensitive to the conformation and mechanical rigidity of the chain. As a result, measurements of J are ideally suited to characterizing the structural and dynamic characteristics of DNA.

Shore, Langowski and Baldwin [52, 74, 83] built upon the work of Wang and Davidson [82, 84] and were the first to measure the J factor using T4 DNA ligase. This advance allowed smaller restriction fragments with shorter complementary ends to be used since the ends did not normally associate with each other strongly enough to be detectable by other means. Since then, much work has been done within the Crothers and Hagerman groups to use this technique to explore the static and dynamic behavior of DNA [50, 53, 57, 59, 60, 71, 85-87]. The theoretical background presented here explains or derives from their seminal works.

The kinetics of cyclizing molecules. A schematic representation of the cyclization of a double stranded piece of DNA with complementary overhanging ends, is shown below:

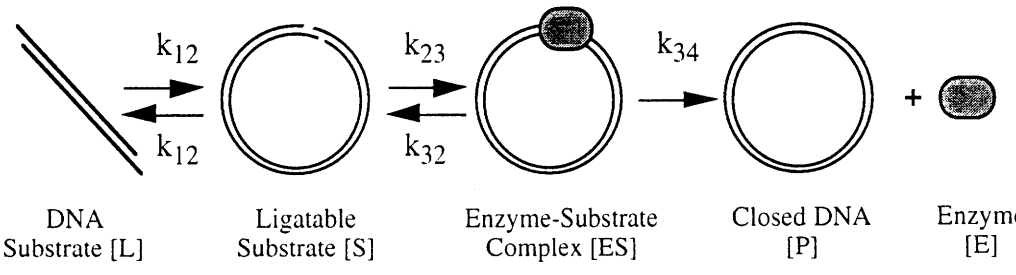

Symbolically,

$$[L] \underset{k_{21}}{\overset{k_{12}}{\rightleftharpoons}} [S] + [E] \underset{k_{32}}{\overset{k_{23}}{\rightleftharpoons}} [ES] \xrightarrow{k_{34}} [P] + [E] \qquad (4.1)$$

This assumes that the second strand of DNA is rapidly ligated after the first and that covalent closure can be considered a single reaction.

To derive a rate constant for the formation of cyclized product [P], we assume that enzymatic modification by the ligase, k_{34}, is the rate limiting step. In other words, the formation of the ligatable substrate and the association of the ligase enzyme occur much faster than the actual enzymatic modification to the DNA. (The validity of this assumption has been demonstrated by the predictive power of the resulting equations.) Since k_{34} is rate limiting, steady state conditions are reached upstream such that

$$\frac{d[S]}{dt} \approx 0 \quad \text{and} \quad \frac{d[ES]}{dt} \approx 0.$$

Applying the second of these conditions to the reaction outlined in equation 4.1 yields

$$[ES] = \frac{k_{23}}{(k_{32} + k_{34})}[S][E]. \qquad (4.2)$$

Similarly, the first steady state condition results in

$$0 = [L]k_{12} - [S]k_{21} - [S][E]k_{23} + [ES]k_{32}.$$

Substituting the latter into the former and solving for [L] gives,

$$[L] = [S]\frac{(k_{21} + [E]\, f_{34}\, k_{23})}{k_{12}} \quad \text{where} \quad f_{34} = \frac{k_{34}}{(k_{32} + k_{34})}. \qquad (4.3)$$

To make use of this result, we must first relate the kinetics of [L] to a measurable rate constant, and then express it in terms of known quantities other than [E] and [S],

which are difficult to determine experimentally. The former is addressed now and the latter in following sections.

The empirically observable quantities in a cyclization experiment are the product, the cyclized DNA [P], and the uncyclized substrate [D] where [D] = [L] + [S]. To relate these quantities to the kinetics of [L], we note that the rate of disappearance of [D] with respect to time -- d[D]/dt -- has been shown to be directly proportional to the amount of uncyclized substrate [52]. In other words, the disappearance of [D] is first order such that

$$\frac{d[D]}{dt} = - k_1 [D] \quad \text{or} \quad k_1 = - \frac{d[D]/dt}{[D]} \tag{4.4}$$

where k_1 is the first order rate constant for the disappearance of uncyclized substrate [D]. From the reaction outline in equation 4.1, the generation of cyclized product [P] is also first order and can be written as

$$\frac{d[P]}{dt} = [ES] k_{34}. \tag{4.5}$$

However, since steady state condition exists in the intervening steps (*i.e.*, d[S]/dt = d[ES]/dt = 0),

$$\frac{d[L]}{dt} = - \frac{d[P]}{dt} . \tag{4.6}$$

We can now relate k_1 to [L] by first noting that [D] = [L] + [S] can be differentiated with respect to time to get

$$\frac{d[D]}{dt} = \frac{d[L]}{dt} + \frac{d[S]}{dt}; \quad \text{or} \quad \frac{d[D]}{dt} = \frac{d[L]}{dt} \tag{4.7}$$

since d[S]/dt = 0 from the assumption of steady state. Substituting equation 4.7 into equation 4.4 gives

$$k_1 [D] = - \frac{d[L]}{dt},$$

which can, by using equations 4.5 and 4.6, be written as

$$k_1 [D] = [ES] k_{34} .$$

Substituting in the earlier expression for [ES], gives

$$k_1\,[D] = \frac{k_{23}}{(k_{32} + k_{34})}\,[S][E]\,k_{34} = [S][E]\,f_{34}\,k_{23},$$

which, since [D] = [L] + [S], can be written as

$$k_1 = \frac{[S][E]\,f_{34}\,k_{23}}{[L] + [S]}.$$

Using equation 4.3 to replace [L] in the above, gives the following expression for k_1;

$$k_1 = \frac{[E]\,f_{34}\,k_{23}\,k_{12}}{k_{12} + k_{21} + [E]\,f_{34}\,k_{23}} \tag{4.8}$$

where k_1 is the observed rate of disappearance of uncyclized DNA and [E] is the concentration of free ligase [52]. Equation 4.8 is premised upon the assumption that the ligation event is rate limiting and that steady state conditions exist prior to ligation.

The kinetics of dimerizing molecules. The process of bimolecular association of identical half molecules with complementary overhanging ends is shown schematically below.

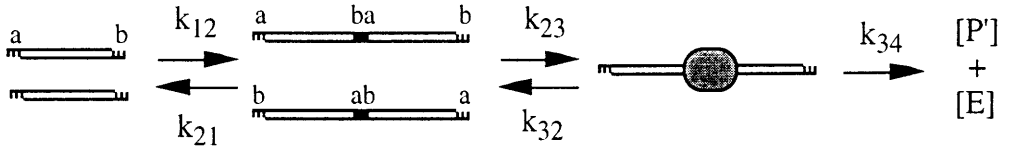

Symbolically, the reaction is,

$$2\,[H] \underset{k_{21}}{\overset{k_{12}}{\rightleftharpoons}} [Sa] + [E] \underset{k_{32}}{\overset{k_{23}}{\rightleftharpoons}} [ES] \xrightarrow{k_{34}} [P'] + [E] \tag{4.9}$$

Analogous to the cyclization reaction, it is assumed that enzymatic ligation is the rate limiting step and that steady state conditions exist upstream. Applying these assumptions, as before, gives the following two expressions;

$$[ES] = \frac{k_{23}}{(k_{32} + k_{34})}[S][E] \tag{4.10}$$

and

$$0 = \frac{1}{2} k_{12} [H]^2 - [S] k_{12} - [S] [E] k_{23} + [ES] k_{32}, \tag{4.11}$$

where the term $(1/2)k_{12} [H]^2$ arises from the fact that 2 molecules of [H] self-react to form only one molecule of [S]. Substituting 4.10 into 4.11 and solving for [S] yields,

$$[Sa] = \frac{\frac{1}{2} k_{12} [H]^2}{k_{21} + [E] k_{23} f_{34}}. \tag{4.12}$$

As before, to make use of this result, we must relate the kinetics of [S] to an experimentally measurable rate constant. It has been observed, that in a reaction in which a linearized half molecule forms a dimer product [P'], the disappearance of [D'], where [D'] is the concentration of undimerized substrate ([H] + 2[S]), with respect to time is second order. Therefore, the rate constant for bimolecular association, k_2 is defined by

$$\frac{d[D']}{dt} = - k_2 [D']^2 \quad \text{or} \quad k_2 = - \frac{\frac{d[D']}{dt}}{[D']^2}. \tag{4.13}$$

From the reaction outlined in 4.11, the generation of dimerized product [P'] is first order, so

$$\frac{d[P']}{dt} = [ES] k_{34} \quad \text{and} \quad \frac{1}{2}\frac{d[H]}{dt} = - \frac{d[P']}{dt}. \tag{4.14) and (4.15}$$

(Equation 4.15 results from the assumption of steady state conditions and the fact that 2 molecules of [H] are used to produce one dimer [P'].) To relate the

experimentally observed k_2 to the kinetic relationship derived above, we note that the equation [D'] = [H] +2[S] can be differentiated with respect to time to get

$$\frac{d[D']}{dt} = \frac{d[H]}{dt} + 2\frac{d[S]}{dt} \quad \text{or} \quad \frac{d[D']}{dt} = \frac{d[H]}{dt} \tag{4.16}$$

(under steady state conditions). Substituting this result into 4.13 results in

$$k_2 = -\frac{\frac{d[H]}{dt}}{[D']^2},$$

which can be further manipulated via equations 4.14, 4.15 and 4.10 to get

$$k_2 = -\frac{2\,[ES]\,k_{34}}{[D']^2} = -\frac{2\left(\frac{k_{23}}{k_{32}+k_{34}}\right)[Sa]\,[E]\,k_{34}}{[D']^2}$$

which simplifies to

$$k_2 = -\frac{2\,f_{34}\,k_{23}\,[Sa]\,[E]}{[D']^2}.$$

Substituting in equation 4.12 for [Sa] gives

$$k_2 = -\frac{1}{[D']^2}\left[\frac{f_{34}\,k_{23}\,k_{12}\,[E]\,[H]^2}{k_{21}+[E]\,k_{23}\,f_{34}}\right] \tag{4.17}$$

where k_2 is the observed rate of disappearance of undimerized DNA, [D'] is the amount of unligated half molecules, [E] is the concentration of free ligase and [H] the concentration of unligated half-molecules. As in the case of cyclizing molecules, it was assumed that the ligation event was rate limiting and that steady state conditions existed prior to ligation.

Monomer kinetics assuming pre-equilibrium and rapid ligase disassociation. Equation 4.8 for cyclizing molecules and equation 4.17 for dimerizing molecules can be further simplified by assuming that the interconversion between the unligatable

substrates, [L] and [H], to the ligatable substrates, [S] and [Sa], occurs extremely fast and that, as a result, these populations exist in a pre-equilibrium state [52]. Therefore, we can define the equilibrium constants K_c and K_a such that

$$K_c = \frac{k_{12}}{k_{21}} \quad \text{for cyclizing molecules, and}$$

$$K_a = \frac{k_{12}}{k_{21}} \quad \text{for dimerizing molecules.}$$

Equation 4.8 can, after dividing by k_{21}/k_{21}, be rewritten as

$$k_1 = \frac{K_c f_{34} [E] k_{23}}{K_c + 1 + [E] f_{34} \frac{k_{23}}{k_{21}}} .$$

Similarly, equation 4.17 can be written in terms of its equilibrium constant as

$$k_2 = - \frac{1}{[D']^2} \left[\frac{K_a f_{34} k_{23} [E] [H]^2}{1 + [E] \frac{k_{23}}{k_{21}} f_{34}} \right] .$$

If we further assume that the ligase disassociates from the ligatable substrate much faster than it binds (*i.e.*, $k_{21} >> k_{23}$), then the above equations can be reduced to

$$k_1 = \left(\frac{K_c}{K_c + 1} \right) f_{34} [E] k_{23} \qquad (4.18)$$

and

$$k_2 = - \frac{K_a f_{34} k_{23} [E] [H]^2}{[D']^2} \qquad (4.19)$$

These equations can be further simplified by defining the term f_s and f_s' as the fractions of ligatable substrate for cyclization, $f_s = \frac{[S]}{[D]}$, and dimerization, $f_s' = \frac{2[S_a]}{[D']}$. Noting that

$$K_C = \frac{[S]}{[L]} = \frac{f_S}{1 - f_S}$$

allows equation 4.18 to be rewritten as

$$k_1 = K_C f_{34} [E] k_{23} (1 - f_S). \tag{4.20}$$

Similarly, by noting that

$$[D'] = [D']\frac{[H]}{[H]} = \frac{[H]}{[H]/[D']} = \frac{[H]}{\frac{[D'] - 2[S]}{[D']}} = \frac{[H]}{1 - f_S'}$$

and that therefore,

$$[D']^2 = \frac{[H]^2}{(1 - f_S')^2}$$

equation 4.19 can be rewritten as

$$k_2 = K_a f_{34} k_{23} [E] (1 - f_S')^2. \tag{4.21}$$

In deriving equations 4.20 and 4.21, two more assumptions were made: 1) the interconversion between the unligatable substrate to the ligatable DNA occurs extremely fast and 2) the rate of ligase disassociation is much greater that the rate of ligase association with the ligatable substrate.

Monomer kinetics in terms of initial ligase concentration. To avoid the need to experimentally determine the concentration of free ligase [E], it is useful to derive expressions for k_1 and k_2 in terms of the total enzyme concentration $[E_o]$ where $[E_o] = [E] + [ES]$. Substituting in the kinetic relationship for [ES], which is the same in either the cyclization or dimerization reactions (equations and 4.2 and 4.10), and solving for [E] results in

$$[E] = \frac{1}{f_{34} k_{23}}\left(\frac{k_{34} [E_O]}{K_m + [S]}\right) \quad \text{where} \quad K_m = \frac{k_{32} + k_{34}}{k_{23}}.$$

Replacing [E] in equations 4.20 and 4.21 with the above expression gives

$$k_1 = \frac{K_c\, k_{34}\, [E_o]\, (1 - f_s)}{K_m + [S]} \tag{4.22}$$

and

$$k_2 = \frac{K_a\, k_{34}\, [E_o]\, (1 - f_s')^2}{K_m + [Sa]} \tag{4.23}$$

where, to summarize:

- k_1 is the rate of disappearance of the uncyclized substrate [D], a first order rate constant;
- K_c is the equilibrium constant between the linear [L], and ligatable [S], substrates;
- k_2 is the rate of disappearance of the monomer substrate [D'], a second order rate constant;
- K_a is the equilibrium constant between the monomer [H], and the ligatable dimer [Sa];
- $[E_o]$ is the total ligase concentration;
- K_m is the rate constant for the DNA ligase; and
- f_s and f_s' are the fractions of ligatable substrate for the cyclization and dimerization reactions respectively.

In deriving these equations it was assumed that: 1) the ligation event is the rate limiting step; 2) steady state conditions exist prior to the ligation event; 3) the interconversion of non-ligatable and ligatable substrate is fast and, as a result, a state of pre-equilibrium exists between the two; and 4) that rate of ligase disassociation is much greater than the rate of association with a ligatable substrate. Shore *et al.* demonstrated the validity of these assumptions empirically, by matching experimental data with the predicted results [52].

Equations 4.22 and 4.23 represent the rate constants for the conversion of a DNA molecule into a polymer or circle respectively. An evaluation of these rates allows a direct determination of the ring closure probability, J, as shown below.

Experimental Design

The ring closure probability, J, can be determined by solving equations 4.22 and 4.23 for the equilibrium constants K_c and K_a and taking the ratio:

$$J = \frac{K_c}{K_a} = \frac{\dfrac{k_1 (K_m + [S])}{1 - f_s}}{\dfrac{k_2 (K_m + [S_a])}{(1 - f_s')^2}}$$

If:
1) the concentration of ligatable substrates [S] and [Sa] are small with respect to K_m and
2) the ratio of ligatable substrate to total unligated DNA f_s and f_s' are much less than 1 (*i.e.*, < 0.03; [52]),

then the above expression reduces to

$$J = \frac{k_1}{k_2}. \qquad (4.24)$$

Therefore, under certain conditions we can approximate the ring closure probability by empirically measuring the two rate constants k_1 and k_2. Our experimental approach was to design a DNA test specimen that allowed us to easily alter the amount of ligatable substrate while developing a robust strategy for measuring the rate constants under a variety of reaction conditions.

Test specimen design. To optimize the change in the probability of cyclization in response to calicheamicin binding, we used test constructs that were polymers of the in-phase binding site construct. Families of different sized polymers were generated by cloning products from the ligation of the in-phase monomer. As a result, we could select the molecule length that gave us structural and dynamic characteristics necessary to remain within the theoretical constraints of our analysis.

In general, the goal was to ensure that the fraction of substrate available for cyclization (f_s) or dimerization (f_s') was very small and that the total amount of ligatable substrate ([S] or [S_a]) was an order of magnitude less than the K_m for the DNA ligase (estimated at 0.6 μM) [75, 76]. The f_s' and f_s can become large if, in the

case of the former, the DNA concentration is high or, in the case of the latter, if the molecule cylcizes easily ($J \approx 10^{-6}$ M) [53]. The amount of ligatable substrate ([S] or [Sa]), is directly dependent on f_s, $f_{s'}$ and the total concentration of DNA. Therefore, the experiments relied upon choosing the correct molecule length and reaction conditions to ensure that none of the assumptions made in the derivations were violated.

Measurement of rate constants. In general, there are two approaches to empirically determine the rate constants k_1 and k_2 for a specific DNA molecule: 1) perform independent reactions or 2) measure k_1 and k_2 simultaneously in one reaction.

To measure the rate constants k_1 and k_2 independently, two separate ligation experiments are performed under conditions designed to produce only one of the two possible reaction products, circles or dimers [56]. This can be achieved in two ways. In the first, the DNA concentration is altered to shift the reaction towards one product while excluding the other. In this case, measurements of k_1 are performed at DNA concentrations too low for dimerization to occur at an appreciable rate, while k_2 is measured at high DNA concentrations, which increases the rate of bimolecular association well above the rate of cyclization. A second technique inhibits cyclization and allows k_2 to be measured directly by using a DNA molecule that is too short to cyclize. Since k_2 is independent of polymer length, the rate constant for the short DNA is equivalent to that of the larger [52]. There are several problems with these approaches. The first technique may not be appropriate for molecules that cyclize easily since the amount of DNA necessary to convert all the substrate directly to dimers may make f_s large and equation 4.24 invalid. The second may not work if the assumption that k_1 and k_2 are independent is wrong. This may be the case when k_1 is large. Last, both techniques are susceptible to errors introduced by having two separate experiments. Differences in ligase concentration or other impurities that influence DNA structure, dynamics or ligation efficiency could all cause experimental artifacts.

To avoid the errors associated with two independent experiments, J can be determined from a reaction in which both circular and polymer products are formed simultaneously. A schematic of such a scenario is shown below.

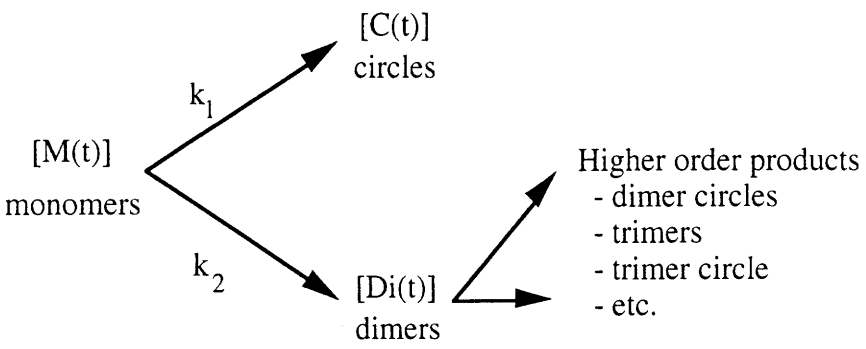

The rate constants k_1 and k_2 are identical to those of the individual reactions in which only one product is formed. In this case,

$$[M(t)] \xrightarrow{k_1} [C(t)] \quad \text{and} \quad 2\,[M(t)] \xrightarrow{k_2} [Di(t)] \qquad (4.25) \text{ and } (4.26)$$

Note, that if dimerization occurs rapidly, then higher order polymers and polymer circles may be generated. This becomes a problem when the proportion of multimers -- which can still act as substrates for dimerization -- is large enough to compete with the existing monomers in further polymerization reactions. Fortunately, the larger polymers often cyclize quickly and are taken out of the pool of reacting substrates.

The kinetics of these competing reactions (neglecting the formation of higher order products) are described by three partial differential equations [53]:

The rate of circle formation; $$\frac{d[C(t)]}{dt} = k_1\,[M(t)]. \qquad (4.27)$$

The rate of dimer formation; $$\frac{d[Di(t)]}{dt} = 2\,k_2\,[M(t)]^2. \qquad (4.28)$$

And, the loss of monomer substrate: $$\frac{d[M(t)]}{dt} = -\,k_1\,[M(t)] - 4\,k_2\,[M(t)]^2. \qquad (4.29)$$

The factor of 2 in equation 4.28 results from the two ways in which polymers with different, but complementary, ends can come together to form a dimer. The coefficient of 4 in equation 4.29 occurs since the rate at which the dimerized product is generated is 1/2 the rate at which monomer, going to form dimer, is lost (two moles of monomer go to form one mole of dimer). Solving the above system of

differential equations with the initial conditions that [C(0)] = [Di(0)] = 0 and [M(0)] = M_o, results in

$$[M(t)] = \frac{M_o e^{-k_1 t}}{1 + 4 M_o (1 - e^{-k_1 t}) \frac{k_2}{k_1}}, \tag{4.30}$$

$$[C(t)] = \frac{k_1}{4 k_2} \left\{ -k_1 t + \ln\left(\frac{M_o}{[M(t)]} \right) \right\}, \text{ and} \tag{4.31}$$

$$[Di(t)] = \frac{1}{2} (M_o - [C(t)] - [M(t)]) . \tag{4.32}$$

The above equations can be used to estimate the rate constants k_1 and k_2 by optimizing their fit to the measured data. (See *Materials and Methods.*) The ring closure probability, J, can then be calculated by taking the ratio of the two reaction rates if the conditions of equation 4.24 are met.

Another method, proposed by Taylor and Hagerman, evaluates J directly by extrapolating the measured data backwards to estimate the reaction products as soon as the reaction starts [57]. If we take the limit of equations 4.26 and 4.26 over a small interval of time,

$$\lim_{t \to 0}[C(t)] = k_1 [M_o] t$$

$$\lim_{t \to 0}[Di(t)] = 2 k_2 [M_o]^2 t$$

then, from equation 4.24, we can then write

$$J = 2 [M_o] \lim_{t \to 0}\left(\frac{[C(t)]}{[Di(t)]} \right) \tag{4.33}$$

Equation 4.33 can be used to solve for J directly by measuring [C(t)] and [Di(t)], extrapolating back to t = 0 to find the limit, and dividing.

Although both the above techniques were tried, the Crother's method allowed an explicit determination of the rate constants, that proved more useful.

Materials and Methods

Reagents and DNA substrates. Calicheamicins γ_1^I and ε were provided by Dr. George Ellestad (Wyeth Ayerst Research) or synthesized as described in Chapter II; calicheamicin θ and the aryltetrasaccharide were provided by Prof. K.C. Nicolaou (Scripps Research Institute). All enzymes were obtained from New England Biolabs. Deoxyoligonucleotides were prepared as described in Chapter II.

Preparation of large quantities of a specific polymer construct. Clones containing specific polymers were constructed and identified as described in Chapter II. Large quantities of the polymer substrate were grown and purified as follows. The appropriate vector was electroporated into the GM1206 *E. coli* host and cultured in LB (10 grams tryptone, 10 grams yeast extract, 5 grams $NaCl_2$ and 2 grams $MgCl_2$ in 1 L H_2O adjusted to pH 7·2 with NaOH) and chloramphenicol as described elsewhere [64]. Plasmid DNA was isolated using Qiagen Giga-Preps (Qiagen) and purified, if necessary, on a CsCl gradient to remove genomic contamination. Polymer constructs were recovered by digesting the plasmids with *Sap* I (1 unit/μg under standard reaction conditions) followed by gel purification.

Preparation of radiolabeled DNA. DNA polymers used in the cyclization experiments were radiolabeled as follows: 1 pM of 5' ends were dephosphorylated for 40 minutes at 37°C with alkaline phosphatase under standard conditions (Boehringer) in a 50 μl reaction containing 0·02 units/pmole of calf intestinal alkaline phosphatase (diluted in 25 mM Tris-HCl, 1 mM $MgCl_2$, 0·1 mM $ZnCl_2$, 50% glycerol, pH 7·4 prior to use). After heating 10 minutes at 65°C to kill the enzyme, the DNA was extracted once with phenol, once with phenol/chloroform and desalted using a G-50 sephadex spin column (Boehringer). Labeling of the 5' end with [^{32}P] was performed in an 80 μl reaction containing 150 μCi of γ-[^{32}P]-ATP (~6,000 mCi/mmole) and 20 units of T4 polynucleotide kinase in standard reaction buffer (NEB) for 1 hr at 37°C. The DNA was then extracted once with phenol, once with phenol/chloroform and the unincorporated ATP removed on a G-50 sephadex spin column. The DNA was immediately diluted to a total volume of 0.1 or 1 ml to reduce radiolytic degradation. The degree of phosphorylation in the radiolabeled substrate was determined by performing overnight ligation reactions at very low DNA concentrations (< 1 fM) under standard conditions and separating the products on a 4% polyacrylamide gel containing 60 μM chloroquine. The gel was dried and

subjected to phosphorimager analysis (Molecular Dynamics). Labeling the DNA in the above manner resulted in greater than 95% phosphorylation of the 5' ends.

DNA cyclization reactions. The circle closure experiments were performed as follows: A mixture of 5'-[^{32}P] end-labeled polymer and unlabeled DNA, at a ratio of less than 1:20, was ligated at 16°C in a 40 µl reaction mixture containing 65 nM DNA, 50 mM Tris-HCl (pH 7·6), 3·5 mM $MgCl_2$, 5 mM KCl_2, 1 mM dithiothreitol, 1 mM ATP, 40 µg/ml bovine serum albumin, 0·1% Nonidet P-40, and 2·5% v/v MeOH containing calicheamicin ε ranging in concentration form 0 to 100 µM. After removing a 4 µl aliquot and quenching as described below, the ligation reaction was initiated by adding 1 µl of T4 DNA Ligase (0·04 to 40 units/µl); diluted in 50 mM KCl_2, 10 mM TrisHCl, 0·1 mM EDTA, 1 mM DTT, 200 µg/ml BSA and 0·1% Nonidet P-40 just prior to use. Ligase stocks were stored in an identical buffer without NP-40 but with 50% glycerol. At specific time intervals, 4 µl aliquots were removed and quenched in 4 µl of preheated (65°C) stop and loading buffer (100 mM EDTA, 5% v/v glycerol and 0·04% w/v bromophenol blue). Samples were then incubated at 65°C for > 10 minutes, cooled to room temperature and loaded directly onto either a 4% composite agarose gel (2% NuSeive GTG and 2% high-melting agarose) or a 4% non-denaturing polyacrylamide gel. In both cases, the gels were dried and subject to phosphorimager analysis.

Methods of Analysis

After performing a cyclization experiment, the reaction products were resolved by polyacrylamide gel electrophoresis and quantified by phosphorimager analysis. The techniques used to evaluate the rate constants were unique to the specific experimental outcome: circles only, polymers only or both circles and polymers.

Case I: Circles only. In ligation experiments where the substrate was converted to circles only, k_1 was determined by measuring the slope of line produced by plotting the natural log of $[M(t)]/[M_O]$ versus time.

From differential equation 4.27, the loss of cyclizable substrate (equation 4.4) is

$$\frac{d[M(t)]}{dt} = - k_1 [M(t)],$$

after separating variables and integrating,

$$\ln[M(t)] - \ln[M_o] = - k_1 t + C_1$$

where $[M_o]$ is $[M(t)]$ at $t = 0$ and C_1 is an integration constant. Since at time $t = 0$, $[M(t)]$ equals $[M_o]$, $C_1 = 0$. The above equation then becomes

$$[M(t)] = \frac{[M_o]}{e^{k_1 t}} \quad \text{or} \quad \ln\left(\frac{[M(t)]}{[M_o]}\right) + k_1 t = 0 . \tag{4.34}$$

Therefore, k_1 can be determined by measuring the slope of line produced by plotting the ln of $[M(t)]/[M_o]$ versus time.

The above analysis assumed that all the substrate could cyclize. In practice, it has been observed that between 5 to 20% of the DNA is unable to ligate [87]. To correct for this, the amount of non-cyclized substrate, measured at a given time t, is

$$[M_m(t)] = [M(t)] + f_d [M_{mo}]$$

where $[M_{mo}]$ is the total amount of measurable substrate ($[M_m(t)]$ at $t = 0$) and f_d is the fraction of total substrate that is not ligatable. Similarly,

$$[M_{mo}] = [M_o] + f_d [M_{mo}].$$

Substituting these last two expressions into equation 4.34 gives the following equation for the measured amount of uncyclized substrate as a function of time and the rate constant k_1

$$[M_m(t)] = [M_{mo}] \left[e^{-k_1 t}(1 - f_d) + f_d\right]. \tag{4.35}$$

In cases where f_d was large, k_1 was obtained by optimizing the fit equation 4.35 to the measured data [71]. To determine f_d, the ligation reaction was allowed to continue until the amount of non-cyclized substrate remained nearly constant. The ratio of

the non-cyclized substrate to total DNA was f_d. All curve fitting was performed on KaleidaGraph (Abelbeck Software).

Case II: Dimers (polymerization) only. In a ligation experiment in which the DNA polymerizes without forming circles, the differential equation describing the disappearance of undimerized substrate (equation 3.18) is

$$\frac{d[M(t)]}{dt} = -k_2 [M(t)]^2 .$$

Again, separate variables and integrate to get

$$-\frac{1}{[M(t)]} + \frac{1}{[M_o]} = -k_2 t + C_1$$

where $[M_o]$ is $[M(t)]$ at $t = 0$ and C_1 is an integration constant. Since at $t = 0$, $[M(t)] = [M_o]$, $C_1 = 0$. Upon rearranging, the above equation becomes

$$[M(t)] = \frac{[M_o]}{k_2 t [M_o] + 1}, \quad \text{or} \quad \frac{\left(1 - \frac{[M(t)]}{[M_o]}\right)}{[M(t)]} - k_2 t = 0. \tag{4.36}$$

An estimate of k_2 can be made from the from the slope of the line fit to the data plotted as $\frac{\left(1 - \frac{[M(t)]}{[M_o]}\right)}{[M(t)]}$ versus time.

For completeness, we can again correct for the proportion of substrate unable to dimerize by using

$$[M_m(t)] = [M_{mo}]\left[\frac{1 - f'_d}{1 + (1 - f'_d)k_2 t} + f'_d\right].$$

where $[M_{mo}]$ is the concentration of initial substrate and f'_d is the percentage of substrate unable to dimerize. In practice, however, it is unlikely that both ends of an individual polymer will be unable to ligate. Therefore, f'_d is much smaller than f_d

and probably much less than 1. In this case, the above equation simplifies to equation 4.36.

Unlike the cyclization reaction, the bimolecular association reaction involves two molecules that can react in two ways with each other to form a dimer. As a result, the rate of dimerization is two times faster than that of a molecule with one reactive end. Therefore, once the reaction rate is computed, the result is divided by 2 to get the true rate of bimolecular association.

Case III: Both circles and dimers. When both circular and dimer products were formed, the individual rate constants were determined by optimizing the fit of equations 4.27 through 4.29 to the experimental data. To begin the optimization, the rate constants were estimated using the methods described assuming that only one product was formed. These were then refined as follows:

- New estimates of k_1 and k_2 were made by fitting the amount of unreacted product to the equation for [M(t)] (equation 4.29).
- A new estimate of k_1 was made by holding k_2 fixed and optimizing the fit of [C(t)] (equation 4.27) to the data.
- The estimate of k_2 was then refined by fixing k_1 and optimizing the fit of [Di(t)] (equation 4.28) to the data.

The last two steps were repeated until the individual rate constants changed by less than two percent upon further iteration. All curve fitting and optimization was performed using a Levenberg-Marquardt algorithm (KaleidaGraph) on a Mac PowerPC.

To measure J directly using equation 4.33, [C(t)] and [Di(t)] were plotted versus time and their respective limits, as t goes to zero, found by extrapolating backwards. Since the radioactivity in the dimers represents twice the concentration of dimers, J was determined from

$$J = 4\,[M_o]\ \lim_{t\to 0}\left(\frac{C(t)_r}{D(t)_r}\right) \tag{4.37}$$

where the subscript r represents measured radioactivity in the band [57].

Results and Discussion

As discussed in Chapter III, the mean of the distribution of circles formed in a DNA polymerization experiment is a relatively insensitive -- and at best -- qualitative measure of cyclization probability. As a result, small changes in DNA structure are likely undetectable. A more rigorous approach is to examine the kinetics of the competing cyclization and bimolecular association reactions directly on a single polymer. To further examine the effects of calicheamicin binding on DNA structure, these experiments were performed on a 273 bp DNA polymer under a wide range of calicheamicin concentrations. The data are consistent with our earlier observations that calicheamicin bends DNA when it binds.

The effect of calicheamicin ε binding on the cyclization kinetics of a 273 bp polymer. To enhance the sensitivity a DNA polymer to bend deformations introduced by calicheamicin binding, a molecule containing 13 repeats (273 bp) of the in-phase binding site construct (pAS1/13m9) was used. As described earlier, calicheamicin-induced bending in-phase with the helical repeat of B-DNA would add constructively to induce a large planar deformation that would bring the ends of the molecule in closer proximity, increasing the probability of cyclization.

The DNA substrate was prepared by cloning the appropriate plasmid (pAS1/13m9 grown in *E. coli* strain GM2163), isolating large quantities of the vector, digesting the DNA with *Sap* I and recovering the polymer by gel electrophoresis. The cyclization reactions were performed over a broad range of calicheamicin concentrations as described in the *Materials and Methods* section using the reaction conditions summarized in Table 4.1. Individual reaction products were resolved as shown in Figures 4.1 through 4.7 and identified by denaturing gel electrophoresis as discussed in Chapter III.

As expected, with increasing amounts of bound calicheamicin ε the reaction shifted from bimolecular association (intermolecular) to cyclization (intramolecular). In other words, calicheamicin binding at phased sites within the DNA molecule led to a greater number of circles being formed. At calicheamicin concentrations greater than 10 μM (approximately six moles of drug for every mole of binding site), only circles were formed.

The quantity of DNA remaining in the wells of each gel was randomly distributed and was not related to any single reaction product. Repeated extractions with phenol/chloroform and chloroform/isoamyl alcohol, and precipatation with

ethanol failed to improve the situation in a consistent manner. In all cases, however, the amount in the wells was small compared to the primary reaction products and had a negligible impact on the analysis.

The rate constants for bimolecular association and cyclization were determined at each drug concentration as described in the *Materials and Methods* section. In those cases where both circular and bimolecular products were measured, the individual rate constants were determined by the fitting the data to the system of partial differential equations (equations 4.30 - 4.32). For each experiment, initial guesses for the rate constants k_1 and k_2 were made by assuming that only circles or dimers formed respectively (equations 4.34 and 4.36) or by fitting the disappearance of unreacted substrate to equation 4.30. Since the percentage of unligatable substrate was less than 5%, the correction to equation 4.34 was unnecessary. An example of the iteration process is shown in Table 2 and graphs of the resulting curve fit in Figure 4.9. The ring closure probability, J, was determined by taking the ratio of the rate constants. For the calicheamicin concentrations shown in Figure 4.1 through 4.7, the results were:

[calicheamicin] (μM)	**k_1** (s^{-1})	**k_2** ($M^{-1}s^{-1}$)	**$J = k_1/k_2$** (Molar)
0	1·52e-4	1·87e+3	8·12e-8
0·1	2·37e-4	2·46e+3	9·65e-8
0·32	3·77e-4	2·56e+3	1·47e-7
1	4·59e-4	1·80e+3	2·55e-7
3.2	8·31e-4	727	1·14e-6
10	1·23e-3	136	9·01e-6
32		All Circles	
100		All Circles	

The calculation of the ring closure probability relies on the assumption that

$$\frac{k1}{k2} \approx \frac{K_C}{K_a} = J.$$

As discussed previously, this is true only if f_s and f_s' are very small and that [S] and [S_a] are much less than the K_m of T4 DNA ligase. Under these reaction conditions

with no calicheamicin ε the ring closure probability of the 13m9 polymer was approximately 10^{-7} M. This value is larger than that determined by other groups for similarly sized DNA fragments [52, 74, 83], but less than that expected for a polymer consisting of phased A-tracts [53, 56]. This is probably due to the increased length of our complementary ends (a 3 bp overhang rather than a 2 bp), which facilitates hydrogen bonding and thus the forming of a greater proportion of ligatable substrate. However, since J is near or below 10^{-6}, the relative amount of DNA available for ligation to a circle (*i.e.*, f_S) is likely small.

To avoid using two reactions to determine the rate constants, it was important that the DNA concentration was high enough to allow intermolecular reactions to occur at a detectable rate. In these experiments, k_2 was -- at most -- $2{\cdot}60 \times 10^3\ M^{-1}s^{-1}$. This is consistent with bimolecular association rates measured with the 5m9 polymer in earlier experiments (data not shown). In a DNA polymer with a two base pair complementary ends, Koo *et al.* [56] measured a k_2 of $2{\cdot}4 \times 10^2\ M^{-1}s^{-1}$, approximately 10-times less than ours. An estimate of K_a, by temperature jump methods, allowed them to calculate, based on a DNA concentration of 10 nM, an f_s' less than or equal to 0·0001. Given that the concentration of DNA used here is 6·7-times greater and the fact that f_s' was very small in their case, it appears reasonable to assume that our assumption that f_s' is small is also reasonable.

Finally, given the relatively small amount of DNA in the cyclization reactions, the concentration of ligatable substrates ([S] and [S_a]) could -- at most -- equal 65 nM which is only 10% of the K_m for T4 DNA ligase. Since f_s and f_s' are certainly much less than one, we can reasonably assume that [S] and [Sa] are much smaller than K_m.

Since all the conditions of the theoretical analysis appear to have been met, the ring closure probability, J, can be reasonably approximated by the ratio of the individual rate constants k_1 and k_2 .

The rate constants for bimolecular association and unimolecular cyclization for the 273 bp polymer of the in-phase binding site construct are shown in Figure 4.10. As more calicheamicin ε binds the DNA, the rate of cyclization, k_1, increases. This slow rise is consistent with bending while the slight oscillatory behavior may be the result of a small twist component. Any twist effects would likely by small since, as mentioned in Chapter III, the intrinsic flexibility of a molecule more than 250 bp in length effectively decouples the influence of one end's position on the other. Interestingly, the rate of dimerization, k_2, drops precipitously causing a near exponential rise in J. This may be the result of steric hindrance as the ends of the

molecule move closer together. (This observation forms the basis of the studies described in Chapter V where it is discussed in more detail.)

The effect of aryltetrasaccharide binding on the cyclization kinetics of a 273 bp polymer. The above experiment was repeated for the oligosaccharide side chain of calicheamicin. The results are plotted in Figure 4.11. The response of the in-phase polymer parallels that seen when calicheamicin ε binds DNA. This result provides further evidence that the aryltetrasaccharide is the structural motif responsible for calicheamicin's effect on DNA topology.

Summary

The effect of calicheamicin binding on the cyclization kinetics of a polymer with phased calicheamicin binding sites has been measured. The experiments were carefully designed to ensure that the individual rate constants for bimolecular association and unimolecular cyclization could be determined and used to estimate ring closure probability. Our results support the hypothesis that calicheamicin bends DNA when it binds and that the oligosaccharide is the structural motif responsible for these changes.

These data provide a unique opportunity to benchmark theoretical models of dynamic DNA behavior. Never before have the cyclization kinetics of the same DNA molecule been measured at different levels of planar bending. Premised on statistical mechanics and polymer chain theory, programs using Monte Carlo simulations of DNA dynamics have been used to fit empirical data to determine the mechanical properties of DNA. These same methods should be capable of estimating how much bending and twisting occurs as calicheamicin binds. The theoretical refinements should prove invaluable to our conceptual understanding of DNA structure and dynamics.

Table 4.1. General reaction conditions and calculated calicheamicin binding data.

[pAS1/13m9] (hot)	< 0·65 nM
[pAS1/13m9] (cold)	65 nM
[calicheamicin-ε] (in MeOH)	0 - 100μM (see below) MeOH = 2.5% v/v
[T4 DNA Ligase]	10 Units/ml

[calicheamicin] μM	moles CAL / moles bp	moles CAL/ moles bind. sites	% of binding sites occupied[a]
0	0	0	0
0·1	0·0056	0·059	2·4
0·32	0·017	0·18	7·5
1	0·056	0·59	21·4
3·2	0·17	1·8	49·8
10	0·56	5·9	78·8
32	1·7	18	92·5
100	5·6	59	97·7

[a] The percentage of sites occupied at a specific drug concentration was determined using equation 3.3 and assuming a K_a of $4{\cdot}3 \times 10^5\ M^{-1}$.

Table 4.2. Estimating rate constants k_1 and k_2 for pAS1/13m9 with 0·32 μM calicheamicin ε.

Iteration #	Equation fit	Fixed variable	new value of k_1	new value of k_2
initial	4.30 [M(t)]	none	-2·9e-3	1·61e+3
1	4.31 [C(t)]	k_2	4·4e-4	-
2	4.32 [D(t)]	k_1	-	2·52e+3
3	4.31 [C(t)]	k_2	3·77e-4	-
4	4.32 [D(t)]	k_1	-	2·56e+3
5	4.31 [C(t)]	k_2	3·77e-4	-

$$[M(t)] = \frac{M_o\, e^{-k_1 t}}{1 + 4\, M_o\, (1 - e^{-k_1 t})\, \frac{k_2}{k_1}} \qquad (4.30)$$

$$[C(t)] = \frac{k_1}{4\, k_2} \left\{ -k_1 t + \ln\left(\frac{M_o}{[M(t)]} \right) \right\} \qquad (4.31)$$

$$[Di(t)] = \frac{1}{2} (M_o - [C(t)] - [M(t)]) \qquad (4.32)$$

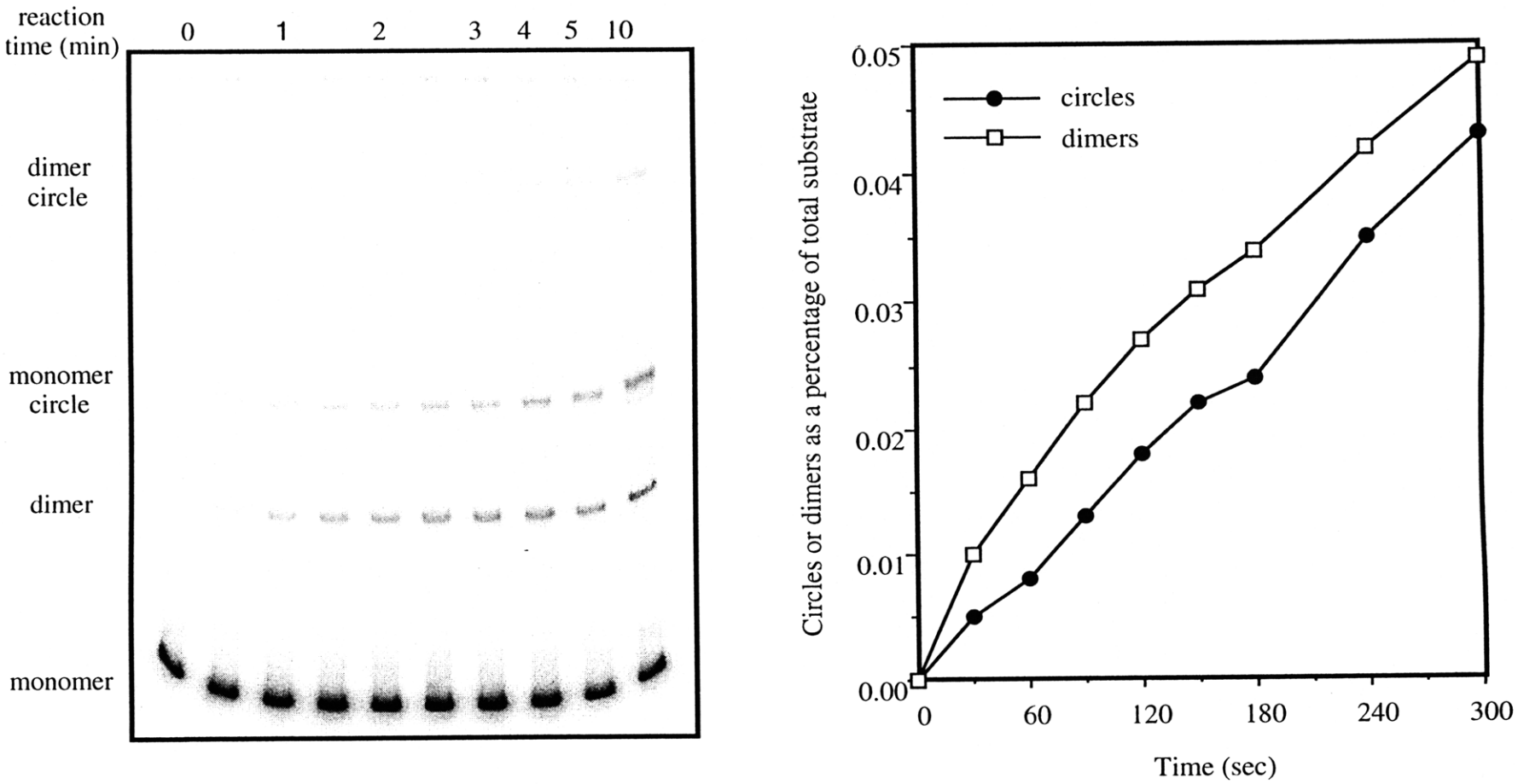

Figure 4.1. The cyclization and bimolecular association behavior of a 273 bp polymer of the in-phase binding site construct. Radiolabeled polymer was mixed with cold polymer at a ratio less than 1:100. MeOH was added to a final concentration of 2% v/v and the mixture allowed to equilibrate at 16° C. The reaction was initiated by adding T4 DNA ligase. At specific time points, aliquots were removed and the reaction stopped by adding EDTA and heat-killing the enzyme. Reaction products were resolved on 4% polyacrylamide gels and quantified by phosphorimager analysis.

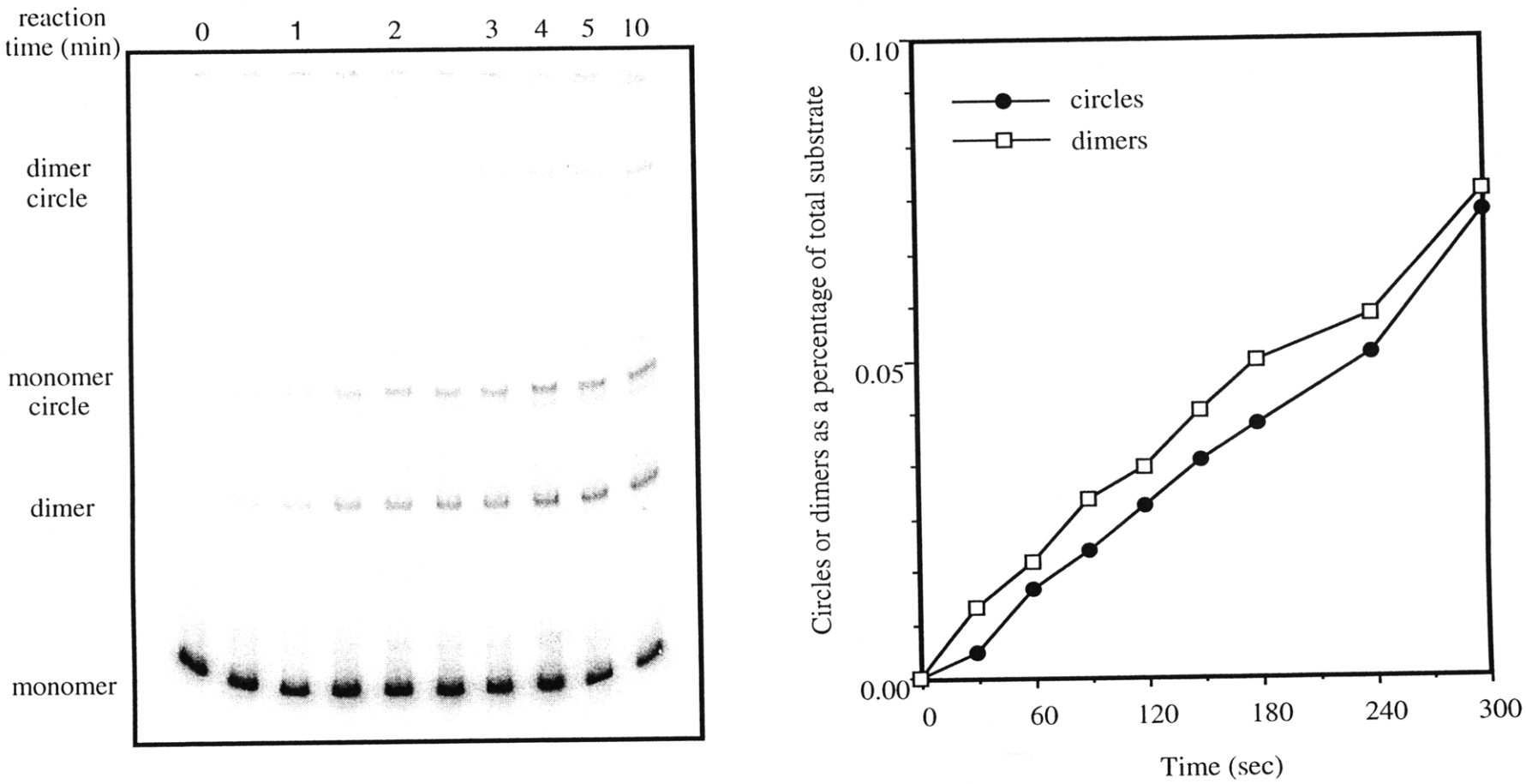

Figure 4.2. The effect of 0.1 μM calicheamicin ε on the cyclization and bimolecular association behavior of a 273 bp polymer of the in-phase binding site construct. Radiolabeled polymer was mixed with cold polymer at a ratio less than 1:100. Calicheamicin ε was added and the mixture allowed to equilibrate at 16° C. The reaction was initiated by adding T4 DNA ligase. At specific time points, aliquots were removed and the reaction stopped by adding EDTA and heat-killing the enzyme. Reaction products were resolved on 4% polyacrylamide gels and quantified by phosphorimager analysis.

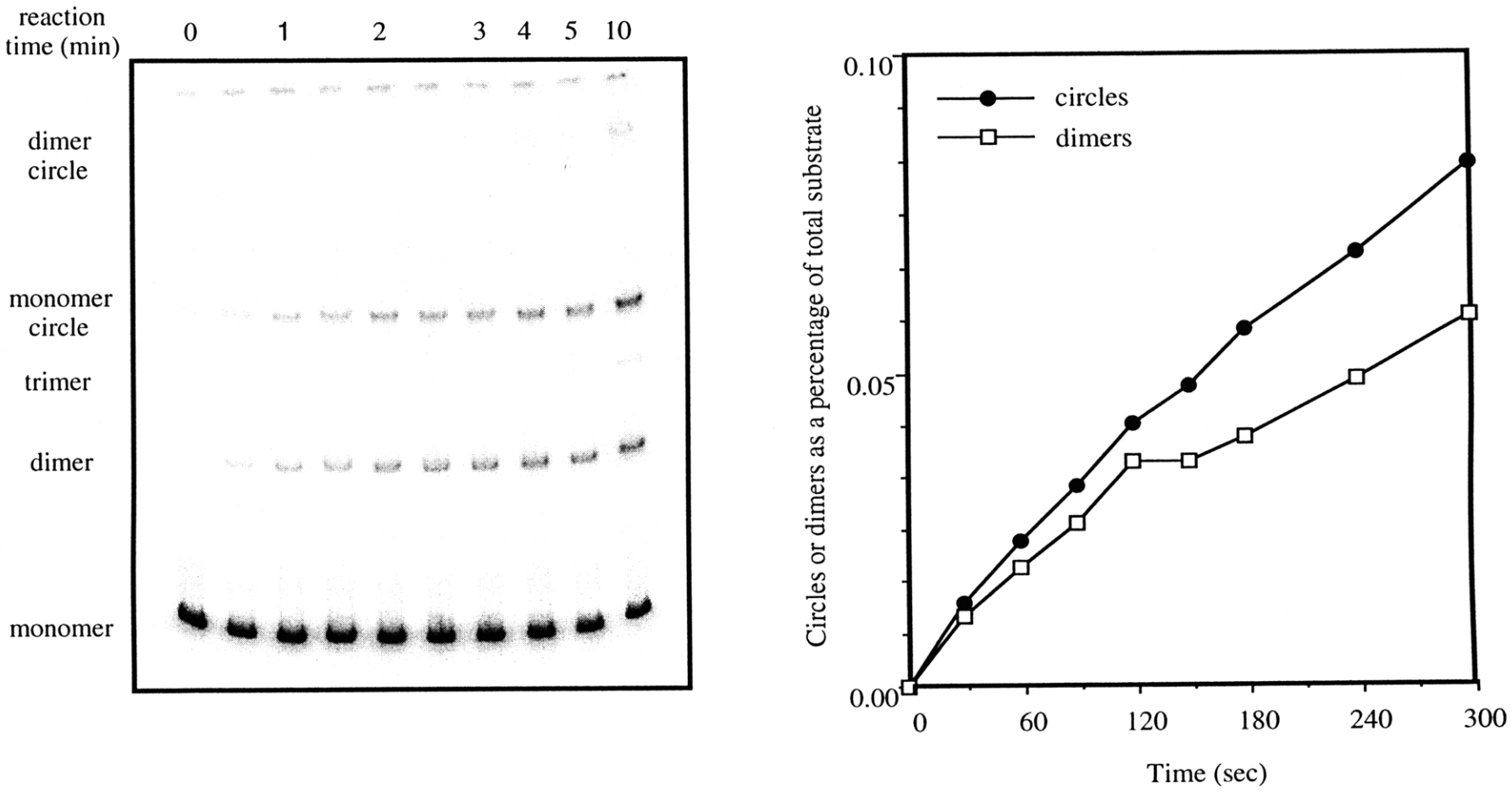

Figure 4.3. The effect of 0.32 μM calicheamicin ε on the cyclization and bimolecular association behavior of a 273 bp polymer of the in-phase binding site construct. Radiolabeled polymer was mixed with cold polymer at a ratio less than 1:100. Calicheamicin ε was added and the mixture allowed to equilibrate at 16° C. The reaction was initiated by adding T4 DNA ligase. At specific time points, aliquots were removed and the reaction stopped by adding EDTA and heat-killing the enzyme. Reaction products were resolved on 4% polyacrylamide gels and quantified by phosphorimager analysis.

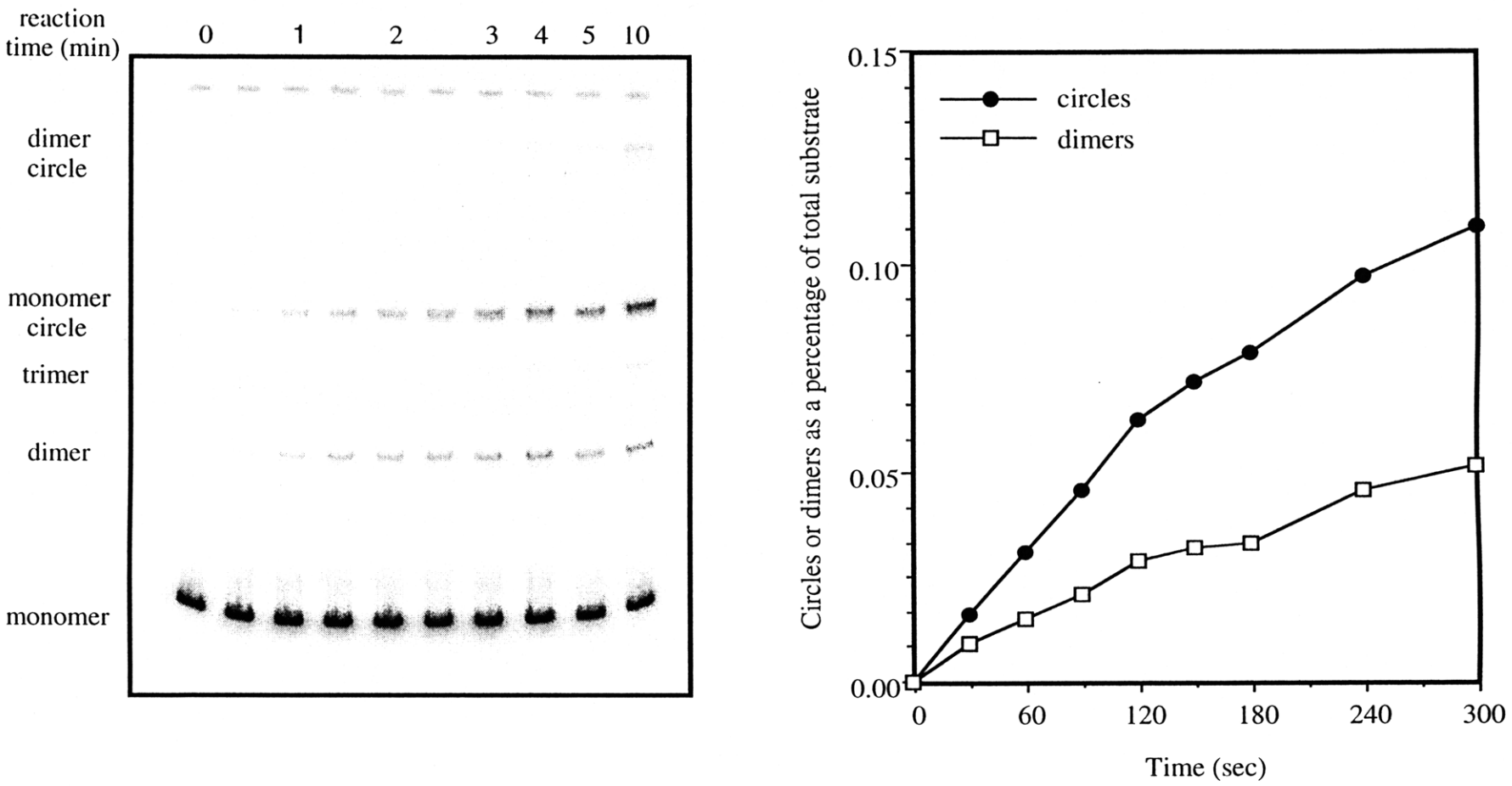

Figure 4.4. The effect of 1 μM calicheamicin ε on the cyclization and bimolecular association behavior of a 273 bp polymer of the in-phase binding site construct. Radiolabeled polymer was mixed with cold polymer at a ratio less than 1:100. Calicheamicin ε was added and the mixture allowed to equilibrate at 16° C. The reaction was initiated by adding T4 DNA ligase. At specific time points, aliquots were removed and the reaction stopped by adding EDTA and heat-killing the enzyme. Reaction products were resolved on 4% polyacrylamide gels and quantified by phosphorimager analysis.

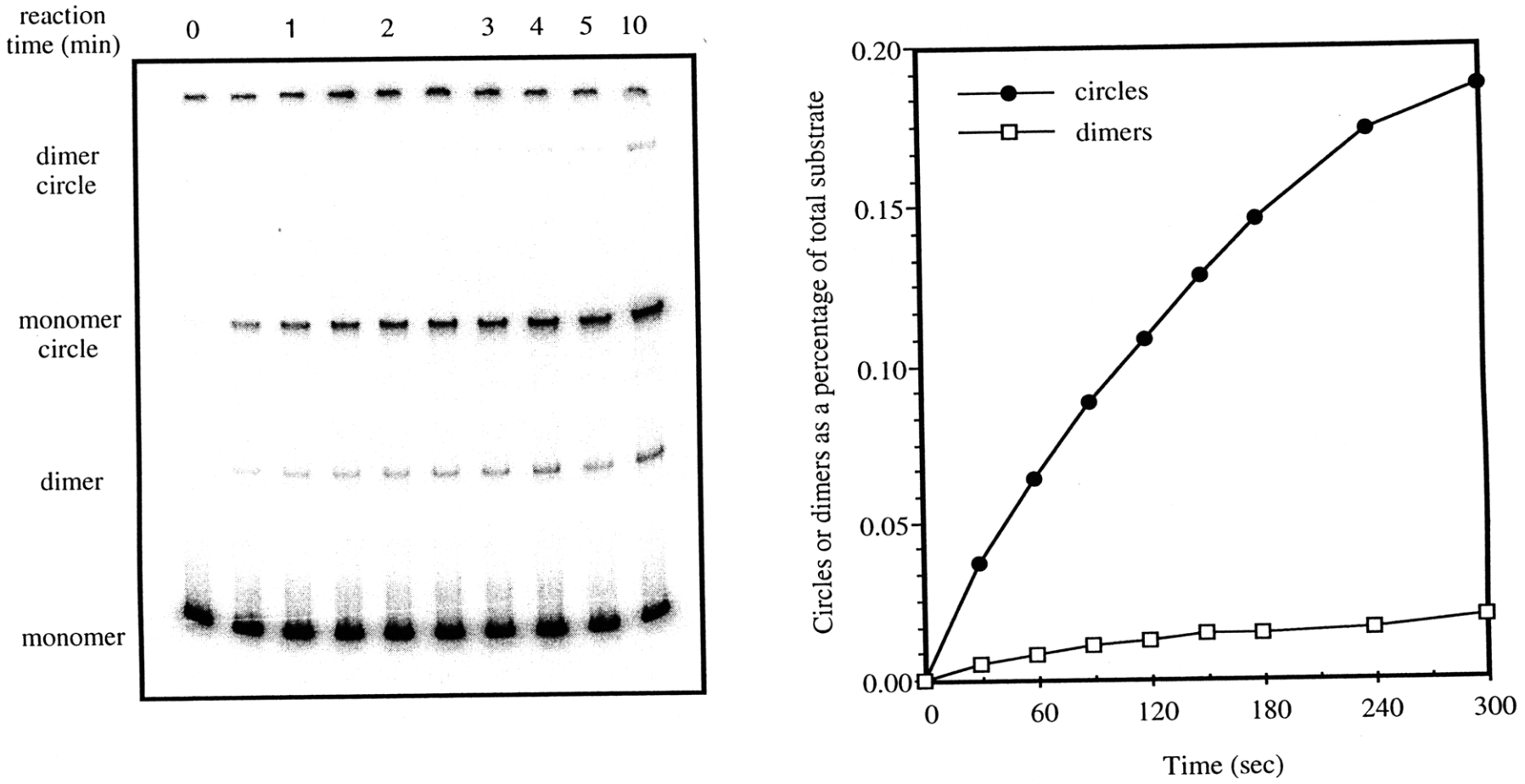

Figure 4.5. The effect of 3.2 μM calicheamicin ε on the cyclization and bimolecular association behavior of a 273 bp polymer of the in-phase binding site construct. Radiolabeled polymer was mixed with cold polymer at a ratio less than 1:100. Calicheamicin ε was added and the mixture allowed to equilibrate at 16° C. The reaction was initiated by adding T4 DNA ligase. At specific time points, aliquots were removed and the reaction stopped by adding EDTA and heat-killing the enzyme. Reaction products were resolved on 4% polyacrylamide gels and quantified by phosphorimager analysis.

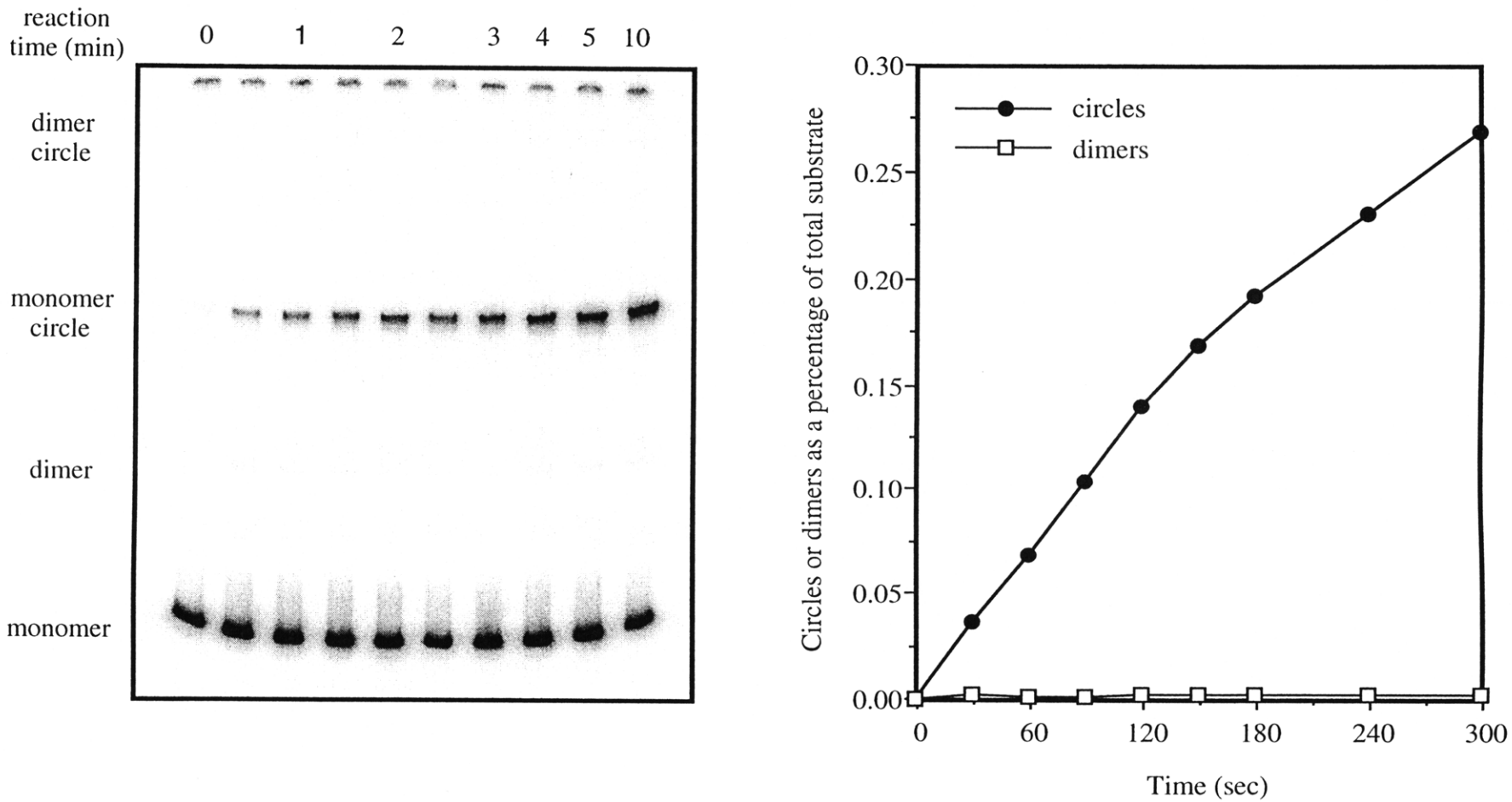

Figure 4.6. The effect of 10 μM calicheamicin ε on the cyclization and bimolecular association behavior of a 273 bp polymer of the in-phase binding site construct. Radiolabeled polymer was mixed with cold polymer at a ratio less than 1:100. Calicheamicin ε was added and the mixture allowed to equilibrate at 16° C. The reaction was initiated by adding T4 DNA ligase. At specific time points, aliquots were removed and the reaction stopped by adding EDTA and heat-killing the enzyme. Reaction products were resolved on 4% polyacrylamide gels and quantified by phosphorimager analysis.

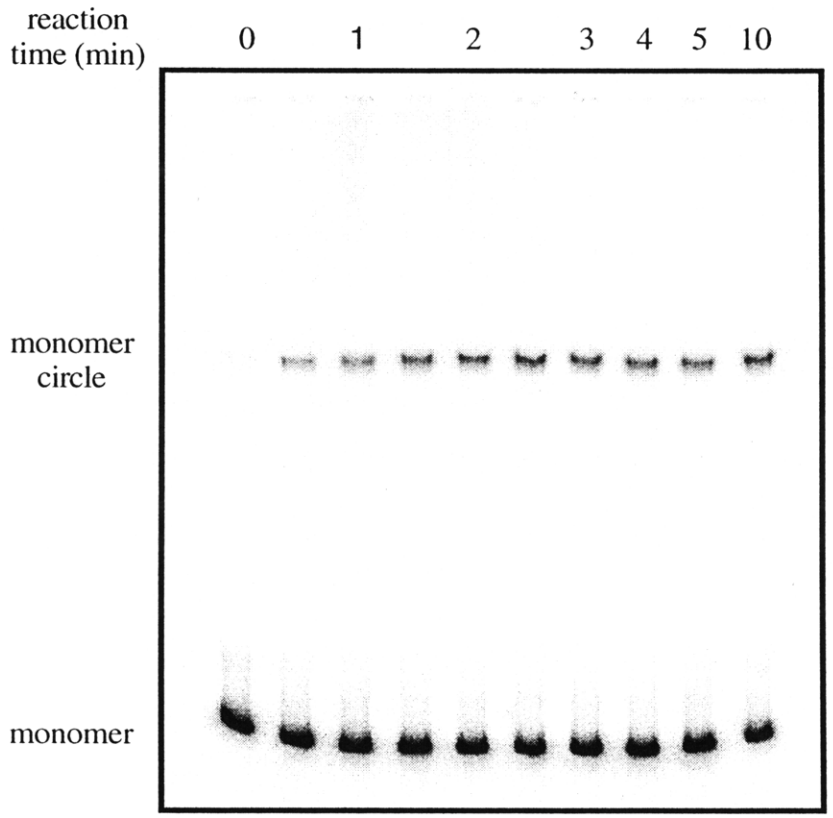

Figure 4.7. The effect of 32 μM calicheamicin ε on the cyclization and bimolecular association behavior of a 273 bp polymer of the in-phase binding site construct. Radiolabeled polymer was mixed with cold polymer at a ratio less than 1:100. Calicheamicin ε was added and the mixture allowed to equilibrate at 16° C. The reaction was initiated by adding T4 DNA ligase. At specific time points, aliquots were removed and the reaction stopped by adding EDTA and heat-killing the enzyme. Reaction products were resolved on 4% polyacrylamide gels and quantified by phosphorimager analysis.

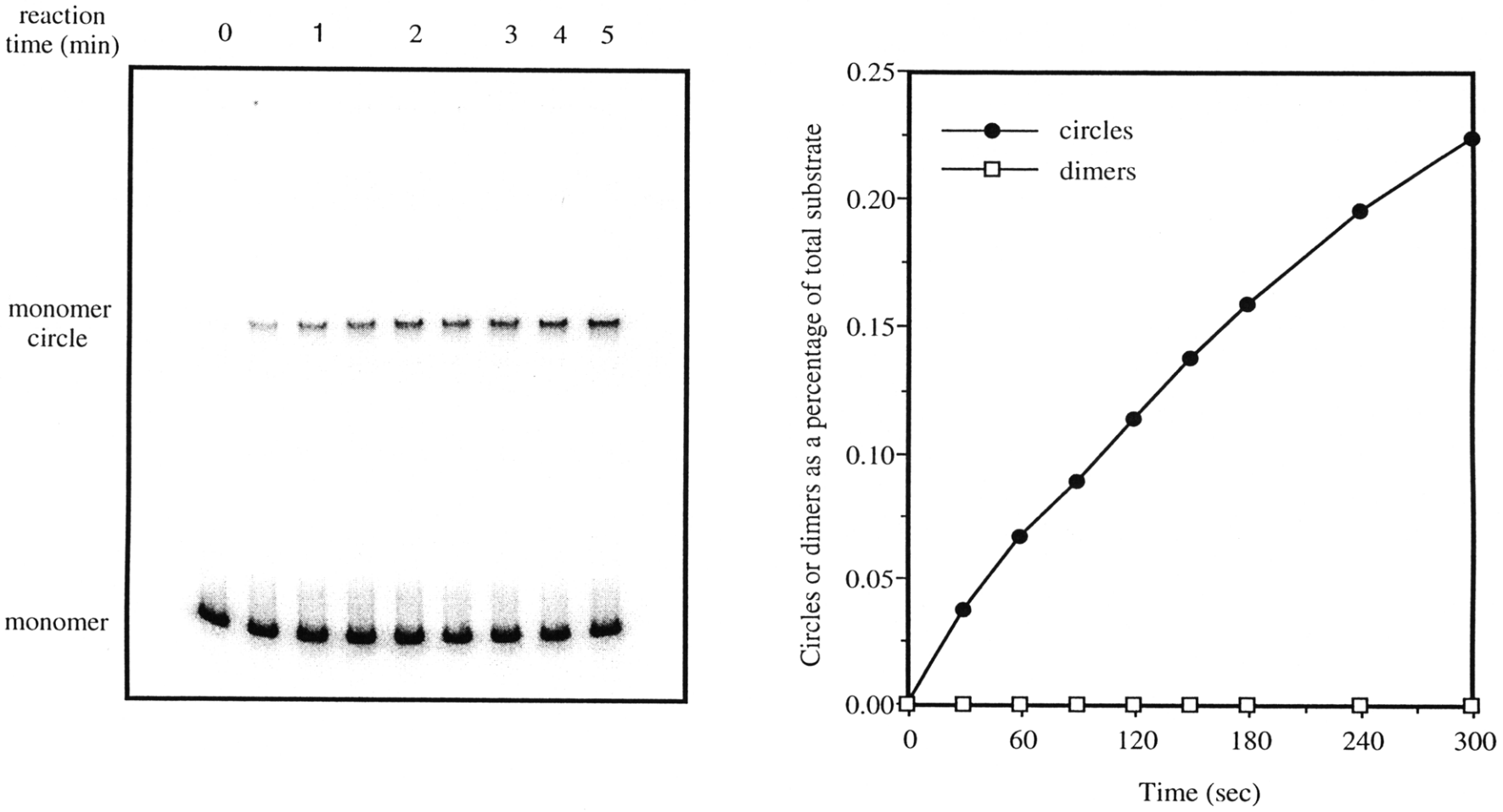

Figure 4.8. The effect of 100 μM calicheamicin ε on the cyclization and bimolecular association behavior of a 273 bp polymer of the in-phase binding site construct. Radiolabeled polymer was mixed with cold polymer at a ratio less than 1:100. Calicheamicin ε was added and the mixture allowed to equilibrate at 16° C. The reaction was initiated by adding T4 DNA ligase. At specific time points, aliquots were removed and the reaction stopped by adding EDTA and heat-killing the enzyme. Reaction products were resolved on 4% polyacrylamide gels and quantified by phosphorimager analysis.

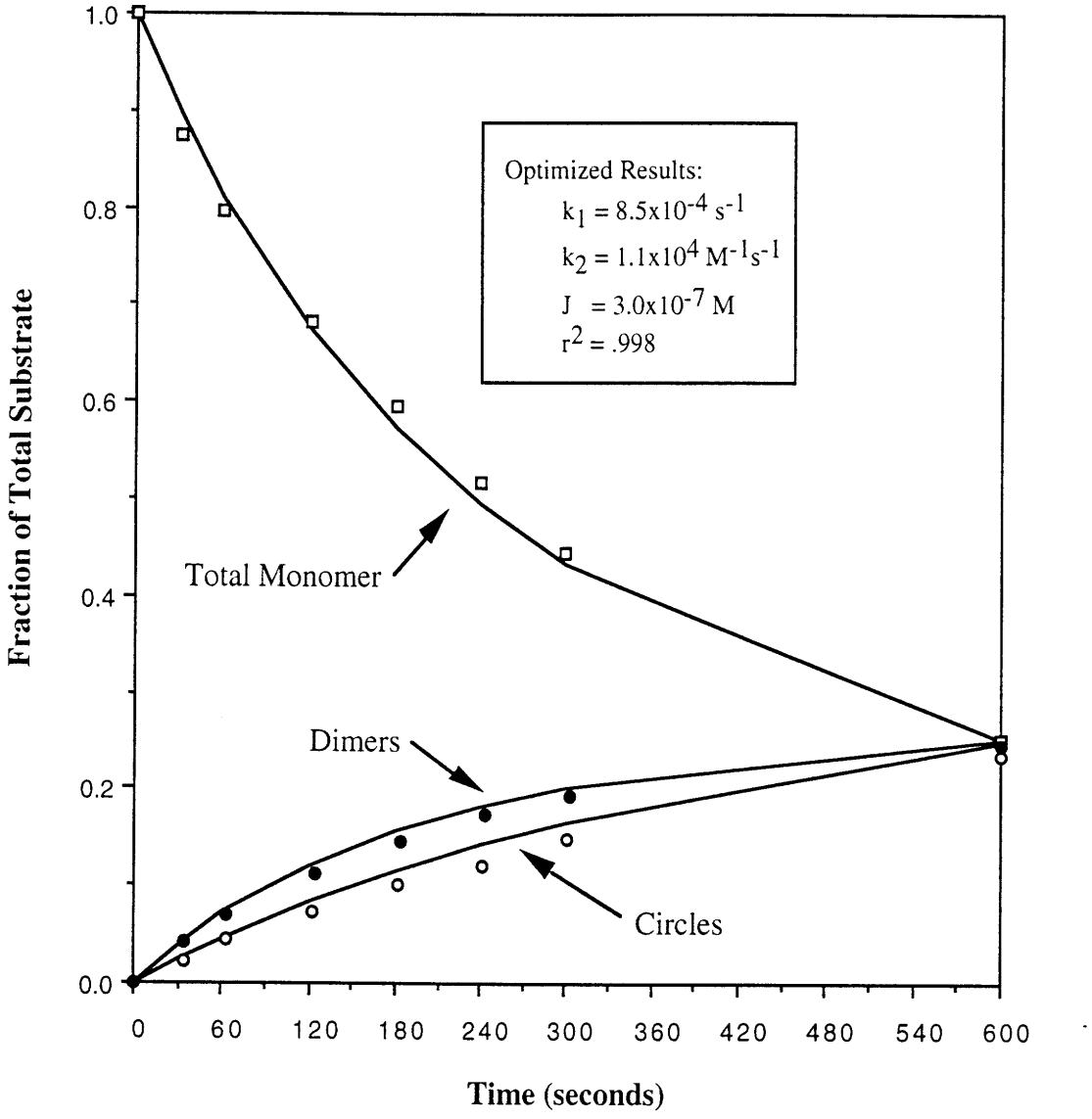

Figure 4.9. Reaction substrate and products versus time for the cyclization of the 273 bp polymer of the in-phase construct. Points represent empirical measurements of the unreacted substrate, M(t), circles, C(t), and polymerized DNA, D(t). Solid lines are plots of equations 4.30, 4.31 and 4.32 after estimates of k_1 and k_2 have been optimized to fit the data.

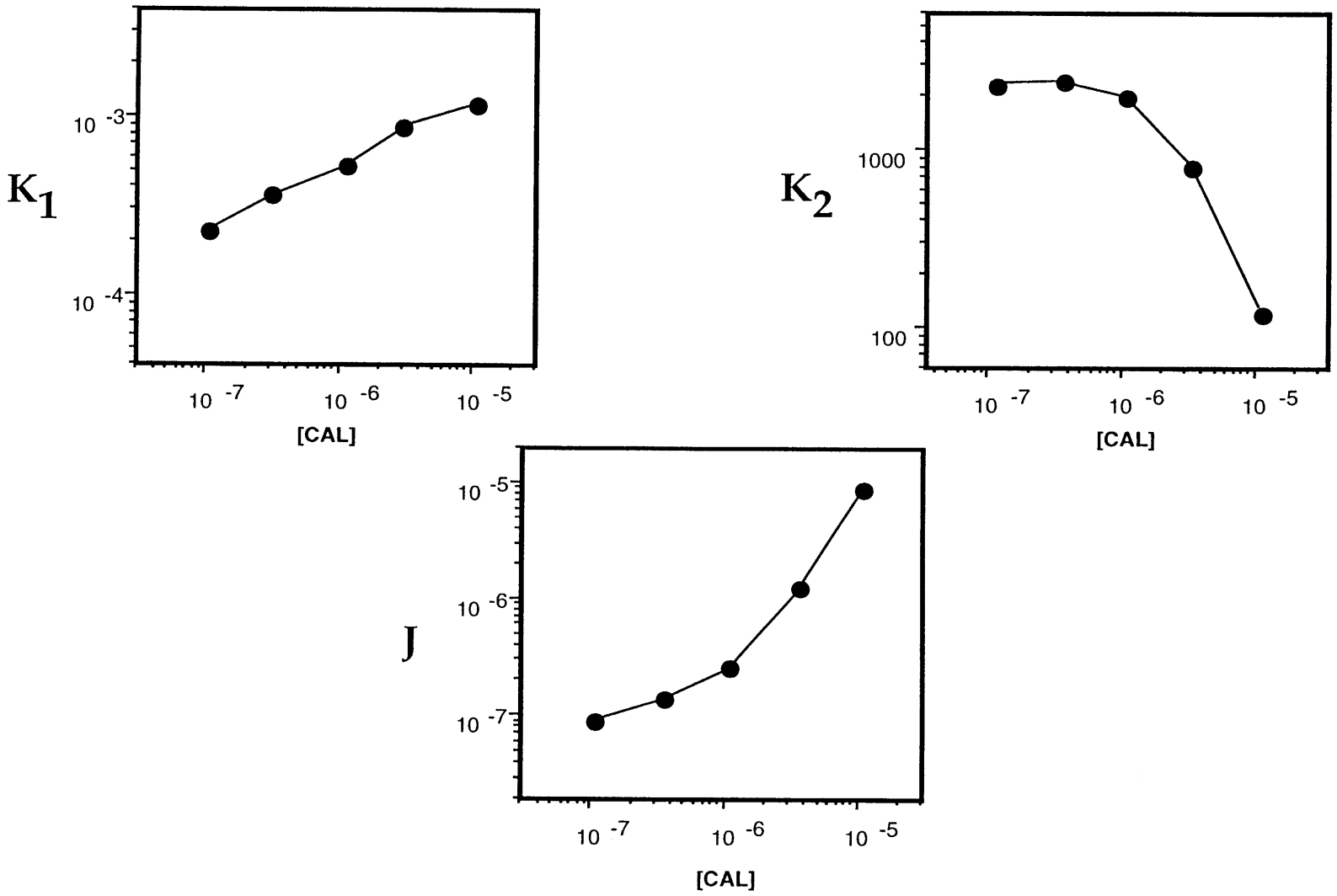

Figure 4.10. The rate constants for cyclization and bimolecular association of the 273 bp in-phase polymer. Estimates of k_1 (s^{-1}) and k_2 ($M^{-1}s^{-1}$) were determined for each drug concentration by optimizing the fit of equations 4.30, 4.31 and 4.32 to the data obtained from the gels shown in Figures 4.1 through 4.8 . The ring closure probability, J (Molar), was estimated by taking the ratio of the two individual rate constants.

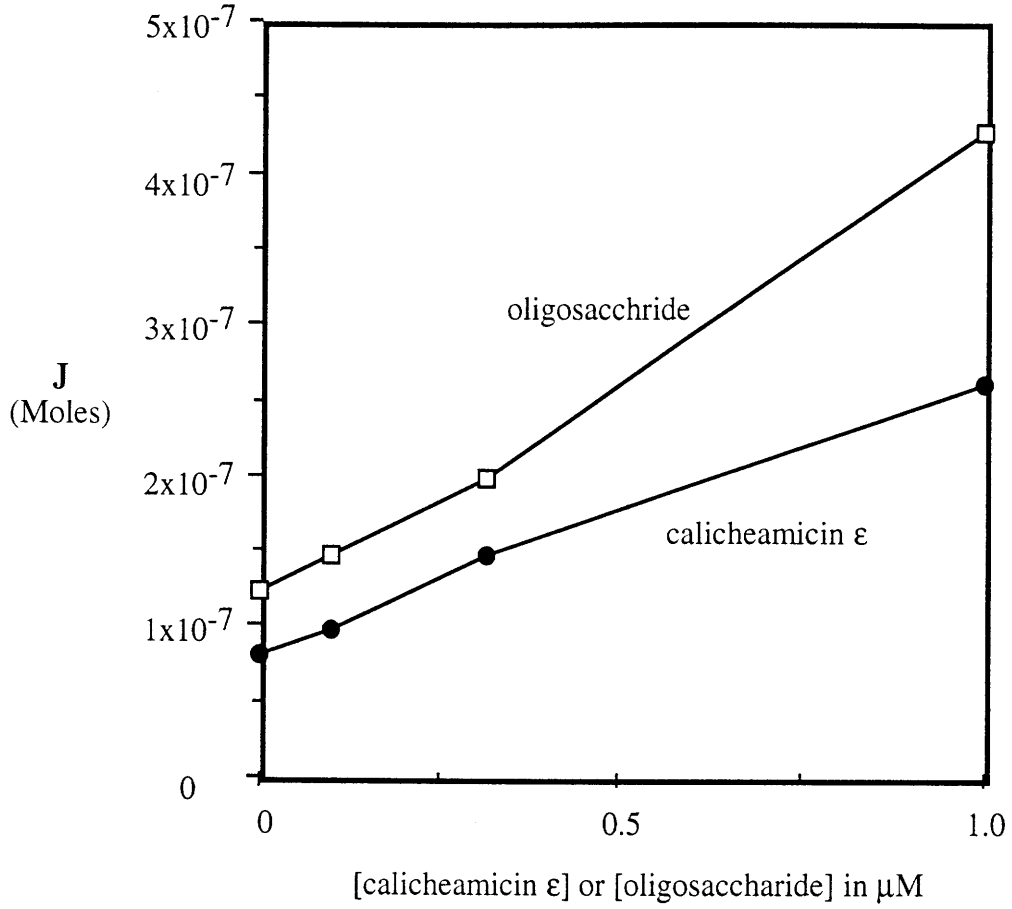

Figure 4.11. The effect of calicheamicin ε and its oligosaccharide on the cyclization kinetics of the 273 bp in-phase polymer. Experiments were performed as described previously.

CHAPTER V

The Influence of DNA Length and Structure on the Kinetics of Bimolecular Association

When calicheamicin ε bound the DNA polymer containing drug binding sites repeated in-phase with the helical repeat of B-DNA, the rate of unimolecular cyclization, k_1, increased while the rate of bimolecular association, k_2, decreased. In other words, at high drug concentrations the addition of calicheamicin ε, or the curvature of the DNA molecule, somehow inhibited the ability of the DNA to dimerize. Since bimolecular association involves the joining of ends from two different molecules, it has long been assumed that the rate of dimerization is independent of the individual molecule's length or curvature [52]. In fact, this assumption is a necessary prerequisite to the determination of the ring closure probability, J, when shorter DNA molecules are used to empirically measure k_2 (see the section "Experimental Design - Measurement of Rate Constants" in Chapter IV). Given the importance of this assumption to measuring the kinetic properties of DNA, an experiment was designed to verify whether this indeed was the case.

Experimental Method

To rule out the possibility that the effects observed in Chapter IV were due to a nonspecific interaction of calicheamicin ε with either the DNA polymer or T4 DNA ligase, we repeated the kinetic studies with a polymer too short to cyclize (3m9 - three 21 bp repeats of the in-phase binding site construct). The short polymer preserved the radius of curvature induced by calicheamicin bending but, because of its reduced length, still kept the ends far apart. As a result, intramolecular cyclization was extremely unlikely. If calicheamicin was responsible for the reduced rate in dimerization, then this effect should be observed in the smaller DNA molecule.

Methods and Materials

Reagents and DNA substrates. Calicheamicin ε was provided by Dr. George Ellestad (Wyeth Ayerst Research) or synthesized as described Chapter II. All enzymes were obtained from New England Biolabs. Deoxyoligonucleotides were prepared as described in Chapter II.

Preparation of large quantities of a specific polymer construct. Clones containing specific polymers were constructed, identified and amplified as described in the *Materials and Methods* section of Chapter IV.

HPLC purification of pAS1 restriction fragments. GM2163 *E. coli* were transfected with the appropriate plasmid containing either the 13m9 or 3m9 polymer and grown in large quantities as described in Chapter IV. The plasmid DNA was isolated using Qiagen Giga-Preps (Qiagen) and purified, if necessary, on CsCl gradient to remove genomic contamination. The DNA was digested with *Sap* I (1 unit/μg under standard reaction conditions), extracted once with phenol/chloroform, once with chloroform/isoamyl alcohol and ethanol precipitated. The polymers were purified by HPLC on a Nucleogen-DEAE 500-7 weak anion exchange column under the following conditions:

time (min)	% Buffer A	% Buffer B
0 - 5	90	10
15 - 20	50	50
80	0	100

where buffer A is 25 mM CHES, buffer B is 25 mM CHES and 1·2 M ammonium sulfate, and the flow rate is 1 ml/min. Using this profile, 3m9, 6m9, 9m9 and 12m9 have been separated from plasmid DNA (See Figure 5.1). The appropriate peak was collected and dialyzed repeatedly (at least four times at a 1:100 v:v ratio) against a 50-fold dilution of TE (1 mM EDTA, 10 mM Tris-HCl pH 7·6). The sample was then lyophilized, resuspended in 200 μl of sterile double deionized H_2O, and dialyzed again against sterile TE. The DNA was quantified by UV absorption at 260 nm.

Preparation of radiolabeled DNA. DNA polymers used in the cyclization experiments were radiolabeled as described in the *Materials and Methods* section of Chapter IV.

DNA cyclization reactions. The circle closure experiments were performed as described in the *Materials and Methods* section of Chapter IV.

Methods of Analysis. The individual rate constants as well as the ring closure probabilities were determined by the protocols described in the *Materials and Methods* section of Chapter IV.

Results and Discussion

The effect of calicheamicin ε binding on the cyclization kinetics of the 13m9 polymer suggested that somehow drug binding inhibited the ability of the DNA molecule to form intermolecular dimers. To determine whether these results were a response to drug interactions with T4 DNA ligase or with the DNA molecule itself, the experiment was repeated with a DNA polymer too short to cyclize under the identical reaction conditions.

The 3m9 DNA was prepared by cloning the appropriate plasmid (pAS1/3m9 grown in *E. coli* strain GM2163), isolating large quantities of the plasmid DNA, digesting with *Sap* I and recovering the polymer by gel electrophoresis or HPLC. The cyclization reactions were performed as described in the *Materials and Methods* section in Chapter IV. Radiolabeled polymer was mixed with cold polymer at a ratio less than 1:100. Calicheamicin ε or MeOH was added and the mixture allowed to equilibrate at 16° C. The reaction was initiated by adding T4 DNA ligase. At specific time points, aliquots were removed and the reaction stopped by adding EDTA and heat-killing the enzyme. The reaction products were then loaded directly on 4% agarose or 4% polyacrylamide gels. Individual reaction products were identified by non-denaturing gel electrophoresis and quantified by phosphorimager analysis as described in Chapter III.

The results for these experiments are shown in Figures 5.2 - 5.5. Since no circles were formed, the rate constant for bimolecular association was determined by optimizing the fit of equation 4.36 to the experimental data. The dimerization rates for both the 13m9 and the 3m9 polymers are shown in Figure 5.6. Unlike the 13m9

DNA, the 3m9 does not show a significant reduction in the rate of bimolecular association over the same drug concentrations. This rules out the possibility that calicheamicin may be interfering with ligase activity or somehow impeding the molecule ends from joining.

An explanation consistent with these results is that the relative proximity of the ends of the DNA molecule affects the polymers ability to dimerize. In other words, if the ends of the molecule are close together, they sterically interfere with other molecules attempting to access the DNA. We could then explain the 13m9 results as follows: With no calicheamicin bound, the polymer cyclizes and dimerizes at rates k_1 and k_2 respectively. At low levels of drug binding, the polymer begins to bend. However, since only a few of the sites are bound, the overall curvature of the molecule is relatively small and the ends remain far apart. The rate of cyclization increases but the rate of dimerization remains unchanged. At high concentrations of calicheamicin ε a significant quantity of drug is bound. The polymer is highly bent and the ends move close together increasing the rate of cyclization. At the same time, however, the relative proximity of the ends inhibits the access of other polymers attempting to dimerize, thereby reducing the rate of dimerization. In other words, the rate of dimerization is dependent upon the relative proximity of the ends which, in turn, is determined by the length and curvature of the DNA. Kahn and Crothers have noted a similar change in the rate of dimerization in a DNA molecule bent by proteins [71].

These results cause us to reconsider the theoretical model for the dimerizing molecule. If the ends of the DNA are in close proximity (*i.e.*, highly curved DNA), then the rate-limiting step of the overall bimolecular association reaction is no longer the ligation process. Instead, formation of the ligatable substrate k_{12} may be rate limiting and k_{21} may be greater than k_{12}.

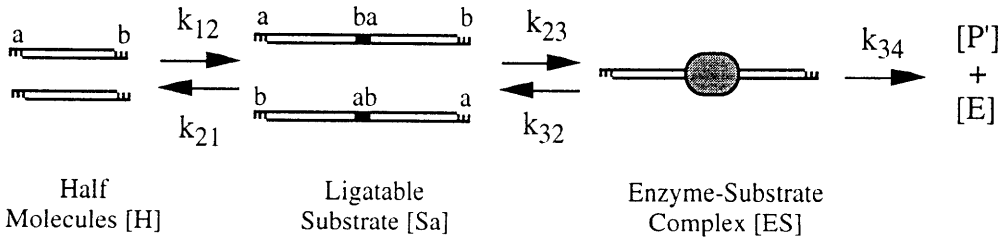

As a result, the expression for k_2 (equation 4.23),

$$k_2 = \frac{K_a k_{34} [E_o] (1 - f_s')^2}{K_m + [Sa]}$$

may not be valid for highly curved DNA molecules since the equilibrium constant, K_a, may not be independent of DNA length and curvature.

These results have serious ramifications for the calculation of k_1, the rate of cyclization, in highly curved DNA molecules. As discussed in Chapter IV, the ring closure probability, J, can be measured directly. The rate of cyclization, k_1, can then be estimated by determining k_2 in a separate reaction on a DNA substrate with ends identical to the original but too short to cyclize and equation 4.24,

$$J = \frac{k_1}{k_2}.$$

However, our results suggest that -- for highly curved DNA -- k_2 in the longer DNA is less than k_2 in the shorter DNA. Therefore, estimates of k_1 based on

$$k_1 = J(\text{long}) \cdot k_2(\text{short})$$

are larger than their actual values. This result, calls into question the cyclization rates measured using this method.

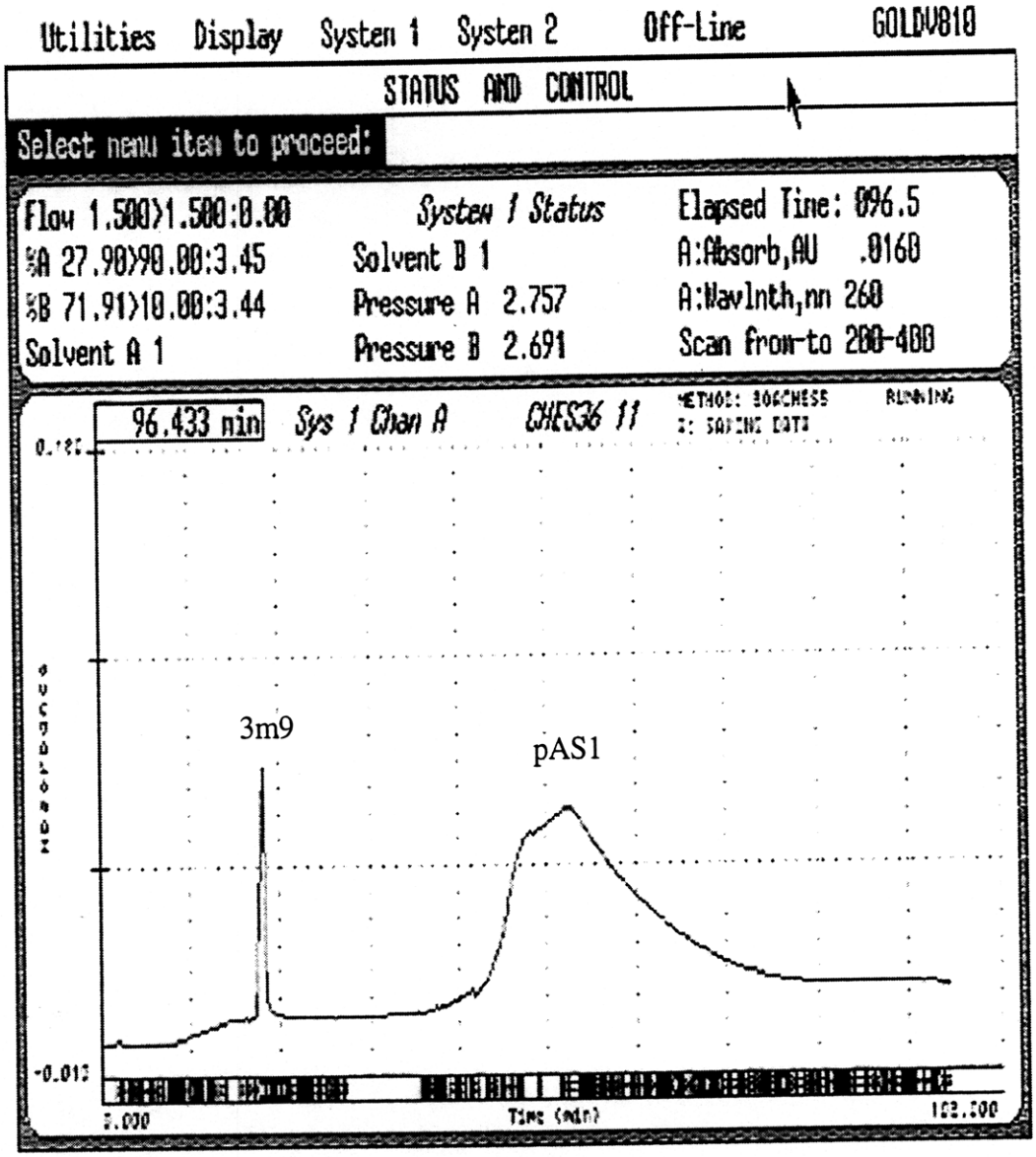

Figure 5.1. HPLC purification of pAS1 restriction fragments. *Sap* I digested pAS1/3m9 was purified by HPLC as described in the text.

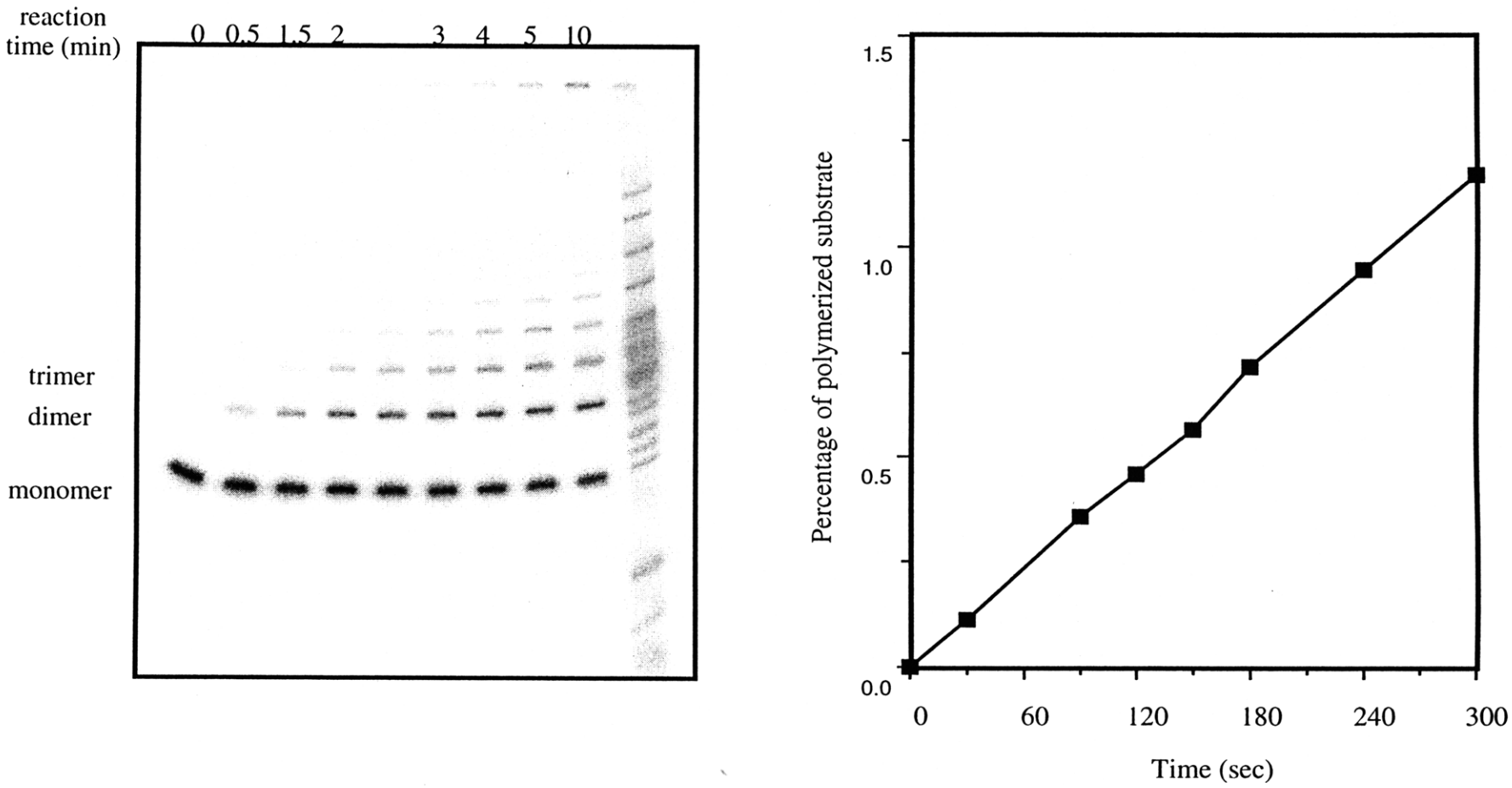

Figure 5.2. The bimolecular association kinetics of the 63 bp polymer of the in-phase binding site construct. Radiolabeled polymer was mixed with cold polymer at a ratio less than 1:100. MeOH was added to a final concentration of 2% v/v and the mixture allowed to equilibrate at 16° C. The reaction was initiated by adding T4 DNA ligase. At specific time points, aliquots were removed and the reaction stopped by adding EDTA and heat-killing the enzyme. Reaction products were resolved on 4% polyacrylamide gels and quantified by phosphorimager analysis.

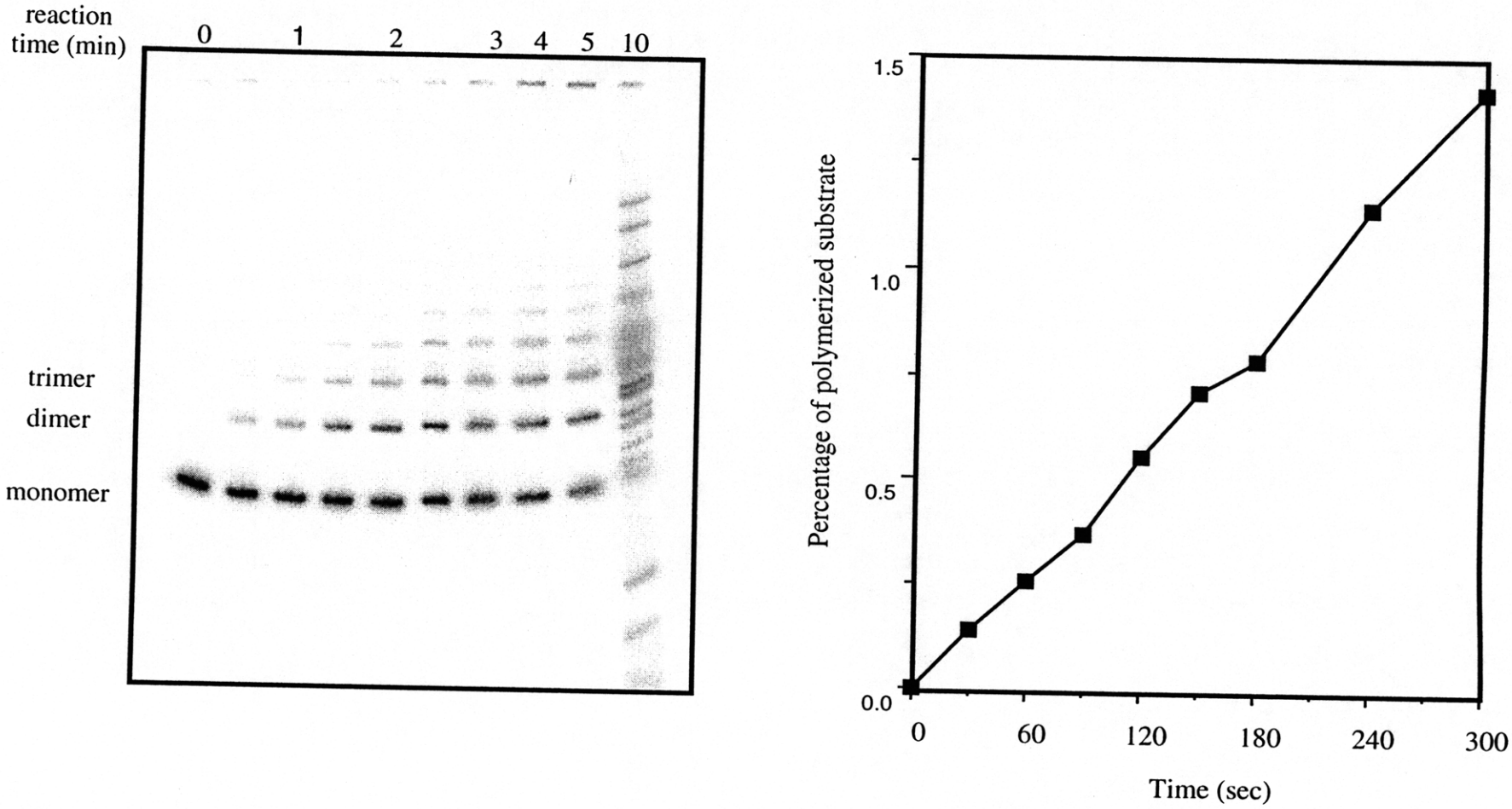

Figure 5.3. The effect of 4 μM calicheamicin ε on the bimolecular association kinetics of a 63 bp polymer of the in-phase binding site construct. Radiolabeled polymer was mixed with cold polymer at a ratio less than 1:100. Calicheamicin ε was added and the mixture allowed to equilibriate at 16° C. The reaction was initiated by adding T4 DNA ligase. At specific time points, aliquots were removed and the reaction stopped by adding EDTA and heat-killing the enzyme. Reaction products were resolved on 4% polyacrylamide gels and quantitated by phosphorimager analysis.

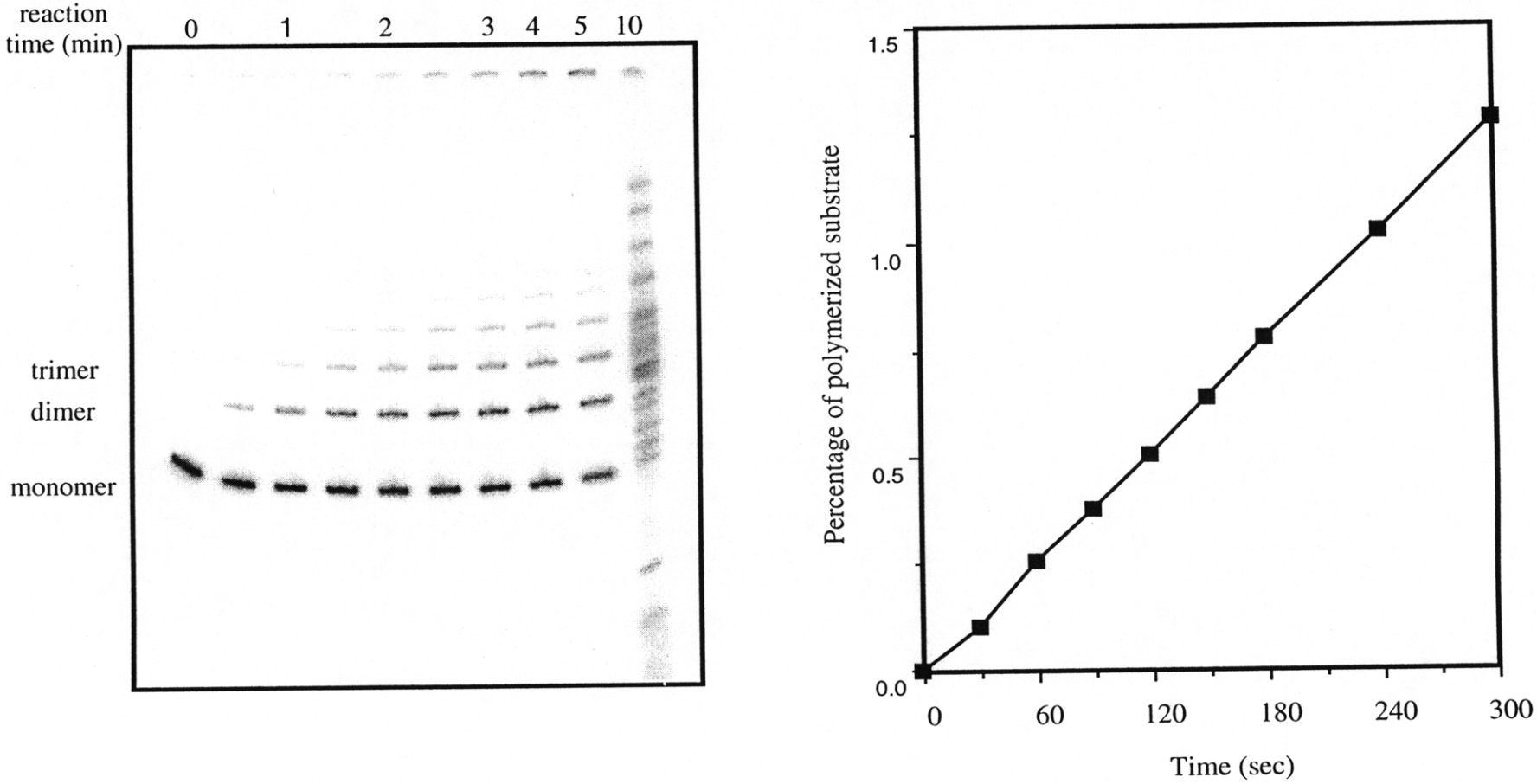

Figure 5.4. The effect of 40 μM calicheamicin ε on the bimolecular association kinetics of a 63 bp polymer of the in-phase binding site construct. Radiolabeled polymer was mixed with cold polymer at a ratio less than 1:100. Calicheamicin ε was added and the mixture allowed to equilibriate at 16° C. The reaction was initiated by adding T4 DNA ligase. At specific time points, aliquots were removed and the reaction stopped by adding EDTA and heat-killing the enzyme. Reaction products were resolved on 4% polyacrylamide gels and quantitated by phosphorimager analysis.

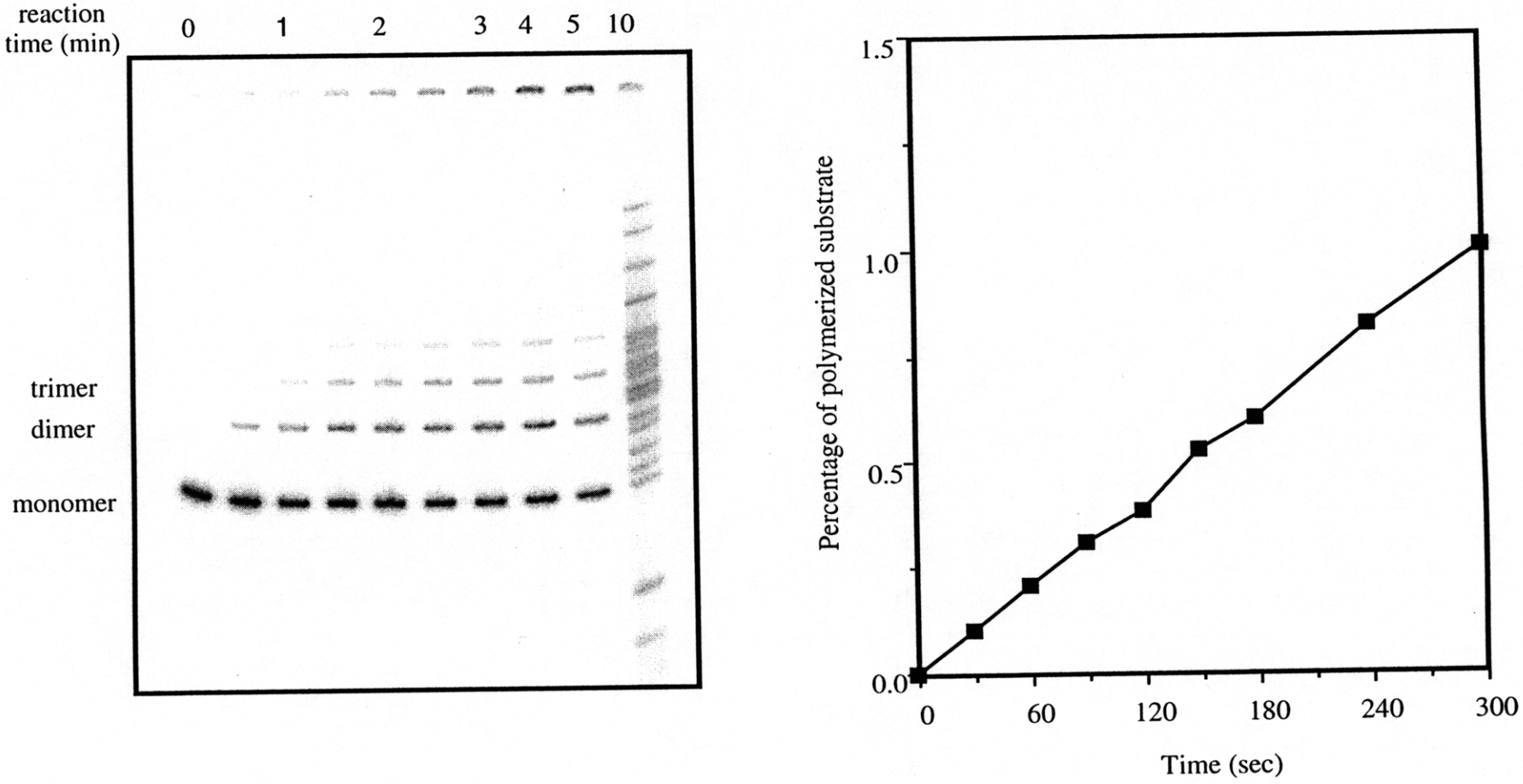

Figure 5.5. The effect of 400 μM calicheamicin ε on the bimolecular association kinetics of a 63 bp polymer of the in-phase binding site construct. Radiolabeled polymer was mixed with cold polymer at a ratio less than 1:100. Calicheamicin ε was added and the mixture allowed to equilibriate at 16° C. The reaction was initiated by adding T4 DNA ligase. At specific time points, aliquots were removed and the reaction stopped by adding EDTA and heat-killing the enzyme. Reaction products were resolved on 4% polyacrylamide gels and quantitated by phosphorimager analysis.

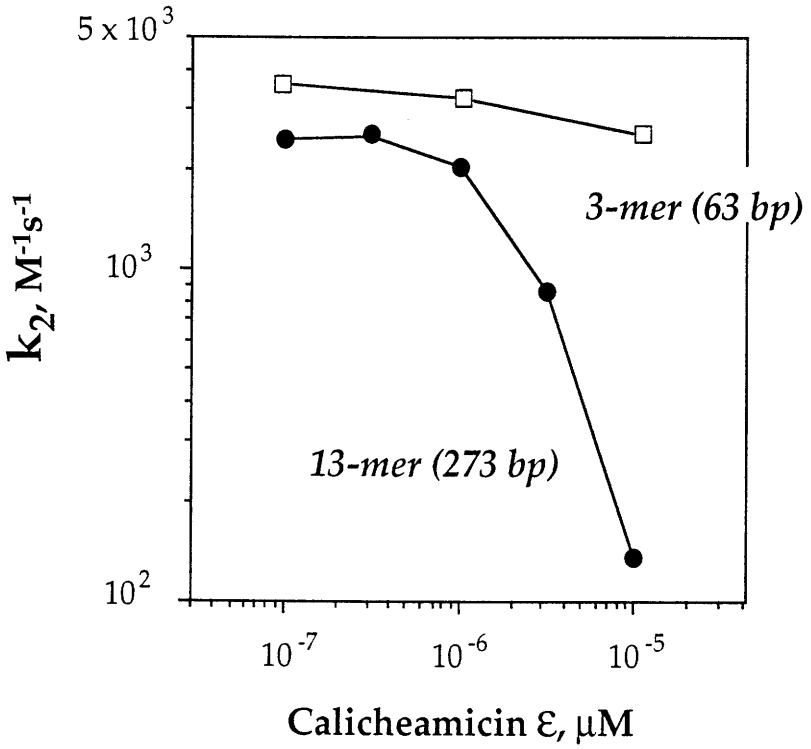

Figure 5.6. Rate of bimolecular association for the 63 and 273 bp polymers of the in-phase DNA construct. The rate of dimerization for 63 bp polymer was determined from the data shown in Figures 5.2 through 5.5 using equation 4.36. The rate constant was then scaled to account for multiple reactive ends and different ligase concentration. The rate of dimerization for 273 bp polymer was calculated as described in Figure 4.10.

CHAPTER VI

Determinants of Calicheamicin-Induced DNA Damage

Calicheamicin is a potent antitumor antibiotic that causes sequence-specific oxidation of the deoxyribose of DNA [2, 7, 8, 88]. Although the drug makes several base-specific contacts along the minor groove, the broad range of sequences bound [8, 35, 36, 43, 81] and the sensitivity of calicheamicin-induced DNA damage to base changes outside the binding site [36, 89] suggest that sequence recognition *per se* is not the primary determinant of target selection. In fact, these observations imply that DNA structure and dynamics mediate, at least in part, the binding of calicheamicin [31, 35, 36, 90]. The evidence presented here has shown that this is indeed the case and that calicheamicin targets those sequences that can be easily bent (*i.e.*, flexible), or already exist in a conformation that optimizes the drug-DNA interactions. This situation is analogous to that of several antibiotics that modify DNA covalently (*e.g.*, [44, 77, 78]).

Although seminal to the recognition process, we are not proposing that DNA structure and dynamics are solitary determinants of calicheamicin binding. In fact, it is clear that calicheamicin target selection is a complex process involving electrostatic and hydrophobic interactions that are optimized by the conformational flexibility of specific DNA sequences. In the following sections, the role of these factors in calicheamicin target selection is discussed.

Sequence-Specific Electrostatic Interactions in Calicheamicin Binding

There is considerable evidence to suggest that the recognition of base-specific charges within the minor groove, plays a role in the targeting of calicheamicin to specific sequences. Figure 6.1 is a pictorial representation of the proposed hydrogen bonding between calicheamicin and the sequence AGGAGT•ACTCCT as determined by NMR in Dinshaw Patel's laboratory [39]. Particularly significant are

the interactions between the thiobenzoate and thiosugar rings of the oligosaccharide tail and the center GGA•TCC sequence. The hydrogen bonding of the thiobenzoate iodine to the amino proton at G03 and the sulfur atom of the S-carbonyl linker to the G04 amino proton suggest a strong affinity for the guanine dinucleotide. Experiments replacing the 03 guanine with inosine, which lacks the 2-amino group, have shown that disruption of this bond greatly reduces the binding of calicheamicin [32]. In fact, a review of approximately 160 sequences, shows that a guanine in the 5' penultimate position of the purine strand leads to reactivity 23% of the time, which is almost 5 times the probability that a sequence without this guanine will react. (See Appendix A for a list of the sequences analyzed and their relative reactivities.) A sequence containing the appropriate GG•CC dinucleotide is reactive in 50% of the cases in which it appears.

Calicheamicin also recognizes the next step on the 3' side, the 05 adenine, by forming a hydrogen bond between the thiosugar hydroxyl and the minor groove-facing imino group. Theoretically, this same bonding could occur between the thiosugar and a guanine, assuming that the exocyclic amine does not sterically interfere. It may even be possible to replace A05 with either a cytosine or thymine, both of which have similar charges in the same relative vicinity. An identical argument can be made for replacing the GG•CC dinucleotide with a CC•GG but both would have to be replaced to preserve the relative orientation of charges across the pair; especially when the propeller twist between the complementary bases is large.[3] One could imagine that this effect would be most dramatic if G04 -- alone -- were replaced since the relationship between all three bases would be disturbed.

Two issues have emerged from this discussion. The first is that charges on the base pairs can, and do, interact with calicheamicin. The second is that the

---

[3] From the perspective of the minor groove, the A·T base pair looks very similar to a T·A since the charge distribution is unchanged when the base pairs are flipped (*i.e.*, -, -). Similarly, a G·C could replace a C·G (*i.e.*, -, +, -). However, when the propellor twist is high (*i.e.*, the complementary bases are rotated in opposite directions about an axis through the C1 atoms) the location of the positive charges with respect to adjacent bases is altered considerably.

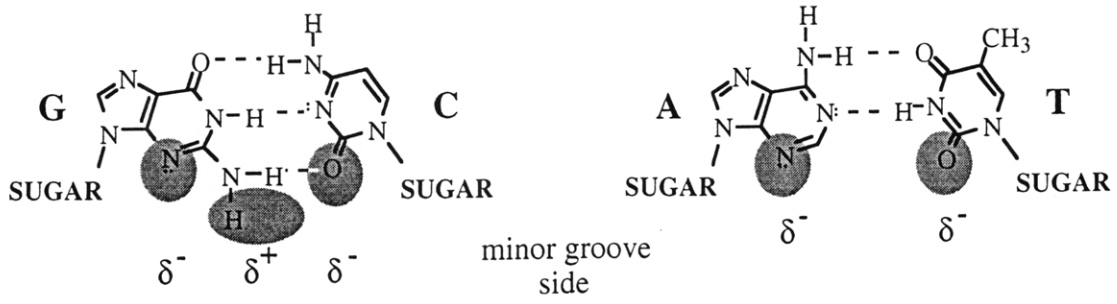

relative location of these partial charges within the minor groove is critical to ensuring that these interactions act cooperatively. Optimizing the first, requires guanines, or possibly cytosines, at 03 and 04; and an adenine, or potentially any of the other three bases, at 05. However, to preserve the relative positions of the partial charges, the purine stacking should be maintained. A homopyrimidine run may allow hydrogen bonding at 03 and 04, but not at 05. The affinity that calicheamicin has for a wide variety of oligopurine runs may result from, at least in part, a balancing of these requirements.

The importance of these interactions is highlighted by the finding that the oligosaccharide tail of calicheamicin is a major contributor to the structural perturbations induced in DNA when the drug binds (see Chapters III and IV).

These observations do not preclude other, mixed, sequences from reacting. The suggestion here is that as the sequence deviates from the archetypal tetrapurine run, the binding interactions are decreased and reactivity falls. However, since this is a multi-factorial process, it is quite possible that other determinants of calicheamicin binding mediate and reduce the significance of base-specific charge recognition.

Shape Recognition and Hydrophobic Forces in Calicheamicin Binding

In addition to the base "sensing" properties of calicheamicin, several experimental observations suggest that the drug is sensitive to the general topological and hydrophobic characteristics of the recognition sequence. In addition to hydrogen bonds with the bases, both Ikemeto *et al.* and Walker *et al.* found that calicheamicin had substantial van der Waals associations with the nucleotides and several hydrogen bonds with the phosphate backbone (see Figure 6.1) [27, 39]. Furthermore, assays in many labs have shown that calicheamicin-induced DNA damage can be affected by changing the 02-15 and 01-16 base pairs in Figure 6.1; substitutions, which according to the hydrogen bonding pattern of the bases discussed above, should have no affect on drug binding [24, 43]. Last, binding experiments conducted in the presence of salt have shown that hydrophobic interactions of the drug with DNA are important mediators of DNA damage [30]. These results suggest that, in addition to specific hydrogen bonding with base substituents, there are other forces arising from the overall conformation and

sequence context of the binding site that play an important role in calicheamicin target recognition.

DNA damage studies performed within our lab have shown that bases not in direct contact with the drug can influence calicheamicin reactivity. Significantly, having an AG•CT dinucleotide at the 5' end almost guarantees that the sequence will be reactive. In sequences beginning with an AG•CT, 7 of 8 were damaged by calicheamicin. The exception was AGCCAA which contains a substantial disruption of the oligopurine tract. The lack of a 5' adenine appears to be partially overcome when the 5' penultimate base is a guanine, but only in a few cases. In fact, only 1 out of 7 sequences beginning with GG•CC were damaged by calicheamicin while no TG•CA or CG•CG beginning sequences were damaged (0/6 and 0/13 respectively). Therefore, a purine (adenine more than guanine) at the 5' end of the sequence stabilizes the binding of calicheamicin to the minor groove. (The guanine may be less desirable becuase the exocyclic amine may sterically interfere with the positioning of the rhamnose sugar ring.)

It is possible that the 5' purine reinforces a helical conformation within the binding site that enhances its affinity for calicheamicin. This may occur if the base contributes to the presence and maintenance of a high degree of propeller twist throughout the oligosaccharide binding region and/or prevents a helical transformation upon dehydration [91]. High levels of propeller twist, known to exist in A-tracts, may expose a greater proportion of the lipophilic base surfaces to the oligosaccharide tail of calicheamicin. This stacking arrangement may cause a narrowing of the minor groove, increasing van der Waals interactions and promoting hydrogen bonding between calicheamicin and the phosphate backbone. It is important to note, however, that a terminal adenine does not -- by itself -- define a calicheamicin binding site since sequences beginning with an adenine followed thymine or cytosine are almost always unreactive.

As mentioned earlier, hydrophobic forces have been shown to be important contributors to the overall binding energy of calicheamicin to DNA. This may explain the generally greater affinity of calicheamicin for homopurine tracts rather than mixed sequence DNA. Since homopurine sequences are more hydrated [92], the increased displacement of water may make drug binding entropically more favorable.

These data suggest that the topological and thermodynamic features of the binding site sequence are likely to contribute along with the base-sensing properties of calicheamicin to determine site selectivity.

DNA Structure and Dynamics

Calicheamicin bends DNA when it binds. Therefore, sequences that can most easily adopt the conformation of the drug-DNA complex are likely energetically favorable targets for binding. However, it is not clear where in the sequence this element of flexibility occurs.

As discussed in Chapter I and shown in Appendix A, calicheamicin damages DNA most frequently at the 3' end of homopurine runs. A closer investigation of target sequences shows that the amount of damage is sensitive to base substitutions all the way up to the 07 position. For example, we have seen that the sequence AGGGTC gets damaged 40% more often than the sequence AGGGTG where the only difference between the two is the 07 base pair which is two bases away from the putative drug binding site. Since the results of the experiments described in Chapters III and IV suggest that calicheamicin binding sites contain some element of flexibility, and further, since the 07 base pair has no contact with the drug, we propose that the ability of the binding site to alter its conformation in response to drug binding occurs as a result of, and near to, the 3' end of the sequence.

Theoretical and empirical evidence suggests that the sugar-phosphate backbones of DNA are relatively flexible and that, while they constrain the bases to a small region of conformational space, they play essentially no role in determining the sequence-dependent structure [93, 94]. As a result, bending is primarily a function of the base-to-base stacking interactions. Since calicheamicin appears to prefer sequences that can be most easily bent, we hypothesize that the drug targets those sequences which can most easily adopt a conformation that could lead to bending of the helical axis. In other words, the drug favors a conformational state that is not often observed naturally, but can exist when supported by other intrinsic or extrinsic forces. Of the six degrees of freedom that each base pair has relative to its neighbor (three translations and three rotations about orthogonal axes through the center of the base-pair), roll is considered to be the motion responsible for bending of the helical axis [45]. Therefore, we posit that the bending observed when calicheamicin binds DNA is the result of a change in one, or more, of the individual roll angles at the 3' end of the oligopurine tract. We further suggest that the drug assists this deformation by reinforcing a high degree of propeller twist throughout the oligopurine tract and widening the minor groove at the site of aglycone binding.

Roll between base-pairs can occur in response to the individual forces mediating the location of one base-pair with respect to another. The classical example, is the highly propeller twisted pyrimidine-purine step, shown below [45].

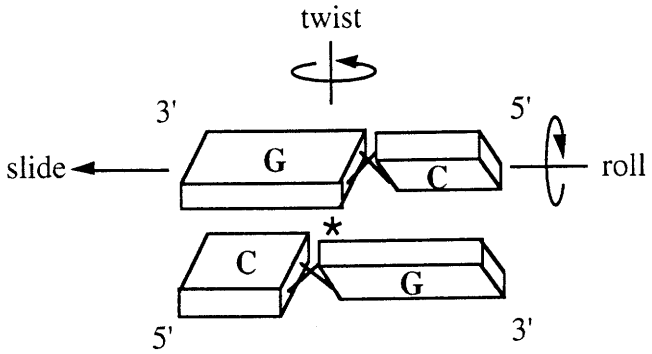

Using the block notation introduced by Calladine & Drew [95], the figure portrays a CG step as seen from the minor groove. The directions of positive slide, roll and twist are shown. Negative propeller twist leads to a cross-strand steric clash between the purines in the major groove (asterisk).

To avoid a steric clash between purines in the minor groove, the 3' base can decrease the propeller twist, reduce its twist angle with respect to the 5' base, slide in either a positive or negative direction, or roll towards the major groove (positive) [96]. The motions are coupled. For example, in this case a negative slide would cause the purines to overlap forcing them to roll such that their surfaces were parallel to one another. This conformation is not only favored sterically, but it also maximizes the favorable hydrophobic and electrostatic interactions [95].

Figure 6.2 is a slide/roll map for each of the possible dinucleotide steps created by Christopher Hunter [95]. Each dinucleotide is plotted in a location that corresponds to the position of the bases that minimizes the unfavorable electrostatic and steric forces acting between them. Interestingly, purine-purine steps are -- for the most part -- comfortable at near zero slide and roll. This is consistent with a model in which the oligopurine tract forms a stable B-DNA type structure. Many of the purine-pyrimidine steps, however, are not comfortable in a zero-slide/zero-roll conformation. In particular, the AT, AC and GT dinucleotides all prefer a similar negative-slide/negative-roll conformation. This is primarily due to a steric clash between the thymine methyl group and the 1' carbon at of the 5' neighboring sugar. It may be, that calicheamicin binding encourages a base slide at dinucleotide steps that are comfortable assuming a high negative slide conformation. The result

would be the introduction of a localized roll possibly leading to bending of the helical axis.

The above rationale appears consistent with both the observed bending and the site selectivity of calicheamicin. Calicheamicin-induced DNA damage occurs predominantly at the 3' ends of oligopurine runs. A wide variety of sequences can facilitate binding but almost all of the most reactive sites contain an AT, AC or GT base step at the 3' end. A review of the damage sequences in Appendix A, shows that this step can occur between 06 and 07, 05 and 06, and even 04 and 05 positions. An explanation for this variability might be that the slide can occur in either the 05, 06 or 07 steps. In fact, it may be the positioning of the aglycone between the phosphate backbones at T07 and C13 that encourages this movement. NMR studies by Ikemeto *et al.* [39] have shown that the minor groove widens at this site; a deformation that might facilatate negative sliding of the base pairs somewhere between 04 and 07.

Calicheamicin Binding to DNA

The data here and elsewhere, suggest that calicheamicin target selection is a result of the electrostatic, hydrophobic and structural properties of the target sequence. It is the optimization of these factors that dictates where, and how often, a specific DNA molecule is damaged. It is important to understand that these forces need not be individually optimized to ensure drug binding. A sequence may be more appropriate in one sense than another but still confer enough of an advantage over an adjacent sequence to make it a target for calicheamicin. As a result of this heterogeneity, we should expect to see a variety of sequences that serve as suitable binding substrates for the drug. Indeed, this is the case.

Our addition to this model has been to establish the role of DNA structure and dynamics in the target recognition process. We have shown that two different high-affinity calicheamicin binding sites are not significantly curved and that when calicheamicin binds to these sequences it bends, and possibly twists, the helix. These results suggest that -- in general -- calicheamicin binding sites are not curved, but are instead flexible DNA sequences that can be easily bent or "trapped" in a conformation that fosters equilibrium drug binding. In addition, these findings imply that sequences already curved or bent into the drug-bound conformation

would also be energetically favorable targets since they do not need to be forced into a bent conformation.

A structure and dynamics based paradigm for calicheamicin target recognition explains why, as discussed earlier, calicheamicin-induced DNA damage is influenced by the sequence context and overall topology of the binding site. Since calicheamicin binding depends on DNA flexibility, adjacent bases can affect drug binding by changing the dynamic behavior of the target sequence; an effect that may extend for several base pairs [79, 80]. In contrast, changes in DNA topology must precisely match the desired drug-bound conformation to facilitate drug binding. For example, in the nucleosome studies described in Chapter I [43, 97], DNA bending reduced or had no effect on calicheamicin-induced DNA damage except at one site. This is consistent with our suggestion that calicheamicin does not target curved or bent DNA indiscriminately but instead, binds only those sequences bent into a specific conformation.

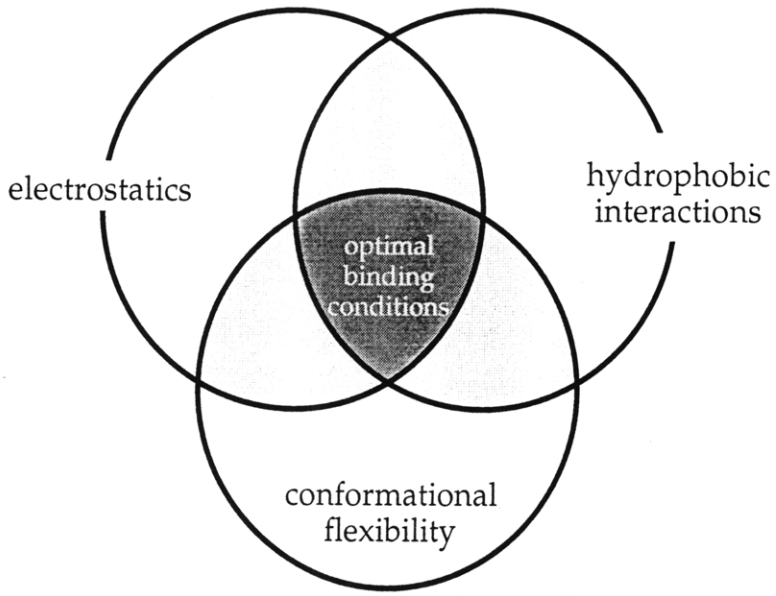

Although DNA structure and dynamics are seminal to drug binding, calicheamicin target selection is a complex process involving several interactions that are optimized -- not necessarily controlled -- by the conformational flexibility of specific DNA sequences. In all cases a balance must be achieved between the DNA's intrinsic resistance to movement and those forces -- electrostatic and hydrophobic -- that bind calicheamicin to DNA. In fact, the above discussion suggests that calicheamicin targets the 3' ends of homopurine runs as a result of their unique thermodynamic and structural properties.

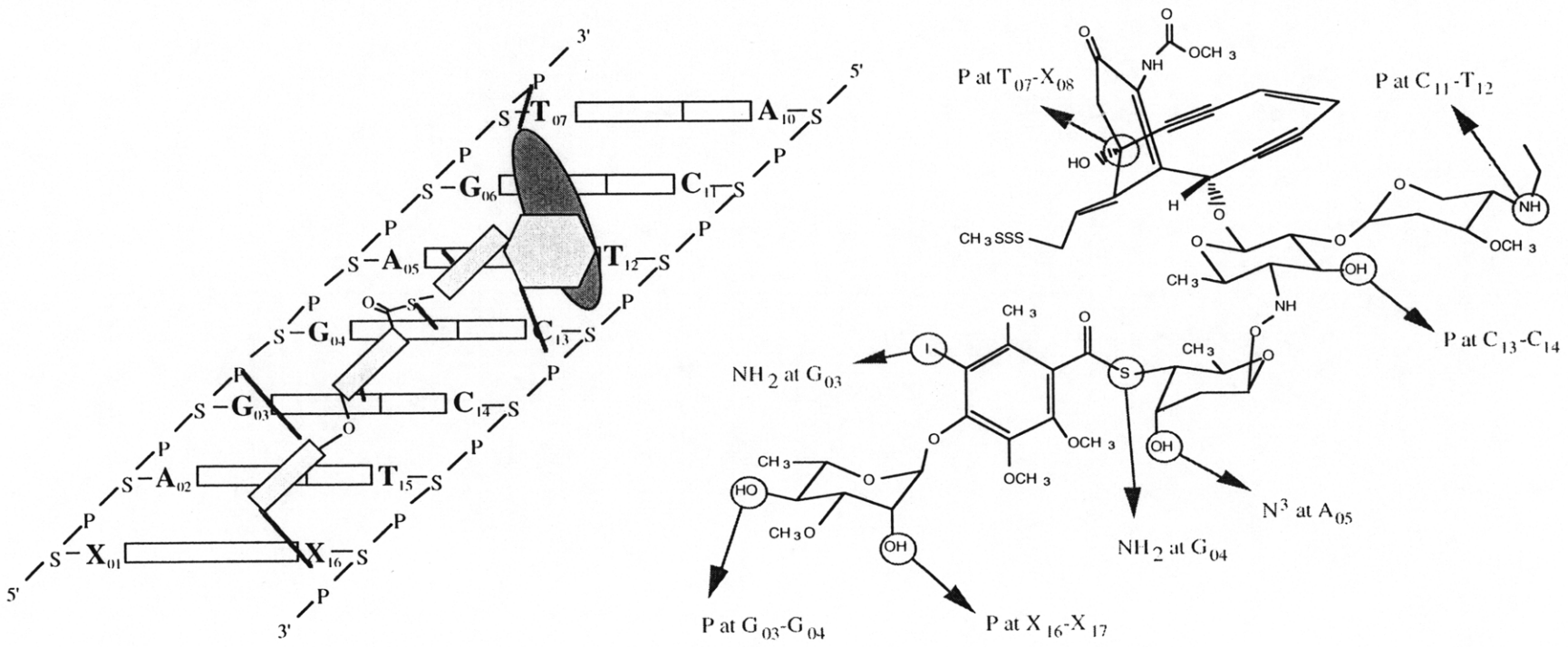

Figure 6.1. Hydrogen bonding of calicheamicin to DNA as determined by NMR. Calicheamicin is represented with a blue aglycone and yellow sugar rings oriented edgewise into the minor groove or lying flat. The ethylamino sugar is left out for clarity. Proposed hydrogen bonds are shown in red, connecting those groups that participate in the bond. The specific atoms involved are shown in the figure on the right. "P" is an abreviation for phosphate. These figures are based upon the NMR data published by Ikemoto *et al.*, [39].

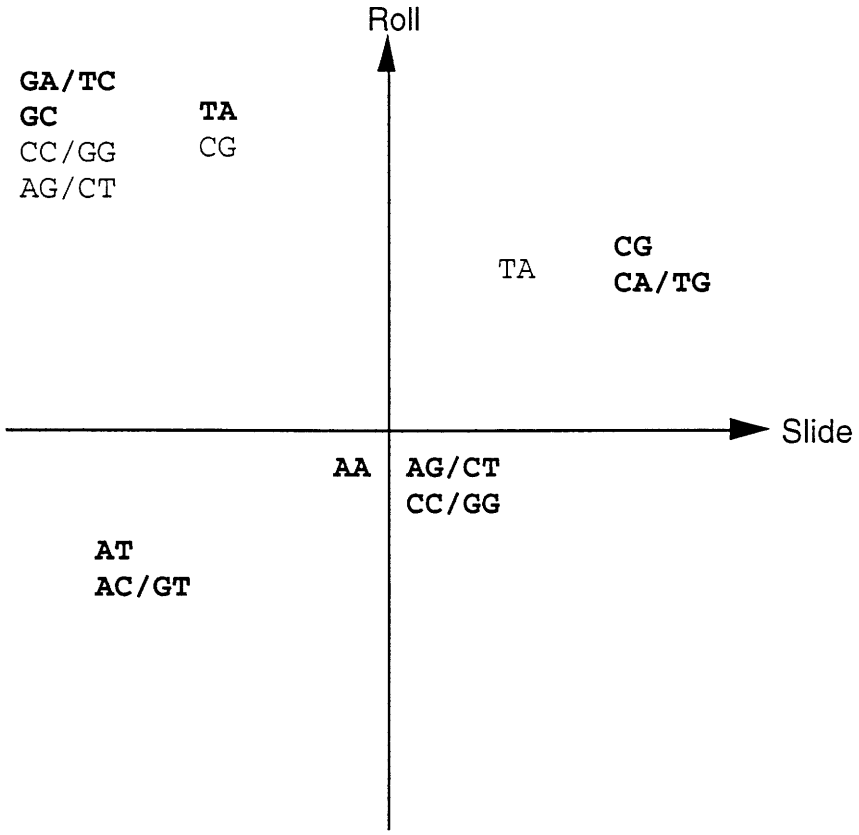

Figure 6.2 A slide/roll map illustrating the positions of the calculated energy minima for all 10 base-pair steps. The lowest energy minima are shown in bold type-face. Secondary energy minima are marked in plain type-face. (Copied from Hunter, 1992)

References

1. Casazza, A.M. and Kelley, S.L. (1995) in *Enediyne Antibiotics as Antitumor Agents* (D.B. Borders and T.W. Doyle, ed) pp. 283-299, Marcel Dekker, New York.

2. Doyle, T.W. and Borders, D.B. (1995) in *Enediyne Antibiotics as Antitumor Agents* (D.B. Borders and T.W. Doyle, ed) pp. 1-15, Marcel Dekker, New York.

3. Nicolaou, K.C., Dai, W.-M., Tsay, S.-C., Estevez, V.A., and Wrasildo, W. (1992) Designed enediynes: A new class of DNA-cleaving molecules with potent and selective anticancer activity. *Science* **256**, 1172-1178.

4. Sullivan, N. and Lyne, L. (1990) Sensitivity of fibroblasts derived from ataxia-telangiectasia patients to calicheamicin γ_1^I. *Mutation Res.* **245**, 171-175.

5. Zhao, B., Konno, S., Wu, J.M., and Oronsky, A.L. (1990) Modulation of nicotinamide adenine dinucleotide and poly(adenosine diphosphoribose) metabolism by calicheamicin γ1 in human HL-60 cells. *Cancer Lett.* **50**, 141-147.

6. Zein, N., Sinha, A.M., McGahren, W.J., and Ellestad, G.A. (1988) Calicheamicin $\gamma 1^I$: an antitumor antibiotic that cleaves double-stranded DNA site specifically. *Science* **240**, 1198-1201.

7. Lee, M.D., Ellestad, G.A., and Borders, D.B. (1991) Calicheamicins: Discovery, structure, chemistry, and interaction with DNA. *Acc. Chem. Res.* **24**, 235-243.

8. Dedon, P.C. and Goldberg, I.H. (1992) Free-radical mechanisms involved in the formation of sequence-dependent bistranded DNA lesions by the antitumor antibiotics bleomycin, neocarzinostatin, and calicheamicin. *Chem. Res. Tox.* **5**, 311-332.

9. LaMarr, W.A., Sandman, K.M., Reeve, J.N., and Dedon, P.C. (1997) Differential effects of DNA supercoiling on radical-mediated DNA strand breaks. *Chem. Res. Toxicol.* **10**, 1118-1122.

10. Xu, J., Wu, J., and Dedon, P.C. (1998) DNA damage produced by enediynes in the human phosphoglycerate kinase gene *in vivo*: Esperamicin A1 as a nucleosome footprinting agent. *Biochemistry* **37**, 1890-1897.

11. Mathur, P., Xu, J., and Dedon, P.C. (1997) Cytosine methylation enhances DNA damage produced by groove binding and intercalating enediynes: Studies with esperamicins A1 and C. *Biochemistry* **36**, 14868-14873.

12. Liang, Q., Choi, D.-J., and Dedon, P.C. (1997) Calicheamicin-induced DNA damage in a reconstituted nucleosome is not affected by histone acetylation: Role of drug structure in the target recognition process. *Biochemistry* **36**, 12653-12659.

13. De Voss, J.J., Hangeland, J.J., and Townsend, C.A. (1990) Characterization of the in vitro cyclization chemistry of calicheamicin and its relation to DNA cleavage. *J. Am. Chem. Soc.* **112**, 4554-4556.

14. Goldberg, I.H. (1987) Free radical mechanisms in neocarzinostatin-induced DNA damage. *Free Radical Biol. Med.* **3**, 41-54.

15. Kishikawa, H., Jiang, Y.-P., Goodisman, J., and Dabrowiak, J.C. (1991) Coupled kinetic analysis of cleavage of DNA by esperamicin and calicheamicin. *J. Am. Chem. Soc.* **113**, 5434-5440.

16. Dedon, P.C., Salzberg, A.A., and Xu, J. (1993) Exclusive production of bistranded DNA damage by calicheamicin. *Biochemistry* **32**, 3617-3622.

17. Kappen, L.S., Goldberg, I.H., and Liesch, J.M. (1982) Identification of thymidine 5'-aldehyde at DNA strand breaks induced by neocarzinostatin chromophore. *Proc. Natl. Acad. Sci. USA* **79**, 744-748.

18. Kappen, L.S., Ellenberger, T.E., and Goldberg, I.H. (1987) Mechanism and base specificity of DNA breakage in intact cells by neocarzinostatin. *Biochemistry* **26**, 384-390.

19. Saito, I., Kawabata, H., Fujiwara, T., Sugiyama, H., and Matsuura, T. (1989) A novel ribose C-4' hydroxylation pathway in neocarzinostatin-mediated degradation of oligonucleotides. *J. Am. Chem. Soc.* **111**, 8302-8303.

20. Kappen, L.S., Goldberg, I.H., Frank, B.L., Worth, L.J., Christner, D.F., Kozarich, J.W., and Stubbe, J. (1991) Neocarzinostatin-induced hydrogen atom abstraction from C-4' and C-5' of the T residue at a d(GT) step in oligonucleotides: shuttling between deoxyribose attack sites based on isotope selection effects. *Biochemistry* **30**, 2034-2042.

21. Frank, B.L., Worth, L., Jr., Christner, D.F., Kozarich, J.W., Stubbe, J., Kappen, L.S., and Goldberg, I.H. (1991) Isotope effects on the sequence-specific cleavage of DNA by neocarzinostatin: kinetic partitioning between 4' and 5'-hydrogen abstraction at unique thymidine sites. *J. Am. Chem. Soc.* **113**, 2271-2275.

22. Hangeland, J.J., De Voss, J.J., Heath, J.A., Townsend, C.A., Ding, W.-d., Ashcroft, J.S., and Ellestad, G.A. (1992) Specific abstraction of the 5'(S)- and 4'-deoxyribosyl hydrogen atoms from DNA by calicheamicin γ_1^I. *J. Am. Chem. Soc.* **114**, 9200-9202.

23. De Voss, J.J., Townsend, C.A., Ding, W.-d., Morton, G.O., Ellestad, G.A., Zein, N., Tabor, A.B., and Schreiber, S.L. (1990) Site-specific atom transfer from DNA to a bound ligand defines the geometry of a DNA-calicheamicin γ_1^I complex. *J. Am. Chem. Soc.* **112**, 9669-9670.

24. Mah, S.C., Price, M.A., Townsend, C.A., and Tullius, T.D. (1994) Features of DNA recognition for oriented binding and cleavage by calicheamicin. *Tetrahedron* **50**, 1361-1378.

25. Paloma, L.G., Smith, J.A., Chazin, W.J., and Nicolaou, K.C. (1994) Interaction of calicheamicin with duplex DNA: Role of the oligosaccharide domain and identification of multiple binding modes. *J. Am. Chem. Soc.* **116**, 3697-3708.

26. Walker, S., Murnick, J., and Kahne, D.J. (1993) Structural characterization of a calicheamicin-DNA complex by NMR. *J. Am. Chem. Soc.* **115**, 7954-7961.

27. Walker, S.L., Andreotti, A.H., and Kahne, D.E. (1994) NMR characterization of calicheamicin γ_1^I bound to DNA. *Tetrahedron* **50**, 1351-1360.

28. Lee, M.D., Dunne, T.S., Marshall, M.S., Chang, C.C., Morton, G.O., and Borders, D.B. (1987) Calicheamicins, a novel family of antitumor antibiotics. 1. Chemistry and partial structure of calicheamicin $\gamma 1^I$. *J. Am. Chem. Soc.* **109**, 3464-3466.

29. Lee, M.D., Dunne, T.S., Chang, C.C., Ellestad, G.A., Siegel, M.M., Morton, G.O., McGahren, W.J., and Borders, D.B. (1987) Calicheamicins, a novel family of antitumor antibiotics. 2. Chemistry and structure of calicheamicin $\gamma 1^I$. *J. Am. Chem. Soc.* **109**, 3466-3468.

30. Ding, W.-d. and Ellestad, G.A. (1991) Evidence for a hydrophobic interaction between calicheamicin and DNA. *J. Am. Chem. Soc.* **113**, 6617-6620.

31. Drak, J., Iwasawa, N., Danishefsky, S., and Crothers, D.M. (1991) The carbohydrate domain of calicheamicin γ_1^I determines its sequence specificity for DNA cleavage. *Proc. Natl. Acad. Sci. USA* **88**, 7464-7468.

32. Li, T., Zeng, Z., Estevez, V.A., Baldenius, K.U., Nicolaou, K.C., and Joyce, G.F. (1994) Carbohydrate-minor groove interactions in the binding of calicheamicin γ_1^I to duplex DNA. *J. Am. Chem. Soc.* **116**, 3709-3715.

33. Mah, S.C., Townsend, C.A., and Tullius, T.D. (1994) Hydroxyl radical footprinting of calicheamicin. Relationship of DNA binding to cleavage. *Biochemistry* **33**, 614-621.

34. Nicolaou, K.C., Tsay, S.-C., Suzuki, T., and Joyce, G.F. (1992) DNA-carbohydrate interactions. Specific binding of the calicheamicin γ_1^I oligosaccharide with duplex DNA. *J Am. Chem. Soc.* **114**, 7555-7557.

35. Walker, S., Landovitz, R., Ding, W.D., Ellestad, G.E., and Kahne, D. (1992) Cleavage behavior of calicheamicin γ^1 and calicheamicin T. *Proc. Natl. Acad. Sci. USA* **89**, 4608-4612.

36. Zein, N., Poncin, M., Nilakantan, R., and Ellestad, G.A. (1989) Calicheamicin $\gamma 1^I$ and DNA: molecular recognition process responsible for site-specificity. *Science* **244**, 697-699.

37. Kohwi-Shigematsu, T. and Kohwi, Y. (1985) Poly(dG)-poly(dC) sequences, under torsional stress, induce an altered DNA conformation upon neighboring DNA sequences. *Cell* **43**, 199-206.

38. Aiyar, J., Danishefsky, S.J., and Crothers, D.M. (1992) Interaction of the aryl tetrasaccharide domain of calicheamicin γ_1^I with DNA: Influence of aglycon and methidiumpropyl-EDTA.iron(II)-mediated DNA cleavage. *J. Am. Chem. Soc.* **114**, 7552-7554.

39. Ikemoto, N., Kumar, R.A., Ling, T.-T., Ellestad, G.A., Danishefsky, S.J., and Patel, D.J. (1995) Calicheamicin-DNA complexes: Warhead alignment and saccharide recognition of the minor groove. *Proc. Natl. Acad. Sci.* **92**, 10506-10510.

40. Langley, D.R., Golik, J., Krishnan, B., Doyle, T.W., and Beveridge, D.L. (1994) The DNA-Esperamicin A1 complex. A model based on solvated molecular dynamics simulations. *J. Am. Chem. Soc.* **116**, 15-29.

41. LaMarr, W.A., Yu, L., Nicolaou, K.C., and Dedon, P.C. (1998) Supercoiling affects the accessibility of glutathione to DNA-bound molecules: Positive supercoiling inhibits calicheamicin-induced DNA damage. *Proc. Natl. Acad. Sci.* **96**, 102-107.

42. Krishnamurthy, G., Ding, W.-d., O'Brien, L., and Ellestad, G.A. (1994) Circular dichroism studies of calicheamicin-DNA interactions: Evidence for a calicheamicin-induced DNA conformational change. *Tetrahedron* **50**, 1341-1349.

43. Yu, L., Salzberg, A.A., and Dedon, P.C. (1995) New insights into calicheamicin-DNA interactions derived from a model nucleosome system. *Bioorg. Med. Chem.* **3**, 729-741.

44. Kizo, R., Draves, P.H., and Hurley, L.H. (1993) Corrolation of DNA sequence specificity of anrthramycin and tomaymycin with reaction kinetics and bending of DNA. *Biochemistry* **32**, 8712-8722.

45. Calladine, C.R. and Drew, H.R. (1992) *Understanding DNA: The Molecule and How It Works,* Academic Press, San Diego.

46. Hansma, H.G., Browne, K.A., Bezanilla, M., and Bruice, T.C. (1994) Bending and straightening of DNA induced by the same ligand: Characterization with atomic force microscope. *Biochemistry* **33**, 8436-8441.

47. Diekmann, S. (1992) Analyzing DNA curvature on polyacrylamide gels. *Meth. Enz.* **212**, 30-46.

48. Crothers, D.M., Haran, T.E., and Nadeau, J.G. (1990) Intrinsically Bent DNA. *J. Biol. Chem.* **265**, 7093-7096.

49. Hagerman, P.J. (1990) Sequence-directed curvature of DNA. *Annu. Rev. Biochem.* **59**, 755-781.

50. Kahn, J.D., Yun, E., and Crothers, D.M. (1994) Detection of localized DNA flexibility. *Nature* **368**, 163-166.

51. McNamara, P.T. and Harrington, R.E. (1991) Characterization of inherent curvature in DNA lacking polyadenine runs. *J. Biol. Chem.* **266**, 12548-12554.

52. Shore, D., Langowski, J., and Baldwin, R.L. (1981) DNA flexibility studied by covalent closure of short fragments into circles. *Proc. Natl. Acad. Sci. USA* **78**, 4833-4837.

53. Crothers, D., Drak, J., Kahn, J., and Levene, S. (1992) DNA bending, flexibility, and helical repeat by cyclization kinetics. *Meth. Enz.* **212**, 3-30.

54. Ulanovsky, L., Bodner, M., Trifonov, E.N., and Choder, M. (1986) Curved DNA: Design, synthesis, and circularization. *Proc. Natl. Acad. Sci. USA* **83**, 862-866.

55. Zahn, K. and Blattner, F.R. (1987) Direct evidence for DNA bending at the lambda replication origen. *Science* **236**, 416-422.

56. Koo, H.-S., Drak, J., Rice, J.A., and Crothers, D.M. (1990) Determination of the extent of DNA bending by an adenine-thymine tract. *Biochemistry* **29**, 4227-4234.

57. Taylor, W.H. and Hagerman, P.J. (1990) Application of the method of phage T4 DNA ligase-catalyzed ring-closure to the study of DNA structure. II. NaCl-dependence of DNA flexibility and helical repeat. *J. Mol. Biol.* **212**, 363-376.

58. Flory, P.J., Suter, U.W., and Mutter, M. (1976) Macrocyclization Equilibria. 1. Theory. *J. Am. Chem. Soc.* **98**, 5733-5739.

59. Levene, S.D. and Crothers, D.M. (1986) Ring closure probabilities for DNA fragments by Monte Carlo simulation. *J. Mol. Biol.* **189**, 61-72.

60. Levene, S.D. and Crothers, D.M. (1986) Topological distributions and the torsional rigidity of DNA. *J. Mol. Biol.* **89**, 73-83.

61. Calladine, C.R., Collis, C.M., Drew, H.R., and Mott, M.R. (1991) A study of electrophoretic mobility of DNA in agarose and polyacrylimide gels. *J. Mol. Biol.* **221**, 981-1005.

62. Hagerman, P.J. (1985) Sequence-dependence of the curvature of DNA: a test of the phasing hypothesis. *Biochemistry* **24**, 7033-7037.

63. Ausubel, F.M., Brent, R., Kingston, R.E., Moore, D.D., Seidman, J.G., Smith, J.A., and Struhl, K. (1989) *Current Protocols in Molecular Biology*, John Wiley and Sons, New York.

64. Sambrook, J., Fritsch, E.F., and Maniatis, T. (1989) *Molecular Cloning, A Laboratory Manual*, Cold Spring Harbor Press, Cold Spring Harbor.

65. Lee, S. and Suraiya, R. (1990) A simple proceedure for maximum yield of high-quality plasmid DNA. *BioTechniques* **9**, 676-679.

66. Salzberg, A., Mathur, P., and Dedon, P. (1995) in *NATO Workshop: DNA Cleavers and Chemotherapy of Cancer or Viral Diseases* (B. Meunier, ed) pp. 23-36, Kluwer Academic Publishers, Dordrecht.

67. Chatterjee, M., Mah, S.C., Tullius, T.D., and Townsend, C.A. (1995) Role of the aryl iodide in the sequence-selective cleavage of DNA by calicheamicin. Importnace of thermodynamic binding vs kinetic activation in the cleavage process. *J. Am. Chem. Soc.* **117**, 8072-8082.

68. Nicolaou, K.C., Li, T., Nakada, M., Hummel, C.W., Hiatt, A., and Wrasildo, W. (1994) Calicheamicin $\emptyset^{I}_{1}$: A rationally designed molecule with extremely potent and selective DNA cleaving properties and apoptosis inducing activity. *Angew. Chem. Int. Ed. Engl.* **33**, 183-186.

69. Lee, M.D., Manning, J.K., Williams, D.R., Kuck, N.A., Testa, R.T., and Borders, D.B. (1989) Calicheamicins, a novel family of antitumor antibiotics. 3. Isolation, purification and characterization of calicheamicins β_1, γ_1^{Br}, α_2^{I}, α_3^{I}, β_1^{I}, γ_1^{I} and δ_1^{I}. *J. Antibiotics* **42**, 1070-1087.

70. Hertzberg, R.P., Caranfa, M.J., and Hecht, S.M. (1985) DNA methylation diminishes bleomycin-mediated strand scission. *Biochemistry* **24**, 5286-5289.

71. Kahn, J.D. and Crothers, D.M. (1992) Protein-induced bending and DNA cyclization. *Proc. Natl. Acad. Sci.* **89**, 6343-6347.

72. Wei, C.-E., Alianell, G.A., Beneen, G.H., and Gray, H.B. (1983) Isolation and comparison of two molecular species of the BAL-31 nuclease from Alteromonas espejiana with disctinct kenietic properties. *J. Biol. Chem.* **258**, 13506-13512.

73. Shishido, K. and Ando, T. (1982) *Nucleases* **14**, 155.

74. Shore, D. and Baldwin, R.L. (1983) Energetics of DNA twisting. II. Topoisomer analysis. *J. Mol. Biol.* **170**, 983-1007.

75. Raae, A.J., Kleppe, R.K., and Kleppe, K. (1975) Kinetics and effects of salts and polyamines on T4 polynucleotide ligase. *Eur. J. Biochem.* **60**, 437-443.

76. Sugino, A., Goodman, H.M., Heynecker, H.L., Shrine, J., Boyer, H.W., and Cozarelli, N.R. (1977) Interaction of bacteriophage T4 RNA and DNA ligases in joining of duplex DNA at base-paired ends. *J. Biol. Chem.* **252**, 3987-3994.

77. Hurley, L., Lee, C.S., McGovren, P., Warpehoski, M., Mitchell, M., Kelly, R., and Aristoff, P. (1988) Molecular basis for sequence-specific DNA alkylation by CC-1065. *Biochemistry* **27**, 3886-3892.

78. Sun, D., Lin, C.H., and Hurley, L.H. (1993) A-tract and (+)-CC-1065-induced DNA bending of DNA. Comparison of structural features using non-denaturing gel analysis, hydroxyl-radical footprinting, and high-field NMR. *Biochemistry* **32**, 4487-4495.

79. Brukner, I., Sanchez, R., Suck, D., and Pongor, S. (1995) Trinucleotide models for DNA bending propensity: comparison of models based on DNaseI digestions and nucleosome packaging data. *Journal of Biomolecular Structures and Dynamics* **13**, 309-317.

80. Dlakic, M. and Harrington, R. (1996) The effects of sequence context on DNA curvature. *Proc. Natl. Acad. Sci.*, 3847-3852.

81. Zein, N., Ding, W.-D., and Ellestad, G.A. (1990) in *Molecular Basis of Specificity in Nucleic Acid-Drug Interactions* (B.P.a.J. Jortner, ed) pp. 323-330, Kluwer Academic Publishers,

82. Wang, J.W. and Davidson, N. (1966) On the probability of ring closure of lambda DNA. *J. Mol. Biol.* **19**, 469-482.

83. Shore, D. and Baldwin, R.L. (1983) Energetics of DNA twisting. I. Relation between twist and cyclization probability. *J. Mol. Biol.* **170**, 957-981.

84. Wang, J.C. and Davidson, N. (1966) Thermodynamic and kinetic studies on the interconversion between the linear and circular forms of phage lambda DNA. *J. Mol. Biol.* **15**, 111-123.

85. Sitlani, A. and Crothers, D.M. (1996) Fos and Jun do not bend the AP-1 recognition site. *Proc. Natl. Acad. Sci. USA* **93**, 3248-3252.
86. Hodges-Garcia, Y. and Hagerman, P.J. (1995) Investigation of the influence of Cytosine Methylation on DNA felxibility. *J. Biol. Chem.* **270**, 197-201.

87. Hagerman, P.J. and Ramadevi, V.A. (1990) Application of the method of phage T4 ligase-catalyzed ring-closure to the study of DNA structure. I. Computational analysis. *J. Mol. Biol.* **212**, 351-362.

88. Nicolaou, K.C., Smith, A.L., and Yue, E.W. (1993) Chemistry and biology of natural and designed enediynes. *Proc. Natl. Acad. Sci. USA* **90**, 5881-5888.

89. Krishnamurthy, G., Brenowitz, M.D., and Ellestad, G.A. (1994) Salt-dependence of calicheamicin-DNA site-specific interactions. *Biochemistry* submitted.

90. Uesugi, M. and Sugiura, Y. (1993) New insights into sequence recognition process of esperamicin A_1 and calicheamicin g_1^I: Origin of their selctivities and "induced fit" mechanism. *Biochemistry* **32**, 4622-4627.

91. Goodfellow, J.M., Cruzeiro-Hansson, L., Norberto de Souza, O., Parker, K., Sayle, T., and Umrania, Y. (1994) DNA structure, hydration and dynamics. *Int. J. Radiat. Biol.* **66**, 471-478.

92. Rentzeperis, D., Kupke, D., and Marky, L. (1992) Differential hydration of homopurine sequences relative to alternating purine/pyrimidine sequences. *Biopolymers* **32**, 1065-1075.

93. Yanagi, K., Prive, G.G., and Dickerson, R.E. (1991) Analysis of local helix geometry in three B-DNA decamers and eight dodecamers. *J. Mol. Biol.* **217**, 201-214.

94. Srinivasan, A.R., Torres, R., Clark, W., and Olson, W.K. (1987) Base sequence effects in double helical DNA. I. Potential energy estimates of local base morphology. *J. Biomol. Struct. Dyn.* **5**, 459-496.

95. Hunter, C.A. (1993) Sequence-dependent DNA structure: The role of base stacking interactions. *J. Mol. Biol.* **230**, 1025-1054.

96. Calladine, C.R. (1982) Mechanics of sequence-dependent stacking of bases in B-DNA. *J. Mol. Biol.* **161**, 343-352.

97. Kuduvalli, P.N., Townsend, C.A., and Tullius, T.D. (1995) Cleavage by calicheamicin γ_1^I of DNA in a nucleosome formed on the 5S RNA gene of *Xenopus borealis*. *Biochemistry* **34**, 3899-3906.

Appendix A

A Compendium of Calicheamicin Binding Sites

DNA sequences damaged by calicheamicin γ_1^I are listed below with references stating where the studies were performed. For each site, the six base pairs preceeding 4' hydrogen abstraction -- going 5' to 3'-- are listed.

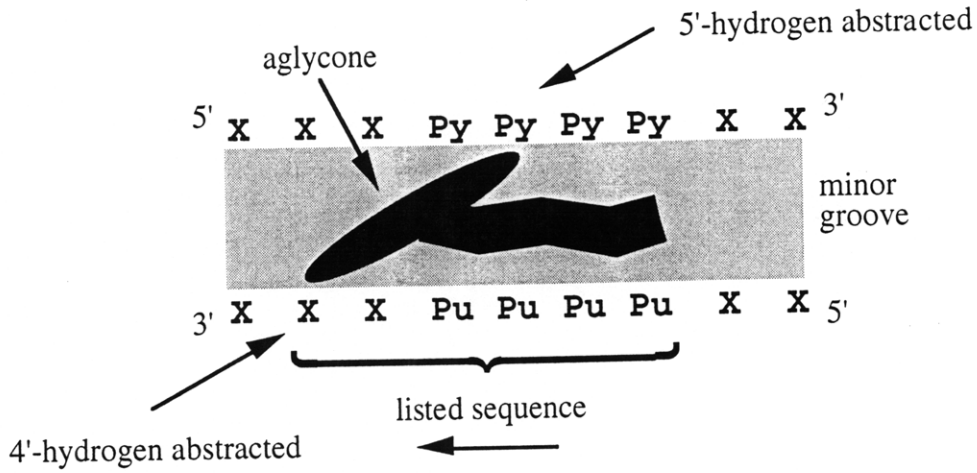

When possible, relative damage intensities are assigned.

Damage Sequences and Relative Damage Intensities

Yu, L., A. A. Salzberg, et al. (1995). "New insights into calicheamicin-DNA interactions derived from a model nucleosome system." *Bioorg. Med. Chem.* **3**(6): 729-741.

Sequence	Damage	Sequence	Damage	Sequence	Damage	Sequence	Damage
CCACCC	0	CACCCT	0	ACCCTG	0	CCCTGA	0
CCTGAA	0	CTGAAA	0	**AGTGCC**	**3**	GTGCCC	0
TGCCCG	0	GCCCGA	0	CCCGAT	0	CGATAT	0
ATATCG	0	TCGTCT	0	CGTCTG	0	GTCTGA	0
TGATCT	0	GATCTC	0	ATCTCG	0	TCTCGG	0
CTCGGA	0	TCGGAA	0	**GGAAGC**	**4**	GAAGCC	0
AAGCCA	0	AGCCAA	0	GCCAAG	0	CCAAGC	0
CAAGCA	0	AAGCAG	0	GCAGGG	0	CAGGGT	0

AGGGTC	**6**	GGGTCG	0	GGTCGG	0	GTCGGG	0
CGGGCC	0	GGGCCT	0	GGCCTG	0	CCTGGT	0
CTGGTT	0	GGTTAG	0	GTTAGT	0	TAGTAC	0
AGTACT	**6**	GTACTT	0	**AGTACT**	**8**	GTACTA	0
TACTAA	0	CTAACC	0	TAACCA	0	AACCAG	0
ACCAGG	0	CCAGGC	0	CAGGCC	0	**AGGCCC**	**2**
GGCCCG	0	GCCCGA	0	CCCGAC	0	CGACCC	0
GACCCT	0	**ACCCTG**	**2**	CCCTGC	0	CCTGCT	0
CTGCTT	0	TGCTTG	0	GCTTGG	0	CTTGGC	0
TTGGCT	0	GCTTCC	0	CTTCCG	0	TTCCGA	0
TCCGAG	0	CCGAGA	0	CGAGAT	0	**GAGATC**	**6**
AGATCA	**8**	GATCAG	0	ATCAGA	0	TCAGAC	0
CAGACG	**2**	GACGAT	0	**ACGATA**	**3**	CGATAT	0
ATATCG	0	TATCGG	0	ATCGGG	0	TCGGGC	0
ACTTTC	**3**	CTTTCA	0	TTTCAG	0	TTCAGG	0
TCAGGG	0	CAGGGT	0	**AGGGTG**	**4**	XXXXXX	X

Mah, S. C., M. A. Price, et al. (1994). "Features of DNA recognition for oriented binding and cleavage by calicheamicin." *Tetrahedron* **50**(5): 1361-1378.

Sequence	Damage	Sequence	Damage	Sequence	Damage	Sequence	Damage
CGCCAG	0	GCCAGG	0	CCAGGG	0	CAGGGT	0
GGGTTT	**4**	GGTTTT	0	GTTTTC	0	TTTTCC	0
TTTCCC	0	TTCCCA	0	TCCCAG	0	CCCAGT	0
CCAGTC	0	CAGTCA	0	AGTCAC	0	GTCACG	0
TCACGA	0	CACGAC	0	ACGACG	0	CGACGT	0
ACGTTG	0	CGTTGT	0	GTTGTA	0	TTGTAA	0
TGTAAA	0	GTAAAA	0	TAAAAC	0	**AAAACG**	**3**
AAACGA	0	AACGAC	0	ACGACG	0	CGACGG	0
GACGGC	0	GCCGTC	0	CCGTCG	0	CGTCGT	0
TCGTTT	0	CGTTTT	0	GTTTTA	0	TTTTAC	0
TTTACA	0	TTACAA	0	TACAAC	0	**ACAACG**	**3**
CAACGT	0	AACGTC	0	ACGTCG	0	CGTCGT	0
GTCGTG	0	TCGTGA	0	CGTGAC	0	GTGACT	0
TGACTG	0	GACTGG	0	ACTGGG	0	CTGGGA	0
TGGGAA	0	GGGAAA	0	GGAAAA	0	**AAAACC**	**6**
AAACCC	0	AACCCT	0	ACCCTG	0	CCCTGG	0

Additional Sequences Damaged by Calicheamicin

Sequence					Reference
AGGATT					[1]
AGGACA	AGGAAT	AGGTTG	AGGAAC	AGGAGT	[2]
AAAACC	AAAACG	TGAATT			[3]
AGGACT					[4]

References

1. Zein, N., Poncin, M., Nilakantan, R., and Ellestad, G.A. (1989) Calicheamicin γ_1^I and DNA: molecular recognition process responsible for site-specificity. *Science* **244**, 697-699.

2. Zein, N., Sinha, A.M., McGahren, W.J., and Ellestad, G.A. (1988) Calicheamicin γ_1^I: an antitumor antibiotic that cleaves double-stranded DNA site specifically. *Science* **240**, 1198-1201.

3. Walker, S., Landovitz, R., Ding, W.D., Ellestad, G.E., and Kahne, D. (1992) Cleavage behavior of calicheamicin g^1 and calicheamicin T. *Proc. Natl. Acad. Sci.* **89**, 4608-4612.

4. Hangeland, J.J., De Voss, J.J., Heath, J.A., Townsend, C.A., Ding, W.-d., Ashcroft, J.S., and Ellestad, G.A. (1992) Specific abstraction of the 5'(S)- and 4'-deoxyribosyl hydrogen atoms from DNA by calicheamicin γ_1^I. *J. Am. Chem. Soc.* **114**, 9200-9202.